1983

Temporal Trends in the Geochemistry and Petrology of the 1980 Mount St. Helens Pyroclastic Flow Deposits

Robert L. Logan

Follow this and additional works at: https://cedar.wwu.edu/wwuet

Part of the Geology Commons

Recommended Citation

Logan, Robert L., "Temporal Trends in the Geochemistry and Petrology of the 1980 Mount St. Helens Pyroclastic Flow Deposits" (1983). *WWU Graduate School Collection*. 819.
https://cedar.wwu.edu/wwuet/819

TEMPORAL TRENDS IN THE GEOCHEMISTRY AND PETROLOGY OF THE

1980 MOUNT ST. HELENS PYROCLASTIC FLOW DEPOSITS

by

Robert Logan

Accepted in Partial Completion

of the Requirements for the Degree

Master of Science

_____

Dean of Graduate School

Advisory Committee

_____

Chairman

_____

MASTER'S THESIS

In presenting this thesis in partial fulfillment of the requirements for a master's degree at Western Washington University, I grant to Western Washington University the non-exclusive royalty-free right to archive, reproduce, distribute, and display the thesis in any and all forms, including electronic format, via any digital library mechanisms maintained by WWU.

I represent and warrant this is my original work and does not infringe or violate any rights of others. I warrant that I have obtained written permissions from the owner of any third party copyrighted material included in these files.

I acknowledge that I retain ownership rights to the copyright of this work, including but not limited to the right to use all or part of this work in future works, such as articles or books.

Library users are granted permission for individual, research and non-commercial reproduction of this work for educational purposes only. Any further digital posting of this document requires specific permission from the author.

Any copying or publication of this thesis for commercial purposes, or for financial gain, is not allowed without my written permission.

Name: _Robert L. Logan_

Signature_____

Date: _5/15/2018_

TEMPORAL TRENDS IN THE GEOCHEMISTRY AND PETROLOGY OF THE 1980

MOUNT ST. HELENS PYROCLASTIC FLOW DEPOSITS

A Thesis

Presented to

The Faculty of

Western Washington State College

In Partial Fulfillment

Of the Requirements for the Degree

Master of Science

by

Robert Logan

ABSTRACT

Petrographic and geochemical analyses were performed on pumice from the May 18, June 12, July 22, August 7, and October 16-18 pyroclastic flow deposits. The pumice is dacitic and contains, in order of decreasing abundance, the minerals plagioclase An_{30-57}, hypersthene, hornblende, magnetite-illmenite, $\pm$ augite, $\pm$ apatite, in a groundmass of highly vesiculated glass and plagioclase microlites. Vesiculation occurred over a period of about one second, but at times during the eruption probably within a zone in the vent rather than at the atmosphere-magma interface.

An increase with time in the crystal to glass ratio indicates continued cooling of the magma. Resorption or recrystallization of hornblende in younger flows indicates degassing by loss of H_2O. Barring new intrusion of magma, these textural trends suggest that less explosive eruptions might be expected in the future.

Using inductively coupled plasma spectroscopy, elemental oxide abundances were determined for Si, Al, Ti, Fe, Mn, Ca, Mg, K, Na, and P; and trace element abundances were determined for Ba, Cr, Cu, La, Nb, Sc, Sr, V, Y, Zn, and Zr. Temporal trends in major and minor element abundances show that SiO_2 decreases, while FeO (total), CaO, MgO, TiO_2, and MnO increase. Temporal trends in trace element abundances show an increase in Cr, Cu, Sc, and V with a decrease in Ba. These trends are toward a more andesitic composition. These data are consistent with the hypothesis that orogenic calk-alkaline rocks are formed by a subcrustal two stage melting process.

TABLE OF CONTENTS

LIST OF FIGURES

LIST OF FIGURES (CONT.)

LIST OF FIGURES (Cont.)

LIST OF TABLES

Page

Table

ACKNOWLEDGMENTS

To my thesis committee, Dr. Scott Babcock, Dr. Ned Brown, and Dr. Dave Pevear, I owe special thanks for help in providing guidance, review of the manuscript, encouragement, and time.

My wife, Terry, has made many sacrifices for my education. For this I owe her, and thank her for years of patience and understanding.

I would like to dedicate this thesis to my children, Molly, Zeke, and Nellie, who were quiet.

INTRODUCTION

Statement of Problem

Mount St. Helens is located in southwest Washington on the western slopes of the Cascade Range (figure 1). On March 20, 1980, this stratovolcano began it latest eruptive cycle. Juvenile ejecta were not produced until the May 18, 1980 event, at which time voluminous outpourings of airfall tephra and pyroclastic flow materials occurred. Most of the airfall tephra was deposited to the northeast of the mountain, following the path of the prevailing winds. The airfall tephra contained a mixture of accidental and juvenile materials, becoming highly enriched in juvenile materials as the eruption progressed, but nevertheless was contaminated by nonjuvenile materials.

Pyroclastic flows occurred on all flanks of the volcano, but most of the flows and the greatest volumes of material were restricted to the valley of the North Fork Toutle River, on the north side of the cone.

Subsequent eruptions of May 25, June 12, July 22, August 7 and October 16-18, 1980, also produced pyroclastic flows. The pumice should better represent the composition of the magmatic source at the time of eruption than airfall tephra, since the latter contain considerable amounts of lithic material (Pevear et al., 1982).

Analyses of airfall tephra, pumice and lava domes for major elements by Melson et al. (1981), Lipman et al. (1981), and Scheidegger et al. (1982), have already shown that significant compositional changes have occurred with time. Irving et al. (1980) published
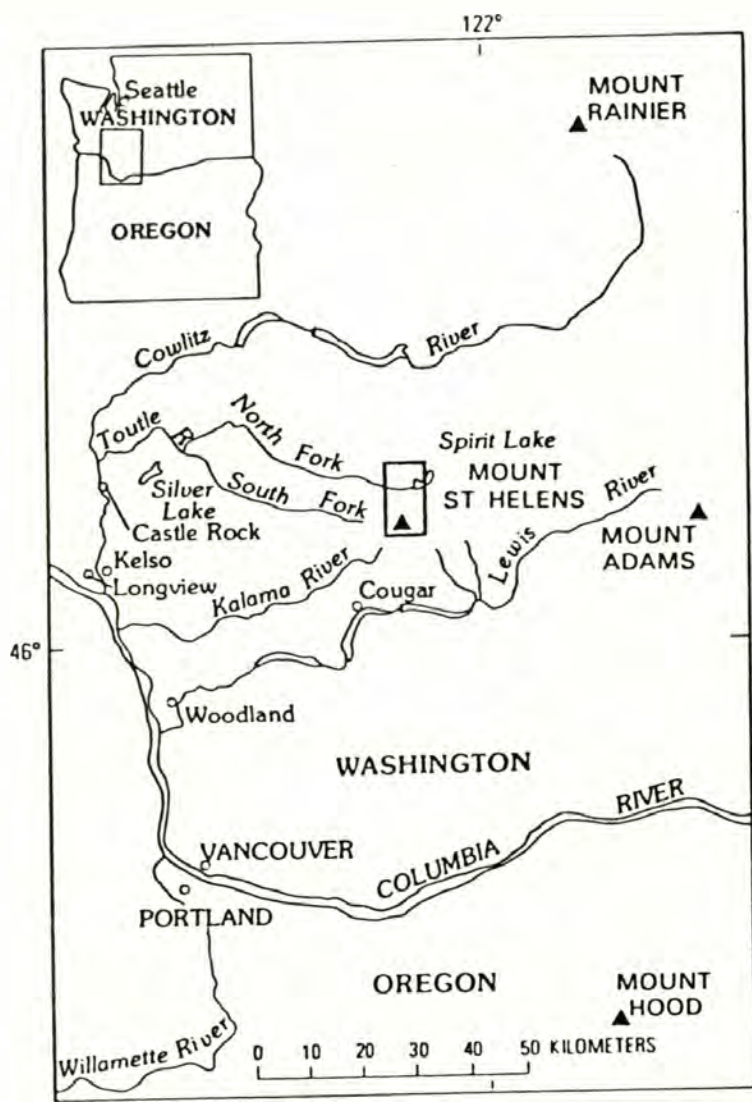
Figure 1. Map showing location of Mount St. Helens and field area.

data on a limited number of trace elements for pumice from the pyro-
clastic flow deposits.

The purpose of this project is to characterize the major, minor
and trace element composition and mineralogy of the pyroclastic flow
deposits as a function of time and to correlate the results with type
of eruptive activity. Such information is potentially useful as a
predictive tool for similar future events and may also be useful for
evolving a better model for Cascade volcanism.

The approach of this study differs from other geochemical studies
of Mount St. Helens ejecta primarily because it concentrates on
poumice from pyroclastic flow deposits. A suite of pumice samples
representing each pyroclastic flow deposit was analyzed. The study
of pyroclastic flow pumice was chosen because each flow deposit
represents a distinct time stratigraphic unit. These units are of
varying size. The size (runout and volume) of the flows are a func-
tion primarily of the eruptive behavior of the volcano (Sykes and
Self, 1981 and Moyer et al., 1982).

Analyses were carried out by Mr. Colin Cool at the University of
Washington by inductively coupled plasma spectroscopy (ICP). ICP is
a relatively new analytical technique which gives results comparable
to other available geochemical technologies.

Field Area

The field area for this study (Figures 1 and 2) is located in the
North Fork of the Toutle River valley, between Mount St. Helens and
Spirit Lake, on a broad, gently sloping area referred to as the
pumice plain. The area was chosen because it contained represen-
tative deposits of pyroclastic flows from each eruption of the
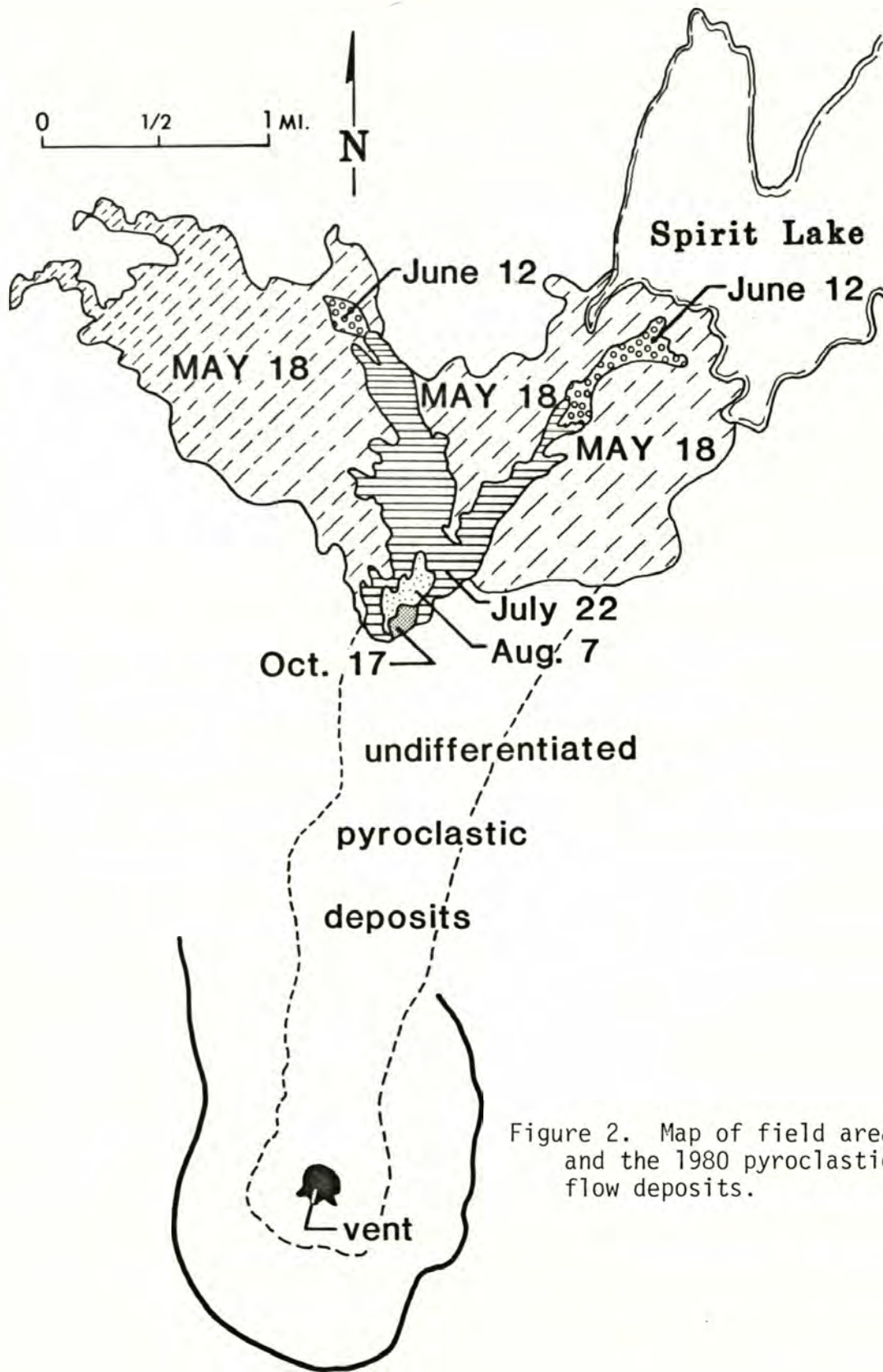
Figure 2. Map of field area and the 1980 pyroclastic flow deposits.

present eruptive cycle and was accessible by helicopter. Figure 2 is a map of the field area showing the extent of the pyroclastic flow deposits.

On May 18, 1980 at 8:32 a.m., a massive landslide occurred on the north flank of Mount St. Helens and filled the valley in places to a depth of about 300 feet with debris flow deposits (Voight et al., 1981). The landslide triggered an enormous eruption which began as a laterally-directed blast devastating a fan-shaped area of 150 square miles, lying to the north of the edifice. The eruption continued throughout the day, during which time numerous pyroclastic flows occurred.

The landslide left a gaping breach in the north flank of the mountain through which the pyroclastic flows were channeled. The emplacement of these flows added a relatively smooth veneer of pyroclastic material on top of the debris deposits in the valley. The largest pyroclastic flows occurred on May 18, 1980, with additional smaller flows being emplaced on May 25, June 12, July 22, August 7, and October 16-18, 1980. Pyroclastic flows also occurred on the east, south, and west flanks during the May 18 eruption but were not studied due to their inaccessibility.

The pyroclastic flows were caused by eruptive column collapse and direct fountaining of ejecta onto the crater floor. The flows consisted of a coarse basal flow accompanied by a hot expanding cloud of ash and gasses. An emplacement velocity of 100 kilometers per hour was reported by Hoblitt (1980).

Rowley et al. (1981) and Wilson and Head (1981) have described in

detail the morphology and extent of pyroclastic flow deposits. They estimate that approximately 0.142 km^3 of pyroclastic debris was erupted during the May 18, May 25, June 12, August 7, and October 16-18 eruptions. These flows covered an area of about 15.5 km^2, and extended as far as Spirit Lake to the north and 15 km to the west down the valley of North Fork Toutle River.

The individual flows formed elongate deposits that bifurcated into tongues and lobes. Levees were common features along the margins of many of the flow deposits. Terminal ends and lobes of flow deposits were commonly steep but sometimes gently tapered. The abruptness of the margins and termini of most flow deposits greatly aided recognition of individual flows especially where color and textural variations between flows were subtle.

The flows were made up primarily of poorly sorted nonwelded pumiceous and lithic ash mixed with pumice clasts. Contaminants included dome rock, breadcrusted clasts, hydrothermally altered pumice, and pumice from previous pyroclastic flows. Charred wood was found in many of the flows. Clast size larger than ash ranged from pebbles to boulders of better than a meter or two in diameter. Figures 3 and 4 illustrate some of these features.

Figure 5 illustrates the general field conditions and textural features of pyroclastic flows as they appeared during the fall of 1980. The pyroclastic flow deposits at that time were intact, and it was not until the winter of 1980-81 that extensive fluvial erosion destroyed the surface features of the flows and eroded deep gullies into the deposits. Reworking of the deposits has become more exten-

Figure 3. Photographs of pyroclastic flow deposit "contaminants".
(a) Breadcrust clast formed when margins chilled while interior
continued to expand by vesiculation. (b) Large hydrothermally
altered pumice clast.

Figure 4. Photographs of pyroclastic flow "contaminants". (a) Charred wood. (b) Large boulder of dome rock containing a greater abundance of crystals and much less vesiculated than pumice clasts.
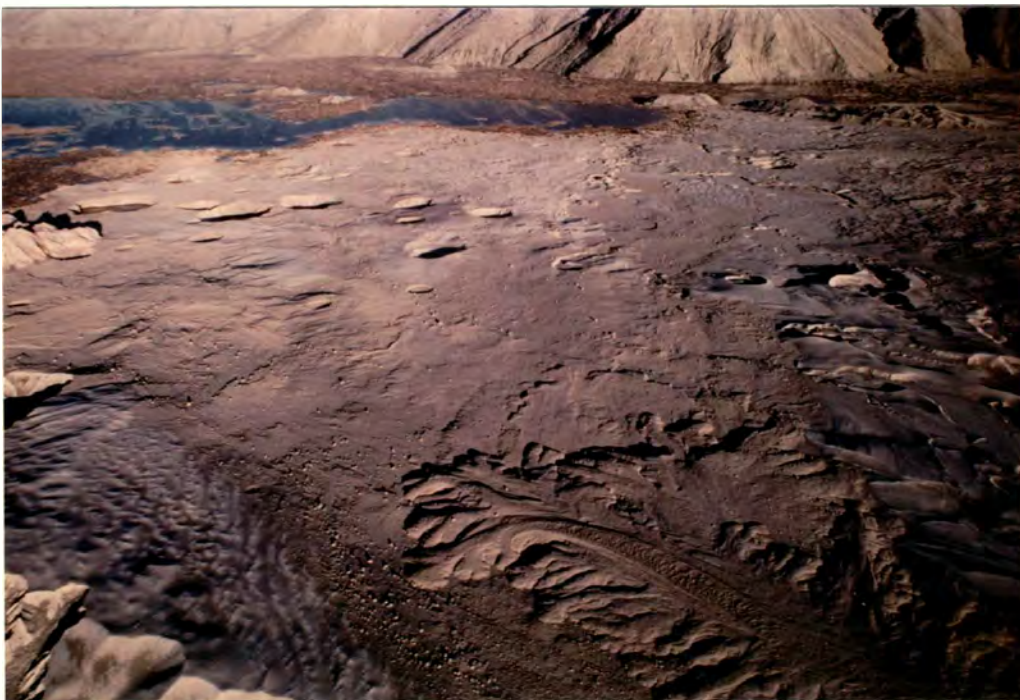
Figure 5. Photographs of (a) Field conditions encountered during the fall of 1980, and (b) Morphological features of pyroclastic flow deposits; note long tongues with marginal and terminal lobes. Relief on these features was generally not greater than a meter or two.

sive with each passing storm, completely destroying the surficial expression of nearly all of the individual flow deposits.

METHODOLOGY

The mapping and sampling phases were completed in the summer and fall of 1980, petrographic analysis in the fall of 1980, and geochemical analysis in January 1983.

Mapping

Shortly after most of the individual eruptive events of Mount St. Helens during 1980, the Washington State Department of Transportation flew aerial photography of the areas surrounding the volcano. The resulting photos have provided an excellent source of data for the compilation of a map of the extent of the various pyroclastic flows (Figure 2). Field checking of the map was accomplished on a limited basis by helicopter reconnaissance and on-ground investigation. The map and air photos were utilized to select 35 sampling sites in the North Fork of the Toutle River valley (Figure 6).

Sampling

Samples were collected on October 7, 16, and 19, 1980, using helicopter transportation to facilitate rapid completion of the task. Samples were collected across pyroclastic flow deposits at proximal, medial, and distal localities in order to obtain representative samples of each flow.

The flows are comprised of coarse pumice clasts in a sandy pumiceous and lithic matrix. Temperatures within the flows ranged up to
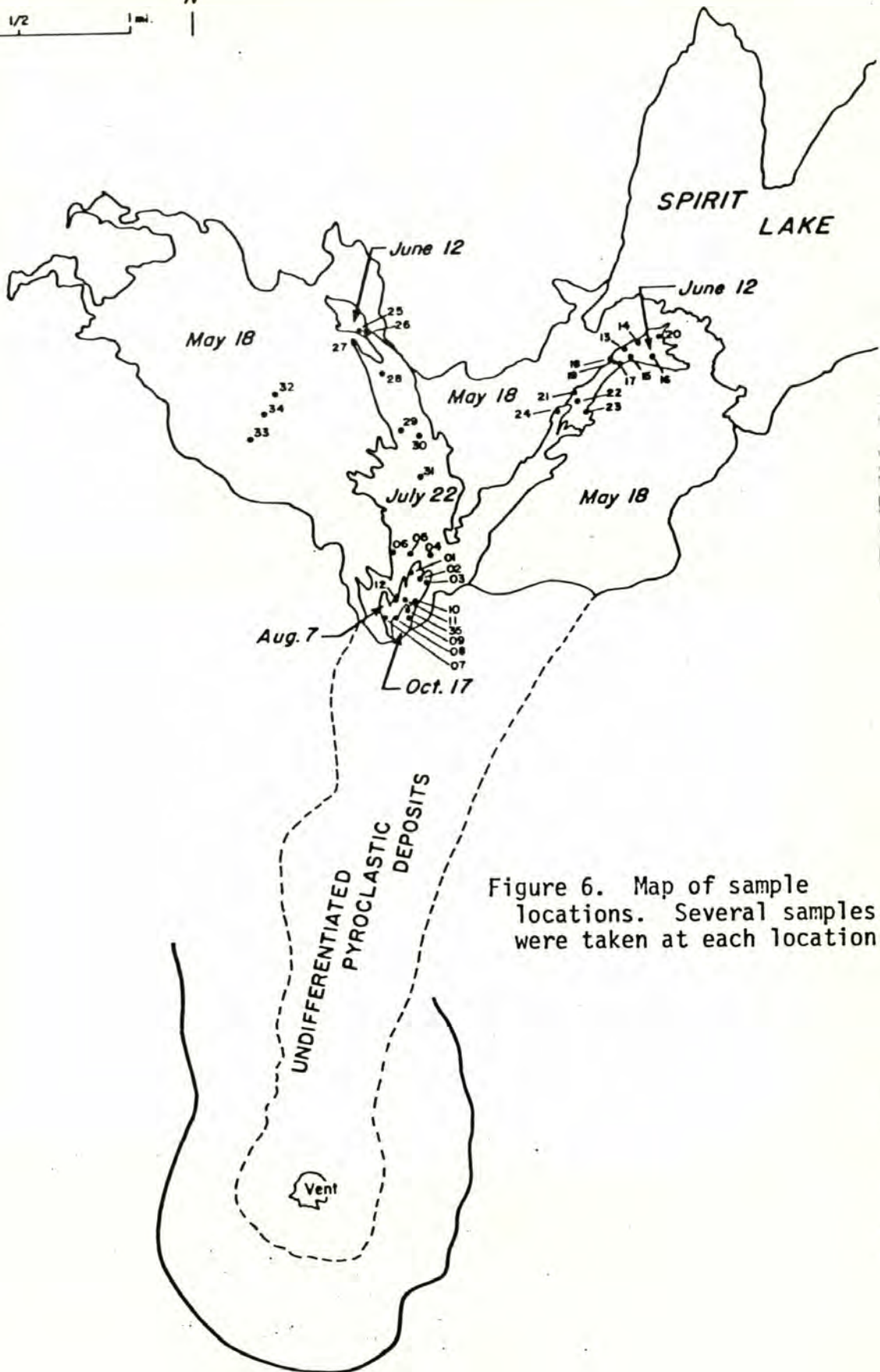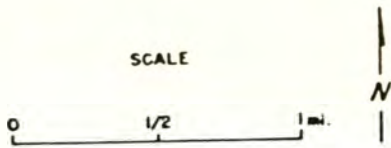
Figure 6. Map of sample locations. Several samples were taken at each location.

about 800°C depending on the depth in the flow, distance from the vent, and time elapsed after the eruption (Banks and Hoblitt, 1981). Although some pumice clasts were disseminated throughout the flows, most were concentrated at or near the surface of each pyroclastic flow where they cooled rapidly, thus reducing the possibility of hydrothermal alteration. The possibility of hydrothermal alteration of the pumice was further avoided by not sampling near the numerous small rootless fumaroles that dotted the surface of all flows. A typical cross-section of a May 18 pyroclastic flow showing the poorly sorted nature of the deposits, and a photograph of a small fumarole in a flow surface are shown in figure 7.

At each sample site, several fist-size pieces of pumice were collected; each sample taken closely resembled the appearance of the bulk of clasts in the pyroclastic flow being sampled. This was done to eliminate breadcrusted, dome and other foreign-appearing acciden-tal materials that might have been mechanically incorporated into the pyroclastic flows during deposition. Some minor contamination of later pyroclastic flows with pumice of similar appearance from earlier 1980 flow deposits remains a possibility. Rowley et al. (1981) have shown that erosion by pyroclastic flows occurred in the rills and canyons of the breached crater through which the flows were channeled.

Laboratory Work and Data Reduction

Analytical techniques used in this study include inductively coupled argon plasma spectrometry (ICP) and petrographic analyses. The geochemical analyses were done by Colin Cool at the University of

Figure 7. Photographs of (a) Streamcut in May 18 pyroclastic flow showing poorly sorted nature of flows, and (b) Small rootless fumarole in May 18, pyroclastic flow deposit. Pumice clasts near many of these fumaroles were often discolored. Sublimates such as halotrichite were commonly found near fumaroles.

Washington, using a Baird inductively coupled argon plasma spectro-
meter. A total of 24 samples were analyzed. The samples were
analyzed in random order to prevent bias. Sample preparation for
geochemical analysis is described in Appendix A. Geochemical data
were normalized and graphically presented using the Statistical
Analysis System package (SAS).

PREVIOUS INVESTIGATIONS

Verhoogen (1937) described the petrography and chemistry of the
various lithologies that comprise the Mount St. Helens edifice. Hyde
(1970), Hyde and Crandell (1972), and Hyde (1973) investigated the
glacial and surficial volcanic deposits of Mount St. Helens to deter-
mine its eruptive history. Greeley and Hyde (1972) studied the lava
tubes of the Cave Basalt. Jillson (1917), Erdmann and Warren (1938),
Holmes (1955), Folsom (1970), and Hopson (1971) discussed the erup-
tive history of the mountain. Studies of tephra deposits from Mount
St. Helens include those by Laurence (1938, 1939, 1941, 1954),
Borchardt et al. (1971), Carithers (1946), Mullineaux (1964, 1975),
Mullineaux et al. (1972, 1975), Smith and Westgate (1969), Okazaki et
al. (1972), Smith et al. (1977), and Smith (1980). Trace element
analyses of Mount St. Helens tephra erupted prior to 1980 include
studies by Randel et al. (1971), Dudas et al. (1973), Sarna-Wojcicki
(personal communication in Smith, 1980), and Smith and Leeman (1982).

The chemistry of the recent eruptive products of Mount St. Helens
has been studied by numerous investigators using a variety of tech-
niques. Fruchter et al. (1980), using ICP and XRF, published data

on the major, minor, and trace element abundances of the May 18 ash. Hooper et al. (1980) analyzed May 18 ash for major elements using XRF. Irving et al. (1980) used XRF and INAA to study the major and trace chemistry of one pumice and various dome and ash samples. Melson et al. (1980a), by using electron microprobe, showed evidence for temporal trends for several major element oxides in probable essential ejecta. The petrology and geochemistry of dome material was studied by Raedeke et al. (1980) using electron microprobe. Major, minor and trace element abundances in the May 18 ash were determined by Taylor and Liehte (1980) using XRF and ICP. Wozniak et al. (1980) used XRF and atomic absorption to analyze May 18 ash for major elements. Sequential INAA was used by Hughes (1981) to study trace element partitioning effects in May 18 pumice. Lipman et al. (1981), using wet chemistry and XRF, analyzed a suite of magmatic material including all eruptions up to October 1980 for major element abundances. Melson et al. (1981) updated his previous electron microprobe study for trends in major elements. Sarna-Wojcicki et al. (1981) used XRF to determine major, minor, and trace element abundances in ashes erupted between May 18 and including August 7, 1980. Scarfe et al. (1982) described the mineralogy and geochemistry of pumice from the March 19, 1982 eruption. Finally, Scheidegger et al. (1982), using electron microprobe, investigated the chemistry of glass from May 18 ash and pumice from several pyroclastic flow deposits.

Investigations dealing primarily with petrology include those by Melson et al. (1980b), Kuntz et al. (1981), and Logan (1981). Rowley

et al. (1981) have described the chronology, morphology, and extent
of the 1980 pyroclastic flows. Melson and Hopson (1981) have pre-
sented estimates of pre-eruption temperatures and oxygen fugacities
in the 1980 eruption sequence. Various observations on conditions of
emplacement of the pyroclastic flows have been presented by Hoblitt
(1980), Hoblitt et al. (1980), Sykes and Self (1981), Wilson and Head
(1981), and Moyer et al. (1982).

GEOLOGIC SETTING AND HISTORY

Mount St. Helens is a Quaternary stratovolcano, consisting of a
composite volcanic pile built upon volcanic and volcaniclastic rocks
of Quaternary and Tertiary age. These basement rocks include the
Marble Mountain microphyric olivine basalt and hornblende andesite of
Quaternary age. Tertiary deposits include the ashflow tuffs and
tuffaceous sedimentary rocks of the Stevens Ridge Formation, and an-
desitic and dacitic, tuff breccia interfingering with pyroxene ande-
site lava flows and associated breccias, and local rhyolites of the
Ohanapecosh Formation. The Ohanapecosh Formation is the most exten-
sive Tertiary unit in the vicinity of Mount St. Helens. Local
Tertiary intrusive rocks include the biotite hornblende dacite
porphyry of the Goat Mountain plug; hypabyssal intrusive rocks,
mainly pyroxene microdiorite and granodiorite; and the epizonal gra-
nodiorite of Cinnamon Peak and Mount Mitchell (Hopson, 1980).

The eruptive history of Mount St. Helens has been complex
(Verhoogen, 1937; Mullineaux and Crandell, 1962; Hopson and Melson,
1980). This complexity is typical of a divergent volcano as

described by McBirney (1968) and Hughes et al. (1980). The oldest known product is a biotite-bearing pumice layer dated at 37,600 years before present (ybp) (Hyde, 1973). This unit marks the beginning of a period of eruptive activity that was characterized by numerous episodes of dacitic to andesitic volcanism, and lasted until about 2,500 ybp, and constitutes the ancestral Mount St. Helens cone upon which the present cone is built (Hoblitt et al., 1980). At approximately 1,950 ybp (Hopson and Melson, 1980), the products became generally more mafic in composition, including not only dacite and andesite but olivine basalt flows as well.

The modern cone yields evidence of several eruptive cycles. Beginning at about 1,700 ybp the orthopyroxene dacite of tephra layer B was erupted and was followed by the emplacement of the orthopyroxene dacite of the East Dome, clinopyroxene-orthopyroxene andesite lava flows, olivine-pyroxene andesite flows and tephra of the upper layer B and finally olivine basalt (Hopson and Melson, 1980). Following a repose interval of 500-600 years the basal W tephra was deposited (Mullineaux et al., 1975), with subsequent emplacement of the orthopyroxene-hornblende dacite Sugarbowl Dome. Hopson and Melson (1980) suggest that the Sugarbowl episode represents an "arrested cycle" since no lava flows are known to have followed. The next cycle, referred to as the Kalama eruptive period by Hoblitt et al. (1980), began about 450 ybp with the Plinian eruption of the orthopyroxene-hornblende dacite pumice tephra of set W, followed by the mineralogically diverse andesite tephra of set X. Ortho-

pyroxene-clinopyroxene andesite lava flows and orthopyroxene-clino-
pyroxene-olivine andesite (Kalama River) pyroclastic flows were then
deposited prior to emplacement of the orthopyroxene-clinopyroxene-
hornblende dacite summit dome at about 350 ybp. After a repose
interval of about 170 years, the Goat Rocks eruptive period was ini-
tiated by the eruption of the orthopyroxene-hornblende-clinopyroxene
dacite tephra of layer T, at about 180 ybp. Again, an andesite flow
of orthopyroxene-clinopyroxene-hornblende mineralogy followed the
initial dacitic tephra eruption. The conclusion of this eruptive
phase at 138 ybp was marked by the emplacement of the Goat Rocks, an
orthopyroxene-clinopyroxene-hornblende dacite dome (Hoblitt et al.,
1980).

The current eruptive cycle began March 27, 1980 with minor lithic
tephra eruptions followed on May 18, 1980 by extensive hornblende-
orthopyroxene dacite airfall ash and pyroclastic flows and a clino-
pyroxene-hornblende-orthopyroxene dacitic dome. Geochemical analyses
of these products indicate a slight trend toward a more mafic com-
position, a subject that will be discussed later in this paper.

PETROGRAPHY

The petrography of the pumice from the 1980 Mount St. Helens
pyroclastic flow deposits has already been described by Melson et al.
(1980b), Logan (1981), and Kuntz et al. (1981). However, a more
detailed presentation of Logan's (1981) preliminary analysis is given
in this thesis which includes a discussion on vesicle textures, and
xenolith influence on petrochemical trends. Thirty-six thin sections

of pumice were analyzed, and the detailed petrography of each section
is given in Appendix A. The mineralogy of each sample is listed in
Table 1.

The pumice is light gray, has a dacitic chemistry based on SiO_2
content, and has fairly constant mineralogy throughout all flows.
The glass in the groundmass is colorless and highly vesiculated. In
addition to glass, minerals present in order of decreasing abundance
include plagioclase feldspar, hypersthene, hornblende, and opaque
minerals. Augite and possibly apatite are present in some samples.

Plagioclase is the most abundant mineral present in all samples
as both phenocrysts and/or xenocrysts and microlites. Although
larger phenocrysts are commonly present in hand specimen, the phe-
nocrysts observed in thin section range in size up to 2.8 mm in
length and are generally euhedral. Both normal and reverse zoning
are common as are inclusions of pink to colorless glass. The inclu-
sions often lie parallel to zoning surfaces within the plagioclase
(Figure 8). The anorthite content, as determined using the
Michel-Levy method, ranges from roughly An_{30} to An_{57}. Carlsbad and
albite twinning are common, whereas pericline twinning is rare.

Pale pink to pale green pleochroic hypersthene is the most abun-
dant mafic phase, usually making up about 5 percent of the rock.
Euhedral crystals with sharp boundaries are the most common (Figure
9). These phenocrysts range in size up to 1.6 mm in length. Many
phenocrysts contain opaque inclusions.

Hornblende phenocrysts ranging up to 2.6 mm in length are usually
present in amounts of less than 5 percent of total phenocrysts.

Table 1. — Mineral Assemblages in Mount St. Helens Pumice

Sample Number	Plagioclase	Hypersthene	Hornblende	Opaque Minerals	Clinopyroxene	Texture	Accessory Minerals	Xenoliths
1	PG	P	Pr	P*Di		R		
2	PG	P	Pr	P*Di		R	a	
3	PG	P	Pr	P*Di	X	R		X
4	PG	P	Pr	P*Di	Gi	R	a	
5	PG	P	Pr	P*Di	Pi	t		
6	PG	P	Pr	P*Di	P	R		
7	PG	P	Pr	P*Di		R		
8	PG	P	Pr	P*Di		R		
9	PG	P	Pr	P*Di	P	t		
10	PG	PG	Pr	P*Di		R		
11	PG	P	Pr	P*Di		R		X
13	PG	P	Pr	P*Di		R		
14	PG	P	Pr	P*Di	P	R		
15	PG	P	Pr	P*Di	i	R		
16	PG	P	Pr	P*Di		R		
17	PG	P	Pr	P*Di		R		X
18	PG	P	Pr	P*Di		R		

P: Phenocryst phase
G: Groundmass phase
r: Reaction rims of hypersthene microlites and/or magnetite
R: Random
t: Subtrachyitic
P*: For magnetite large crystals
D: Disseminated in groundmass
a: Apatite
i: As inclusions
X: In xenoliths

Table 1. — Mineral Assemblages in Mount St. Helens Pumice (Cont.)

Sample Number	Plagioclase	Hypersthene	Hornblende	Opaque Minerals	Clinopyroxene	Texture	Accessory Minerals	Xenoliths
19	PG	P	Pr	P*Di		R		
20	PG	P	Pr	P*Di		R		
21	PG	P	Pr	P*Di		R		
22	PG	P	Pr	P*Di		R		
23	PG	P	Pr	P*Di	x	R		x
24	PG	P	Pr	P*Di		R		
25	PG	P	Pr	P*Di	P	t		
26	PG	P	Pr	P*Di	P	R	a	
27	PG	P	Pr	P*Di		t		
28	PG	P	Pr	P*Di		R		
29	PG	P	Pr	P*Di	x	R		x
30	PG	P	Pr	P*Di		R		
31	PG	P	Pr	P*Di	P	R		
32	PG	P	P	P*Di		R		
33	PG	P	Pr	P*Di		R		
34	PG	P	Pr	P*Di		R		
35	PG	P	Pr	P*Di	PX	R		x

P: Phenocryst phase
G: Groundmass phase
r: Reaction rims of hypersthene microlites and/or magnetite
R: Random
t: Subtrachyitic
P*: For magnetite large crystals
D: Disseminated in groundmass
a: Apatite
i: As inclusions
X: In Xenoliths
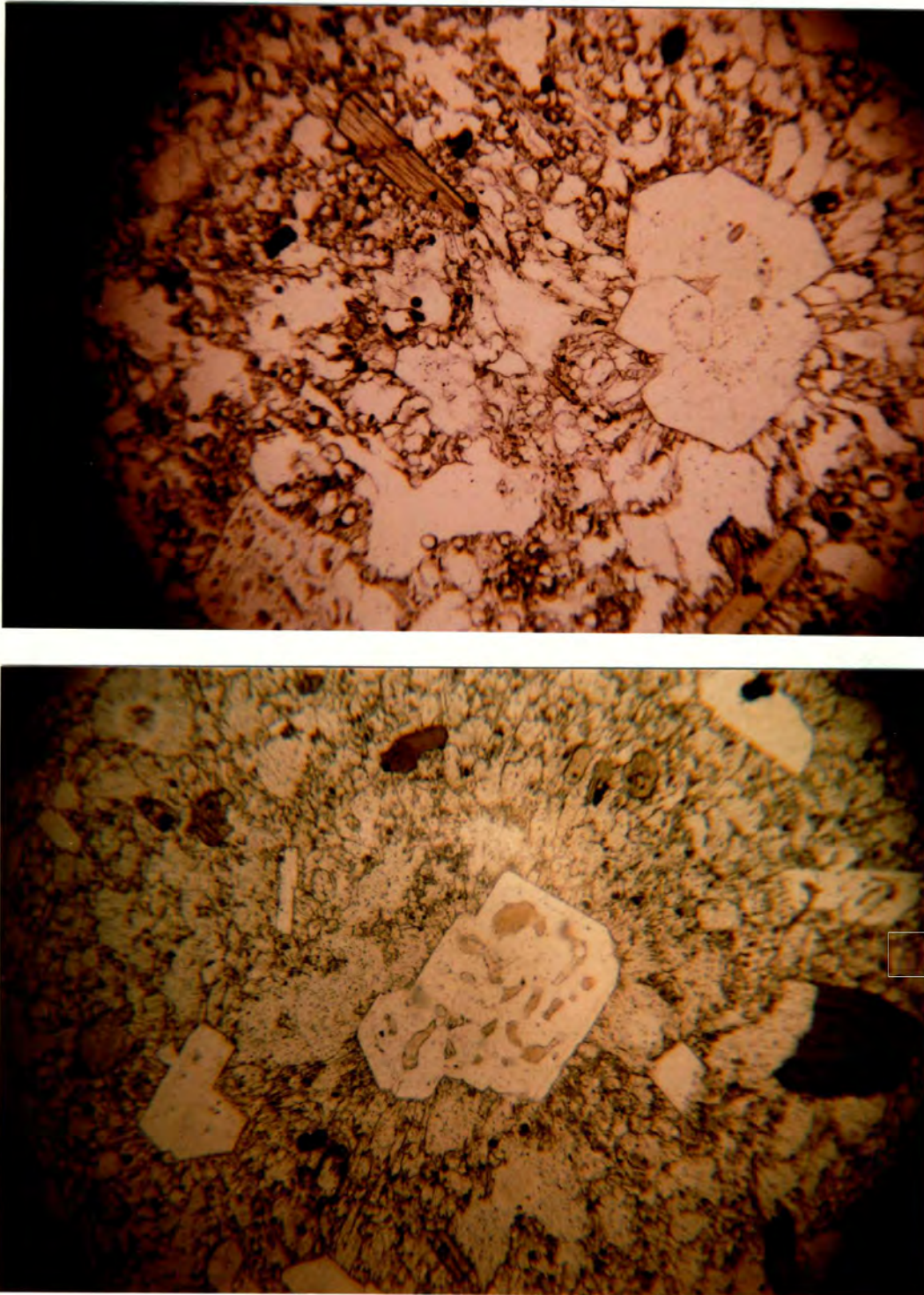
Figure 8. Photomicrographs showing glass inclusions in plagioclase feldspar, (a) Parallel to zoning surfaces, and (b) In core of reversely zoned phenocryst.
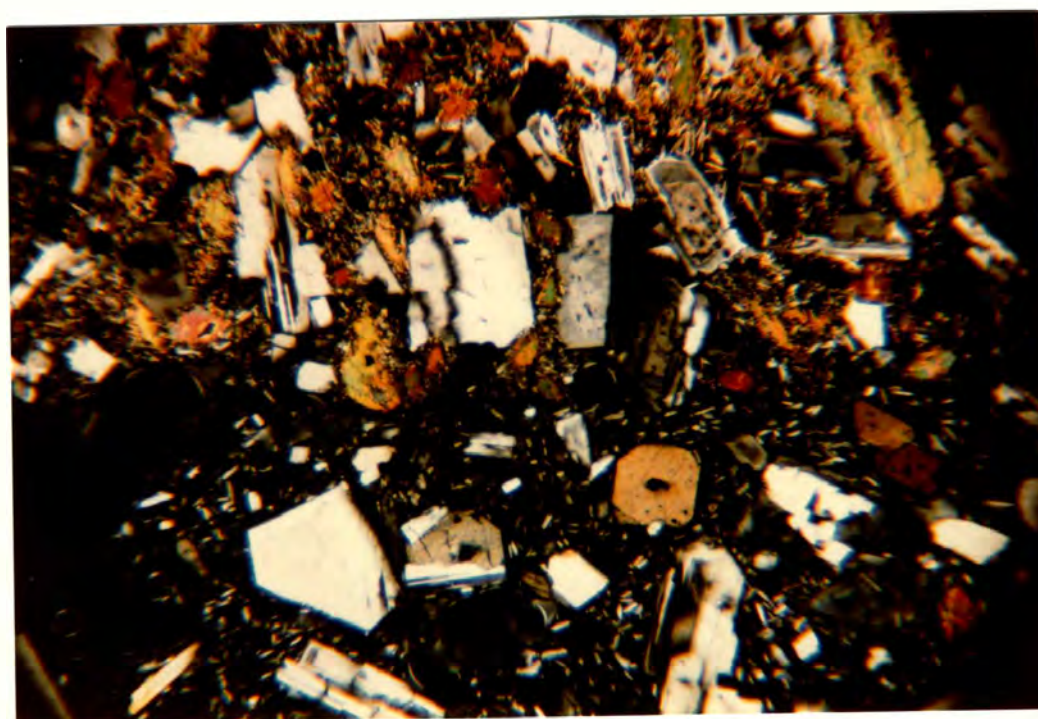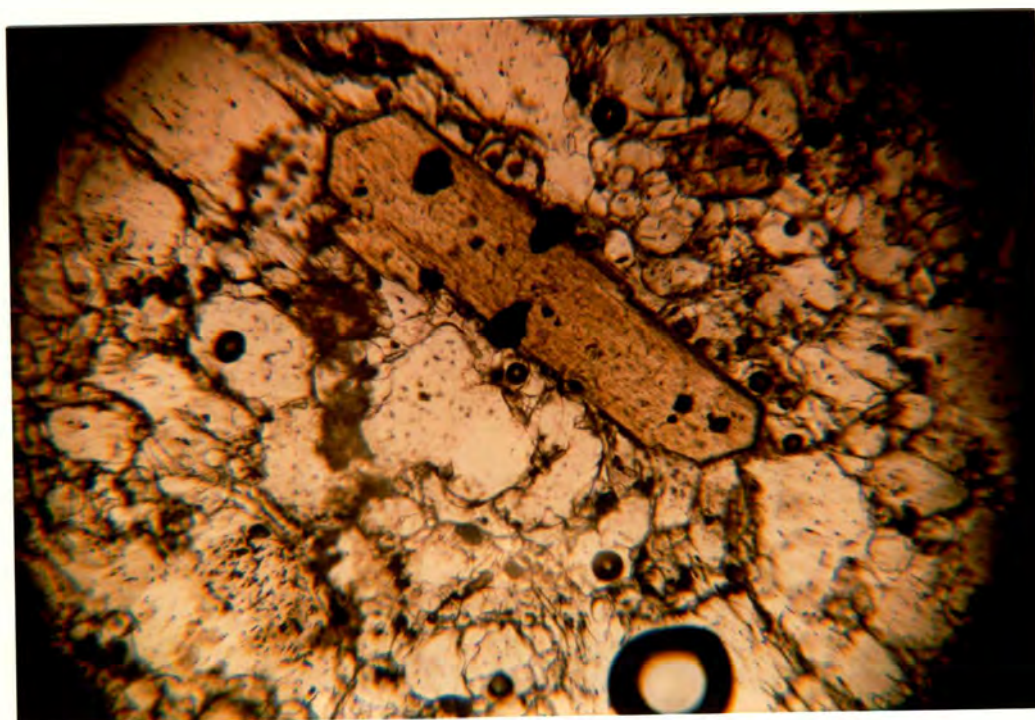
Figure 9. Photomicrographs of euhedral hypersthene, (a) Parallel to c,
(b) Basal section.

Pleochroism ranges from light to dark green or dark olive green in phenocrysts from earlier flows, to a generally more brownish hue in crystals from later pyroclastic material.

Hornblende grain boundaries are relatively sharp in May 18 material, but are commonly embayed and partially recrystallized in later pumice (Figure 10). Complete recrystallization of the hornblende to hypersthene microlites has resulted in the presence of ghost phenocrysts in many of the post-May 18 samples (Figure 11).

Opaque minerals are commonly present in amounts of 1 percent or less of the total rock and occur as irregular subhedral to euhedral grains. These grains are typically scattered throughout the groundmass, but are concentrated as inclusions within some hypersthene phenocrysts (Figure 12). Because thin section analysis was the only technique used for the petrography presented in this paper, the various opaque mineral phases were not specifically identified.

However, the opaque minerals have been identified as iron-titanium oxides of the species ulvospinel-magnetite and ilmenite-hematite by Kuntz et al. (1981) using polished grain mounts submersed in oil under reflected light. Their results are comparable to those of Smith (1980) who analyzed the opaque minerals of pre-1980 Mount St. Helens ejecta, using an electron microprobe.

Kuntz et al. (1981) noted that there are two distinct populations of iron-titanium oxides, the first, a highly oxidized "contaminant" variety that probably represents a xenocryst phase, and the second, an optically homogeneous unaltered variety. The unaltered state of the second variety indicates that post-emplacement hydrothermal
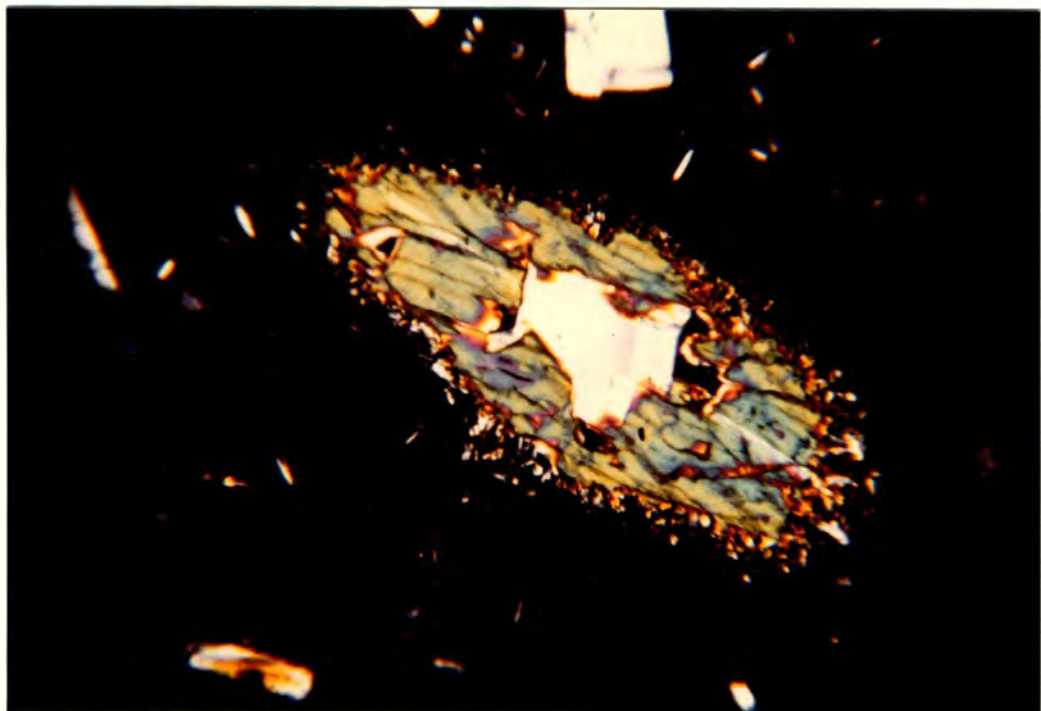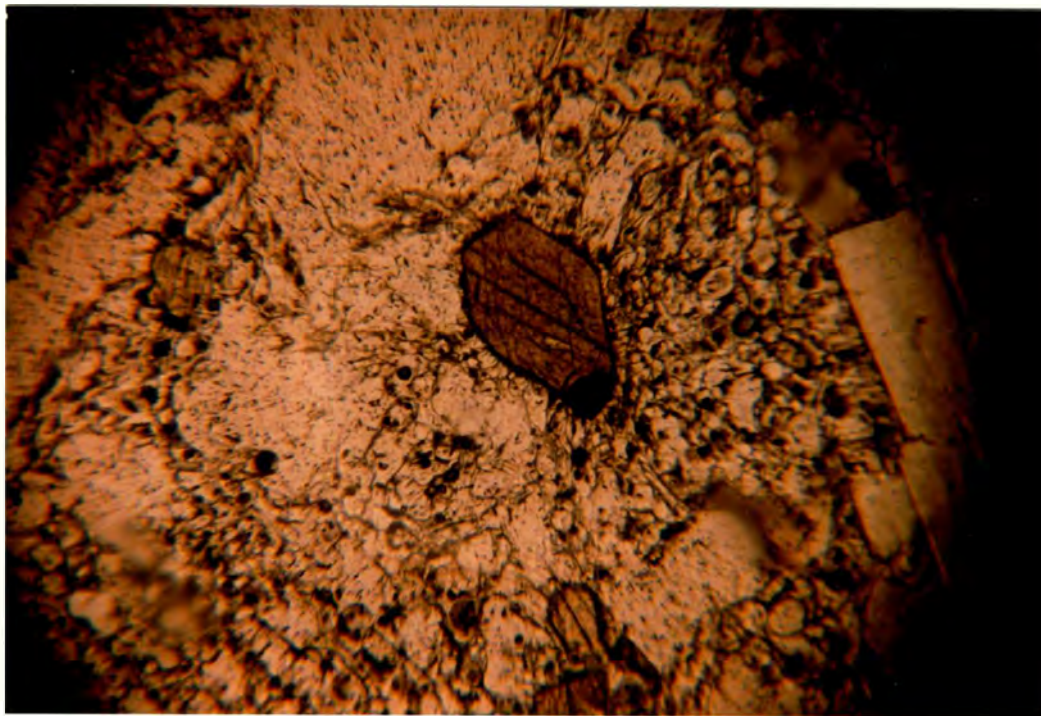
Figure 10. Photomicrograph of hornblende showing, (a) Euhedral crystal showing no signs of resorption in May 18 pumice, (b) Partially re-sorbed crystal in August 7 pumice.
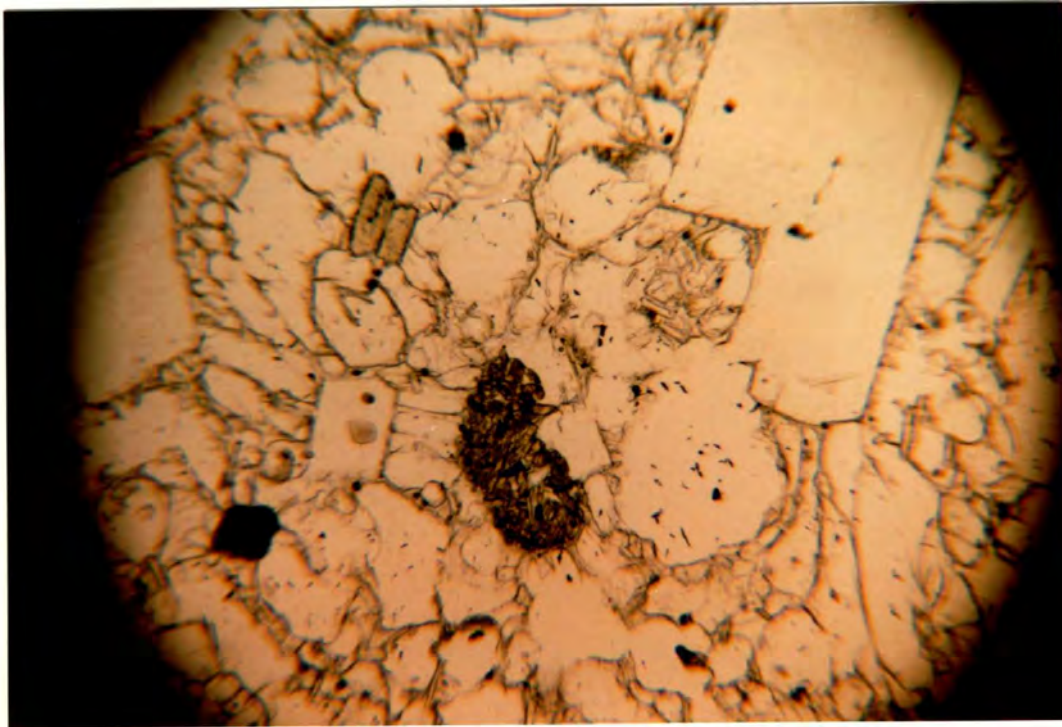
Figure 11. Photomicrograph of ghost hornblende in August 7 pumice.
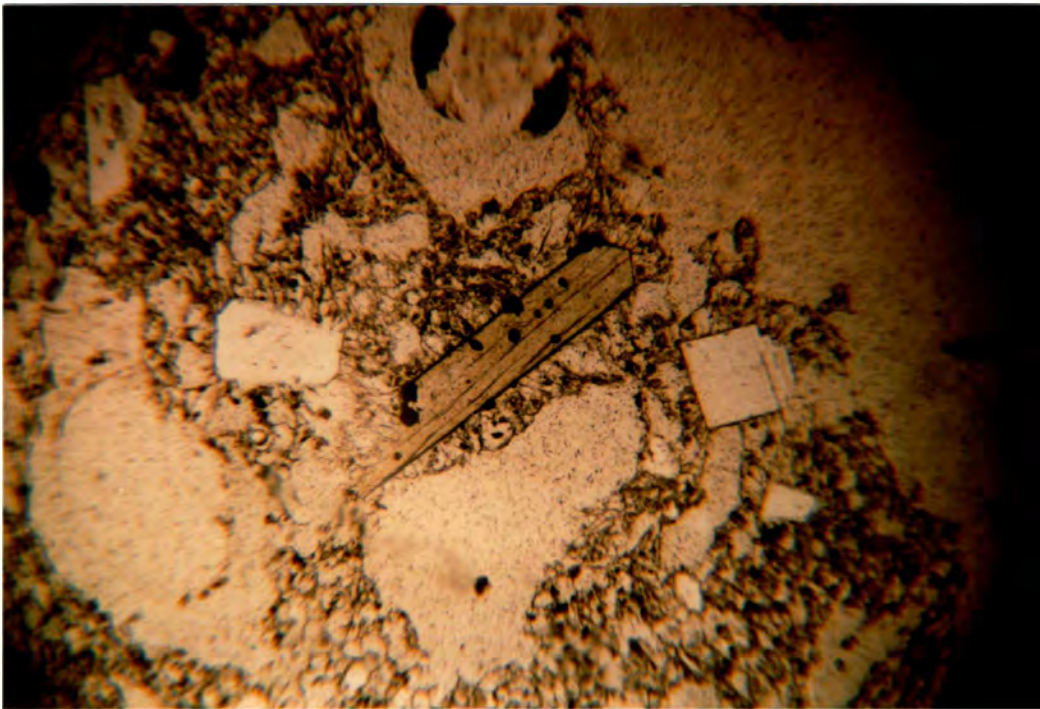
Figure 12. Photomicrograph showing magnetite inclusion in hypersthene phenocryst.

alteration of pyroclastic materials is virtually absent, and, there-
fore, would not influence the bulk chemistry of the pumice.

Progressive changes in ejecta textures have occurred with time.
The most apparent change is in the realtive abundance of glass and
crystals. Figure 13 illustrates this empirical textural change bet-
ween May 18 pumice and October 17 pumice. As noted above, the pro-
gressive recrystallization of the hornblende phase becomes more
apparent within younger flows. The instability of hornblende is
likely due to loss of volatiles (mainly water) through the continued
degassing of the magma chamber.

The glass matrix displays a highly vesiculated texture and many
of the phenocrysts are surrounded by elongate vesicles arranged with
their long axis normal to the surface of the phenocrysts. This
radial vesicle pattern in volcanic ejecta has been attributed to pool
boiling (Heiken and Eichelberger, 1980), and results when a hot sur-
face is submersed into a cooler liquid. Closely spaced nucleation of
bubbles occurs at the solid/liquid interface, followed by outward
migration of bubbles (Tong, 1972).

If it is assumed that the liquid and crystals of the magma were
at thermal equilibrium prior to eruption, then cooling of the liquid
through adiabatic expansion of the contained gasses would occur
during vesiculation. Heiken and Eichelberger (1980) have shown that
vesiculation at temperatures within the range of those estimated for
Mount St. Helens magma by Melson and Hopson (1981) and Scheidegger
et al. (1982) must be very rapid, i.e., about one second. If vesi-
culation occurs at shallow depths, deformation of the radial pattern
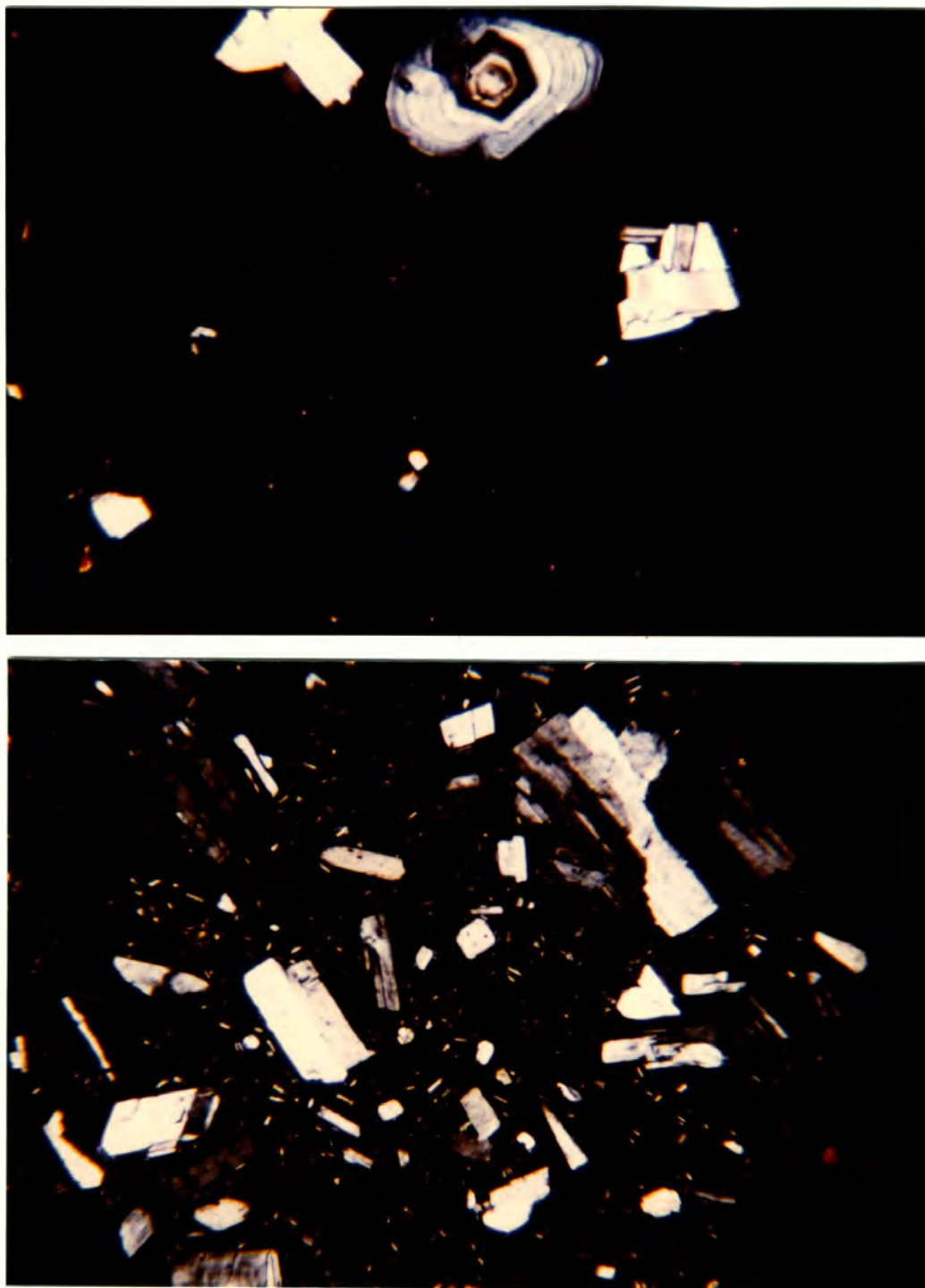
Figure 13. Photomicrographs illustrating temporal trend toward increased density of crystal phases. Comparison of May 18 pumice with fewer crystals versus October 17 with noticeably more crystals.

should not occur. Radial vesicle patterns in the 1980 Mount St. Helens pumice were preserved in most of the thin sections observed. However, there is some evidence of disturbed radial vesicles (Figure 14), indicating some flowage of magma within the vent shortly before eruption. Further evidence for flowage during vesiculation is subtrachyitic textures in several of the pumice clasts studied.

In addition to the specimens listed in Table 1, several other thin sections of pumice containing xenoliths were examined. These are listed with their mineral phases in Table 2, but are given only a cursory discussion in this paper as several other workers, i.e., Heliker (personal communication, 1983) and A. Irving (personal communication, 1982) are currently doing detailed studies of xenoliths in the 1980 pumice and domal dacite from Mount St. Helens. Paine (1982) has described xenoliths fround in Mount St. Helens dome material, reporting two populations of gabbroic mineralogy. The most abundant groups are the gabbronorites, containing 50 to 80 percent plagioclase with subordinate augite and hypersthene. The second group he refers to as olivine-normative gabbros, which contain abundant olivine, hornblende, orthopyroxene, clinopyroxene and plagioclase. The majority of xenoliths studied for this paper have mineralogies similar to the pumice, i.e., hornblende, hypersthene, plagioclase and accessory minerals. Examples are shown in Figure 15. Xenolith boundaries show very little evidence of resorption. Microlitic accumulations are present along boundaries of some xenoliths, but appear to be the result of "piling up" of matrix microlites on the xenolith surface as it moved through the melt. Resorption
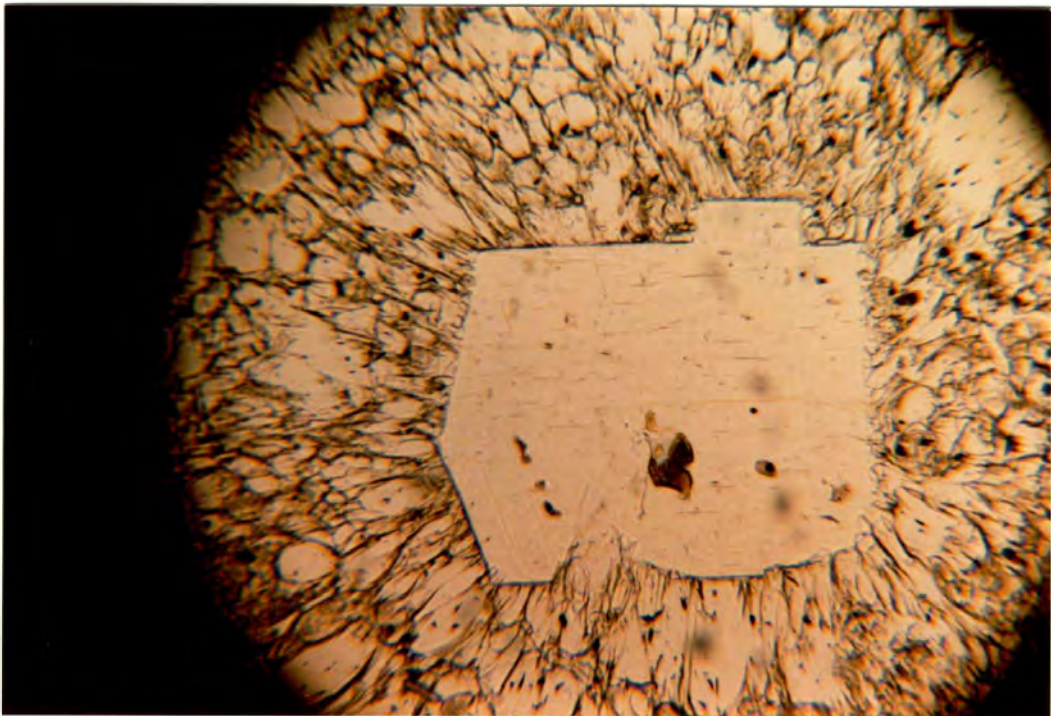
Figure 14.   Photomicrographs of radial vesicle patterns, (a) Undisturbed
radial vesicles, (b) Disturbed radial vesicles.

Table 2. — Mineralogy of Xenoliths

Sample	Plagioclase	Hornblende	Clinopyroxene	Hypersthene	Opaque Minerals	Biotite	Olivine
XP-11	X	X			X		
XP-10	X	X			X	X	X
XP-1	X	X		X	X		
XP-7	X	X		X	X		
D-1	X			X	X		
D-2	X		Xr	X	X		
D-3 (C)	X	X	X	X	X		
D-9 (C)	X	X		X	X		

(C):   Crystal cummulate

XP: Xenolith in pyroclastic pumice

D: Xenolith in dome rock

r: Resorbed
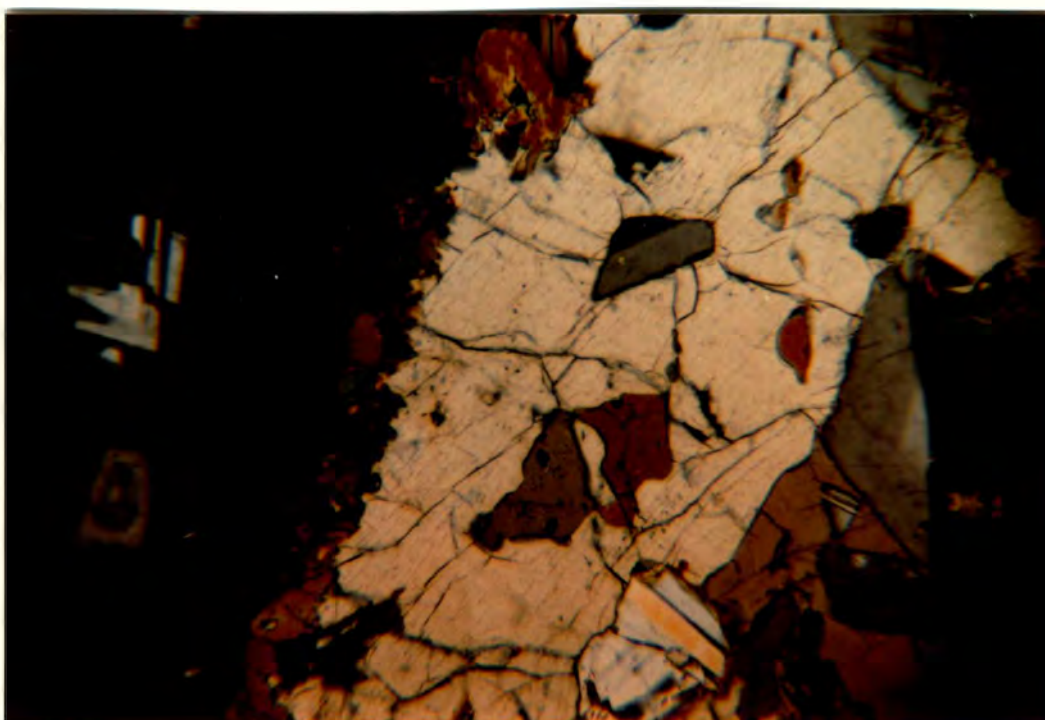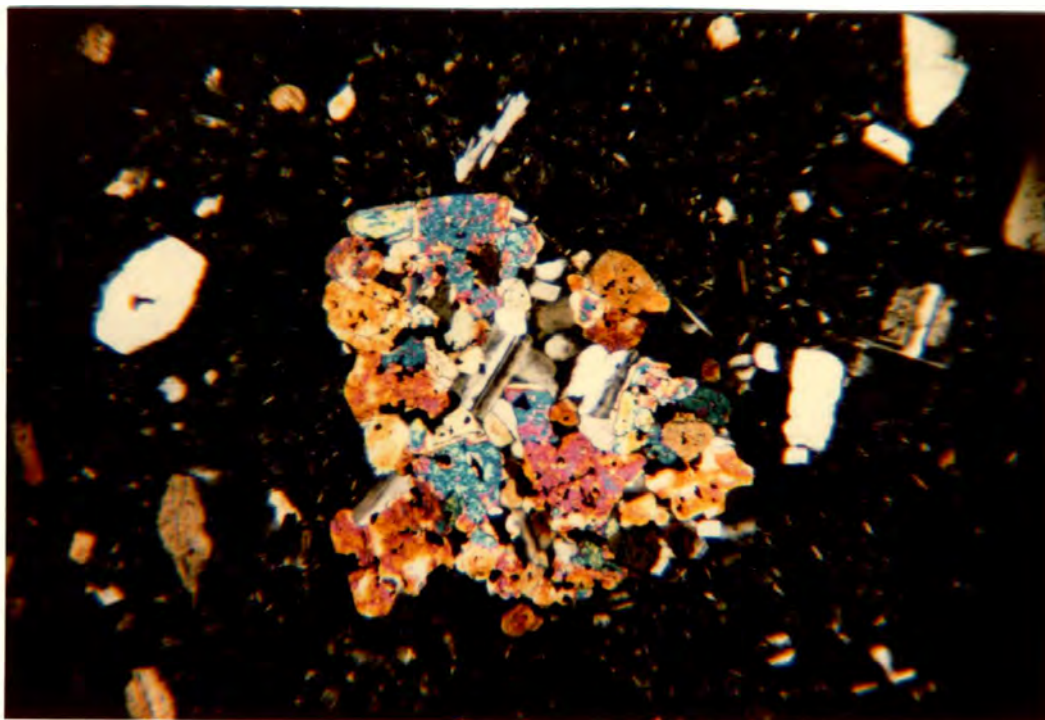
Figure 15. Photomicrographs of xenolith boundaries showing (a) No
resorption, (b) Partial recrystallization.

embayments are rare. Microlite accumulation rather than resorption or recrystallization seems more probable since magma chamber temperatures as estimated by Scheidegger et al. (1982) and Melson and Hopson (1981) of 965-1016°C do not seem hot enough to cause assimilation to any great extent. Heliker (personal communication, 1983) cites evidence of mechanical assimilation of xenoliths in domal material as well as the presence of interstitial glass within the xenoliths. To what extent assimilation is responsible for temporal trends in the petrochemistry of the pumice is impossible to estimate from the petrographic evidence available in the limited number of samples examined.

GEOCHEMISTRY

Whole rock chemical analyses were obtained for 24 samples of pumice from the May 18, June 12, August 7, July 22, and October 16-18, 1980 pyroclastic flows. The rocks were analyzed at the University of Washington by Colin Cool using a Baird, model PS101, inductively coupled argon plasma spectrometer. Analytical procedures are described in Appendix B.

Weight percentages of the major and minor oxides SiO_2, Al_2O_3, TiO_2, FeO (total), MnO, CaO, MgO, K_2O, Na_2O and P_2O_5 are listed in Table 3. In addition, the abundances of the trace elements Ba, Cr, Cu, La, Nb, Sc, Sr, V, Y, Zn, and Zr were determined and are listed in Table 4. Analytical precision was checked by analyzing the USGS standard AGV-1. A comparison between the ICP results and the published values for the standard (Abbey, 1980) are given in Table 5.

Table 3. — Mount St. Helens Pyroclastic Flow Geochemistry
ICP Major and Minor Oxide Data

Sample	Date	SIO_2	AL_2O_3	TIO_2	FEO	MNO	CAO	MGO	K_2O	NA_2O	P_2O_5	Total
33	18 May 1980	64.29	17.67	0.59	3.90	0.11	4.82	1.87	1.31	4.96	0.21	99.73
34	18 May 1980	63.91	17.46	0.59	3.92	0.11	4.97	1.86	1.32	4.98	0.22	99.34
14	12 Jun 1980	63.69	17.51	0.62	4.06	0.13	4.93	1.96	1.33	4.99	0.22	99.44
15	12 Jun 1980	63.28	17.77	0.62	4.08	0.12	5.07	1.98	1.41	5.01	0.22	99.56
17	12 Jun 1980	63.22	17.98	0.60	4.04	0.11	4.82	1.94	1.24	5.03	0.21	99.19
19	12 Jun 1980	63.99	17.31	0.64	4.25	0.12	4.99	1.99	1.38	4.79	0.21	99.67
22	12 Jun 1980	63.14	17.68	0.62	4.20	0.11	4.77	2.03	1.27	5.00	0.22	99.04
23	12 Jun 1980	63.47	17.56	0.61	4.16	0.12	5.02	2.09	1.36	4.88	0.23	99.50
26	12 Jun 1980	63.40	17.72	0.64	4.29	0.12	5.12	2.19	1.33	4.88	0.23	99.92
5	22 Jul 1980	63.27	17.68	0.66	4.35	0.14	5.29	2.22	1.31	4.96	0.22	100.10
6	22 Jul 1980	63.96	17.88	0.64	4.32	0.12	5.23	2.18	1.37	4.92	0.23	100.85
24	22 Jul 1980	64.22	17.86	0.64	4.40	0.12	5.07	2.13	1.35	5.08	0.22	101.09
25	22 Jul 1980	64.30	17.86	0.61	4.18	0.12	4.99	2.04	1.39	4.98	0.21	100.68
28	22 Jul 1980	61.66	18.06	0.67	4.50	0.14	5.46	2.42	1.29	4.92	0.22	99.34

Table 3. — Mount St. Helens Pyroclastic Flow Geochemistry
ICP Major and Minor Oxide Date (Cont.)

Sample	Date	SIO_2	AL_2O_3	TIO_2	FEO	MNO	CAO	MGO	K_2O	NA_2O	P_2O_5	Total
31	22 Jul 1980	63.33	17.45	0.59	4.15	0.12	5.03	2.02	1.31	4.72	0.22	98.94
1	7 Aug 1980	63.82	18.00	0.67	4.42	0.12	5.30	2.25	1.33	4.84	0.23	100.98
2	7 Aug 1980	63.16	17.71	0.65	4.34	0.13	5.28	2.17	1.31	4.88	0.24	99.87
7	7 Aug 1980	63.46	17.80	0.65	4.36	0.12	5.31	2.22	1.35	4.97	0.22	100.46
10	7 Aug 1980	63.14	17.83	0.68	4.43	0.12	5.20	2.23	1.34	4.98	0.22	100.17
11	7 Aug 1980	62.78	17.76	0.67	4.39	0.12	5.24	2.21	1.37	4.93	0.22	99.69
12	7 Aug 1980	62.63	17.78	0.65	4.29	0.12	5.26	2.19	1.37	4.96	0.22	99.47
8	17 Oct 1980	62.73	17.93	0.68	4.62	0.13	5.37	2.42	1.32	4.98	0.23	100.41
9	17 Oct 1980	62.07	17.89	0.71	4.58	0.14	5.50	2.42	1.26	4.99	0.23	99.79

Table 4. — Mount St. Helens Pyroclastic Flow Geochemistry
ICP Trace Element Data

Sample	Date	Ba	CR	CU	LA	NB	SC	SR	V	Y	ZN	ZR
33	18 May 1980	281	11	29	11	12	8	430	77	12	57	114
34	18 May 1980	296	11	32	11	11	9	451	81	13	58	120
14	12 Jun 1980	279	11	50	9	12	9	426	87	13	71	116
15	12 Jun 1980	273	6	34	9	9	9	427	80	12	54	114
17	12 Jun 1980	276	9	27	10	12	8	456	93	13	56	145
19	12 Jun 1980	277	11	34	9	11	9	441	92	13	57	119
22	12 Jun 1980	274	9	28	10	11	9	435	84	12	58	115
23	12 Jun 1980	272	9	37	9	11	9	432	83	12	57	113
26	12 Jun 1980	271	12	37	9	11	9	432	88	13	67	113
5	22 Jul 1980	269	12	37	9	11	9	448	92	13	58	112
6	22 Jul 1980	264	8	36	8	11	9	428	87	13	55	114
24	22 Jul 1980	278	12	38	10	11	9	432	90	13	69	113
25	22 Jul 1980	283	9	34	10	11	9	432	94	13	63	157
28	22 Jul 1980	271	9	36	9	12	9	423	90	13	60	119

Table 4. — Mount St. Helens Pyroclastic Flow Geochemistry
ICP Trace Element Data (Cont.)

Sample	Date	Ba	CR	CU	LA	NB	SC	SR	V	Y	ZN	ZR
31	22 Jul 1980	273	10	38	10	12	9	438	97	12	56	159
1	7 Aug 1980	271	9	41	9	11	9	442	96	13	58	129
2	7 Aug 1980	270	9	38	9	11	9	452	92	13	61	121
7	7 Aug 1980	295	12	38	10	11	10	451	99	13	67	126
10	7 Aug 1980	272	9	39	9	12	10	441	90	13	73	116
11	7 Aug 1980	277	16	39	9	11	10	447	89	13	70	116
12	7 Aug 1980	262	9	36	9	11	9	431	83	12	55	112
8	17 Oct 1980	259	23	47	9	11	10	429	92	13	67	111
9	17 Oct 1980	255	13	40	10	12	9	448	106	13	59	147

Major and Minor Oxides

	ICP Analysis for AGV-1	USGS Values for AGV-1
SiO_2	59.64 ± 0.27	59.61
Al_2O_3	17.26 ± 0.058	17.19
TiO_2	1.02 —	1.06
FeO (total)	5.83 —	6.59
MnO	0.13 ± 0.004	0.10
CaO	4.82 ± 0.06	4.94
MgO	1.53 ± 0.005	1.52
K_2O	3.02 ± 0.01	2.92
Na_2O	4.55 ± 0.04	4.32
P_2O_5	0.51 ± 0.01	0.51
	98.31	99.93

Trace Elements

	ICP	USGS
Ba	1165	1200
Cr	18	10
Cu	66	59
La	40	36
Nb	15	16
Sc	10	12.5
Sr	602	660.
V	123	125
Y	19	19
Zn	88	86
Zr	·254	230

Table 5 - Comparison of ICP analysis of USGS Standard AGV-1 with published USGS "Usable Values" (from Abbey, 1980).

A major purpose of this study is identification of trends in whole rock chemistry with time. Before analyzing for trends, all geochemical data were normalized to the average SiO_2 weight percent with the following computation:

$$NOXIDE = OXIDE \times \frac{SiO_2}{SiMEAN}$$

where NOXIDE = normalized oxide or trace element concentration, OXIDE = unnormalized oxide or trace element concentration, SiO_2 = weight percent SiO_2 determined for the sample, and SiMEAN = average weight percent SiO_2 for all samples. SiMEAN is equal to 63.344 percent. The normalized major and minor element oxide data are presented in Table 6 and the normalized trace element data in Table 7.

Trends were determined using standard linear regression techniques where a straight-line equation of the form $Y = Bo + B_1X$ was fit to a set of values. In this work, Y is the response variable, namely the oxide and trace element concentrations determined for the pyroclastic flows, X the regressor variable, or days after the May 18, 1980 eruption, and B_0 and B_1 the equation parameters of Y-intercept and slope, respectively.

The linear regression technique uses the method of least squares where the sum of squares of the differences between the actual response value and the value predicted by the equation is the criteria used to estimate the best values of the equation parameters B_0 and B_1. The best fit equation is defined as that line which minimizes the sum of the squares of differences. The "goodness of fit"

Table 6. — Mount St. Helens Pyroclastic Flow Geochemistry
Normalized ICP Major and Minor Oxide Data

Sample	Date	SIO_2	AL_2O_3	TIO_2	FEO	MNO	CAO	MGO	K_2O	NA_2O	P_2O_5	Total
33	18 May 1980	64.29	17.93	0.60	3.96	0.11	4.89	1.90	1.33	5.03	0.21	100.26
34	18 May 1980	63.91	17.62	0.60	3.96	0.11	5.01	1.88	1.33	5.02	0.22	99.66
14	12 Jun 1980	63.69	17.61	0.62	4.08	0.13	4.96	1.97	1.34	5.02	0.22	99.64
15	12 Jun 1980	63.28	17.75	0.62	4.08	0.12	5.06	1.98	1.41	5.00	0.22	99.52
17	12 Jun 1980	63.22	17.94	0.60	4.03	0.11	4.81	1.94	1.24	5.02	0.21	99.12
19	12 Jun 1980	63.99	17.49	0.65	4.29	0.12	5.04	2.01	1.39	4.84	0.21	100.03
22	12 Jun 1980	63.14	17.62	0.62	4.19	0.11	4.75	2.02	1.27	4.98	0.22	98.92
23	12 Jun 1980	63.47	17.59	0.61	4.17	0.12	5.03	2.09	1.36	4.89	0.23	99.57
26	12 Jun 1980	63.40	17.74	0.64	4.29	0.12	5.12	2.19	1.33	4.88	0.23	99.95
5	22 Jul 1980	63.27	17.66	0.66	4.34	0.14	5.28	2.22	1.31	4.95	0.22	100.06
6	22 Jul 1980	63.96	18.05	0.65	4.36	0.12	5.28	2.20	1.38	4.97	0.23	101.21
24	22 Jul 1980	64.22	18.11	0.65	4.46	0.12	5.14	2.16	1.37	5.15	0.22	101.60
25	22 Jul 1980	64.30	18.13	0.62	4.24	0.12	5.07	2.07	1.41	5.06	0.21	101.23
28	22 Jul 1980	61.66	17.58	0.65	4.38	0.14	5.31	2.36	1.26	4.79	0.21	98.34
31	22 Jul 1980	63.33	17.45	0.59	4.15	0.12	5.03	2.02	1.31	4.72	0.22	98.93

Table 6. — Mount St. Helens Pyroclastic Flow Geochemistry
Normalized ICP Major and Minor Oxide Data (Cont.)

Sample	Date	SIO_2	AL_2O_3	TIO_2	FEO	MNO	CAO	MGO	K_2O	NA_2O	P_2O_5	Total
1	7 Aug 1980	63.82	18.14	0.68	4.45	0.12	5.34	2.27	1.34	4.88	0.23	101.26
2	7 Aug 1980	63.16	17.66	0.65	4.33	0.13	5.26	2.16	1.31	4.87	0.24	99.76
7	7 Aug 1980	63.46	17.83	0.65	4.37	0.12	5.32	2.22	1.35	4.98	0.22	100.53
10	7 Aug 1980	63.14	17.77	0.68	4.42	0.12	5.18	2.22	1.34	4.96	0.22	100.05
11	7 Aug 1980	62.78	17.60	0.66	4.35	0.12	5.19	2.19	1.36	4.89	0.22	99.36
12	7 Aug 1980	62.63	17.58	0.64	4.24	0.12	5.20	2.17	1.35	4.90	0.22	99.05
8	17 Oct 1980	62.73	17.76	0.67	4.58	0.13	5.32	2.40	1.31	4.93	0.23	100.04
9	17 Oct 1980	62.07	17.53	0.70	4.49	0.14	5.39	2.37	1.23	4.89	0.23	99.03

Table 7. — Mount St. Helens Pyroclastic Flow Geochemistry
Normalized ICP Trace Element Data

Sample	Date	BA	CR	CU	LA	NB	SC	SR	V	Y	ZN	ZR
33	18 May 1980	285	11	29	11	12	8	436	78	12	58	116
34	18 May 1980	299	11	32	11	11	9	455	82	13	59	121
14	12 Jun 1980	281	11	50	9	12	9	428	87	13	71	117
15	12 Jun 1980	273	6	34	9	9	9	427	80	12	54	114
17	12 Jun 1980	275	9	27	10	12	8	455	93	13	56	145
19	12 Jun 1980	280	11	34	9	11	9	445	93	13	58	120
22	12 Jun 1980	273	9	28	10	11	9	434	84	12	58	115
23	12 Jun 1980	273	9	37	9	11	9	433	83	12	57	113
26	12 Jun 1980	271	12	37	9	11	9	432	88	13	67	113
5	22 Jul 1980	269	12	37	9	11	9	447	92	13	58	112
6	22 Jul 1980	267	8	36	8	11	9	432	88	13	56	115
24	22 Jul 1980	282	12	39	10	11	9	438	91	13	70	115
25	22 Jul 1980	287	9	35	10	11	9	439	95	13	64	159
28	22 Jul 1980	264	9	35	9	12	9	412	88	13	58	116
31	22 Jul 1980	273	10	38	10	12	9	438	97	12	56	159

Table 7. — Mount St. Helens Pyroclastic Flow Geochemistry
Normalized ICP Trace Element Data (Cont.)

Sample	Date	BA	CR	CU	LA	NB	SC	SR	V	Y	ZN	ZR
1	7 Aug 1980	273	9	41	9	11	9	445	97	13	58	130
2	7 Aug 1980	269	9	38	9	11	9	451	92	13	61	121
7	7 Aug 1980	296	12	38	10	11	10	452	99	13	67	126
10	7 Aug 1980	271	9	39	9	12	10	440	90	13	73	116
11	7 Aug 1980	275	16	39	9	11	10	443	88	13	69	115
12	7 Aug 1980	259	9	36	9	11	9	426	82	12	54	111
8	17 Oct 1980	256	23	47	9	11	10	425	91	13	66	110
9	17 Oct 1980	250	13	39	10	12	9	439	104	13	68	144

for the estimated equation may be conveniently described by the
sample regression coefficient, R. Computational formulas for R are
given in most standard statistics texts, i.e., Huntsberger and
Billingsley (1973). For any linear regression, R has a value between
-1 and +1. When response variable values are close to the best-fit
line, R will be close to /1/. As scatter of the points becomes
greater, R. will approach zero. For this reason, R is a useful
measure of the strength of the relationship between the best-fit line
and the response data.

It is always wise to place confidence limits on the calculated
estimate of R. If the confidence interval about the estimate of R
includes zero, R is not significant at the given level of signifi-
cance. Krumbien and Graybill (1965) provide a convenient nomogram
where a confidence belt for R at a 95 percent confidence interval can
be determined for n = 3 to 400.

A linear regression of oxide or trace element concentration ver-
sus days after the May 18, 1980 eruption was computed for each of the
oxides and trace elements measured. Results of the regressions are
tabulated in Table 8. The best-fit equation is also plotted on
scatter plots in Figures 17 to 37. In addition, oxide or trace ele-
ment means for each eruption are shown on the scatter plots to faci-
litate subjective evaluation of chemical variation between eruption
dates.

A plot of the average total alkali against silica for the 1980
pyroclastic flow pumice shows that these rocks are very near the
lower boundary of average dacitic rocks for the Cascade Range

Table 8. — Results of Simple Linear Regression Oxide/Element
Concentrations vs. Days after 18 May 1980 Eruption

S = Significant   N - Not Significant   M = Marginal

Oxide/ Element	Bo (Y-intercept)	B_1 (Slope)	Sample Regression Coefficient R	Confidence Belt at 95% Confidence Interval	Sig.
SiO_2	63.86%	-0.0088	-0.525	-0.775 to -0.075	S
TiO_2	0.61%	0.0006	0.761	-0.900 to -0.450	S
CaO	4.93%	0.0034	0.773	-0.950 to -0.500	S
K_2O	1.35%	0.0003	0.240	-0.200 to 0.600	N
P_2O_5	0.217%	0.0001	0.424	0.000 to 0.725	M
Na_2O	4.98%	-0.0006	-0.250	0.225 to -0.600	N
MnO	0.114%	0.0001	0.599	0.800 to 0.250	S
FeO	4.06%	0.0035	0.835	0.925 to 0.600	S
MgO	1.95%	0.0031	0.848	0.950 to 0.650	S
Al_2O_3	17.75%	-0.00001	-0.003	0.400 to -0.425	N
BA	284.5	-0.179	-0.625	-0.825 to -0.200	S
CR	8.3	0.044	0.527	0.125 to 0.775	S
CU	32.6	0.070	0.537	0.150 to 0.775	S
LA	9.8	-0.274	-0.005	-0.400 to 0.400	N
NB	11.2	-0.115	0.002	-0.400 to 0.400	N
SC	8.7	0.555	0.007	-0.400 to 0.400	N
SR	439.7	-0.116	-0.306	-0.625 to 0.125	N
V	83.7	0.100	0.628	0.275 to 0.825	S
Y	12.6	0.334	0.004	-0.400 to 0.400	N
ZN	59.5	0.196	0.029	-0.425 to 0.375	N
ZR	119.6	0.147	0.054	-0.325 to 0.450	N

(Figure 16). The plot also shows that a trend toward a more andesitic composition would be indicated by a depletion of both total alkali and silica.

Silica and the alkalis, Na_2O and K_2O, for the 1980 pumice are shown on separate diagrams (Figures 17-19). And, although a subjective analysis of the mean values might lead one to interpret the alkali diagrams as showing a slight depletion, the regression coefficients indicate no apparent trend exists. Silica, on the other hand, shows a significant depletion trend.

Major element oxides showing an increase in overall abundance with time are Fe (total), CaO, and MgO (see Figures 20, 21, and 22). The minor element oxides TiO_2 and MnO also show an increase in abundance (see Figures 23, 24, and 25). The apparent increase in P_2O_5 is questionable. Alumina is the only other major constituent besides the alkalais that does not show a definite trend toward either enrichment or depletion (see Figure 26).

Regression coefficients for TiO_2, FeO (total), CaO, MgO, MnO, and SiO_2 are high enough to be significant. The relationship for Na_2O, K_2O, and Al_2O_3 is weak, and P_2O_5 questionable.

The above data are in agreement with those of Lipman et al. (1981), Melson et al. (1980a), and Melson et al. (1981), indicating that a trend toward a more andesitic composition is occurring in the pyroclastic flow pumice. If the amount of change in composition is considered, it is noted that CaO, FeO, TiO_2, and MgO are increasing in abundance at a rate that is an order of magnitude greater than the rate of decrease in the alkalis, i.e., CaO increases an average of
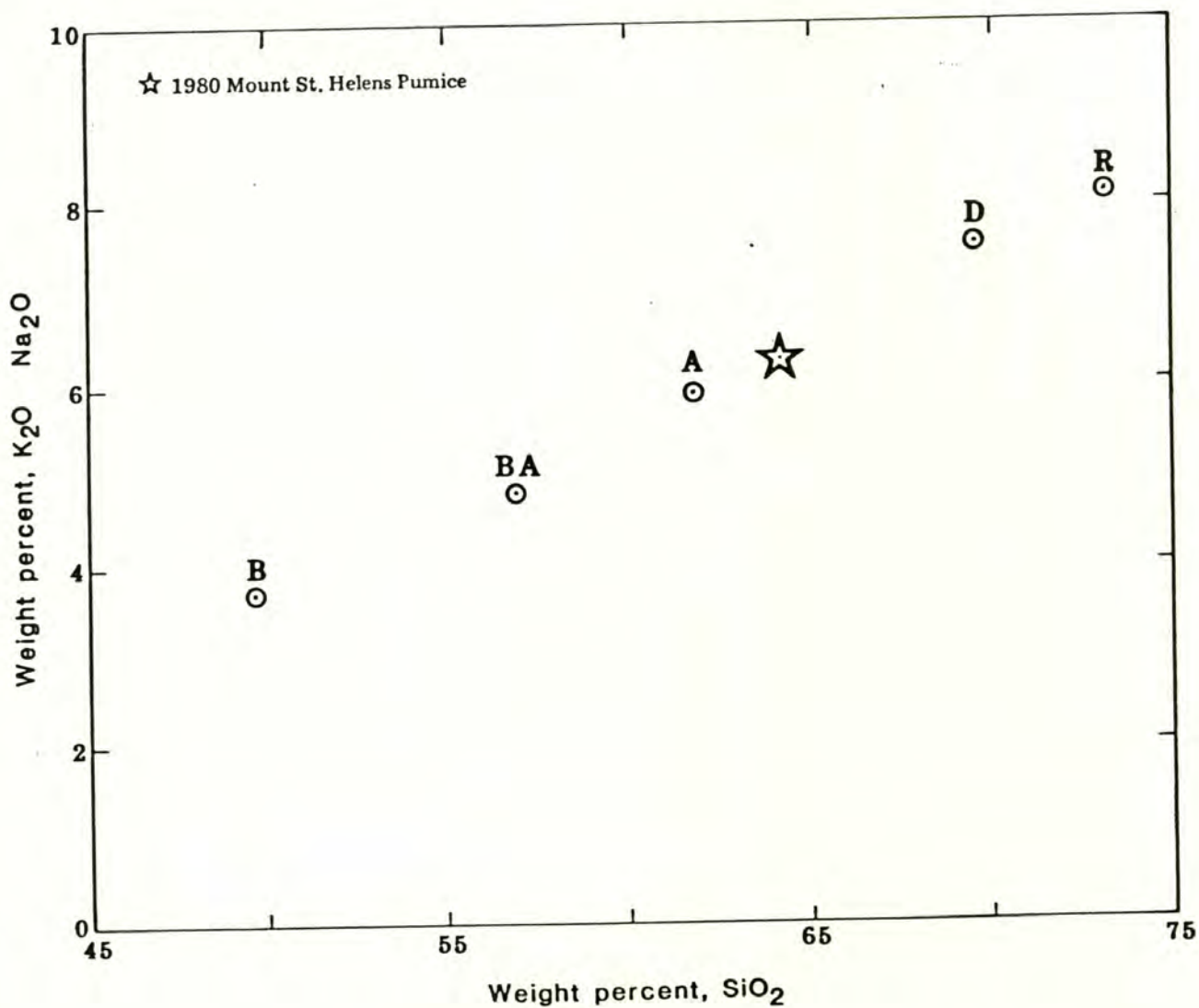
Figure 16. Plot of total alkali against silica; B, BA, A, D, and R refer to the average basalt, basaltic andesite, andesite, dacite and rhyolite of the North American Cascades. The average value for the 1980 Mount St. Helens pumice is shown by the star.
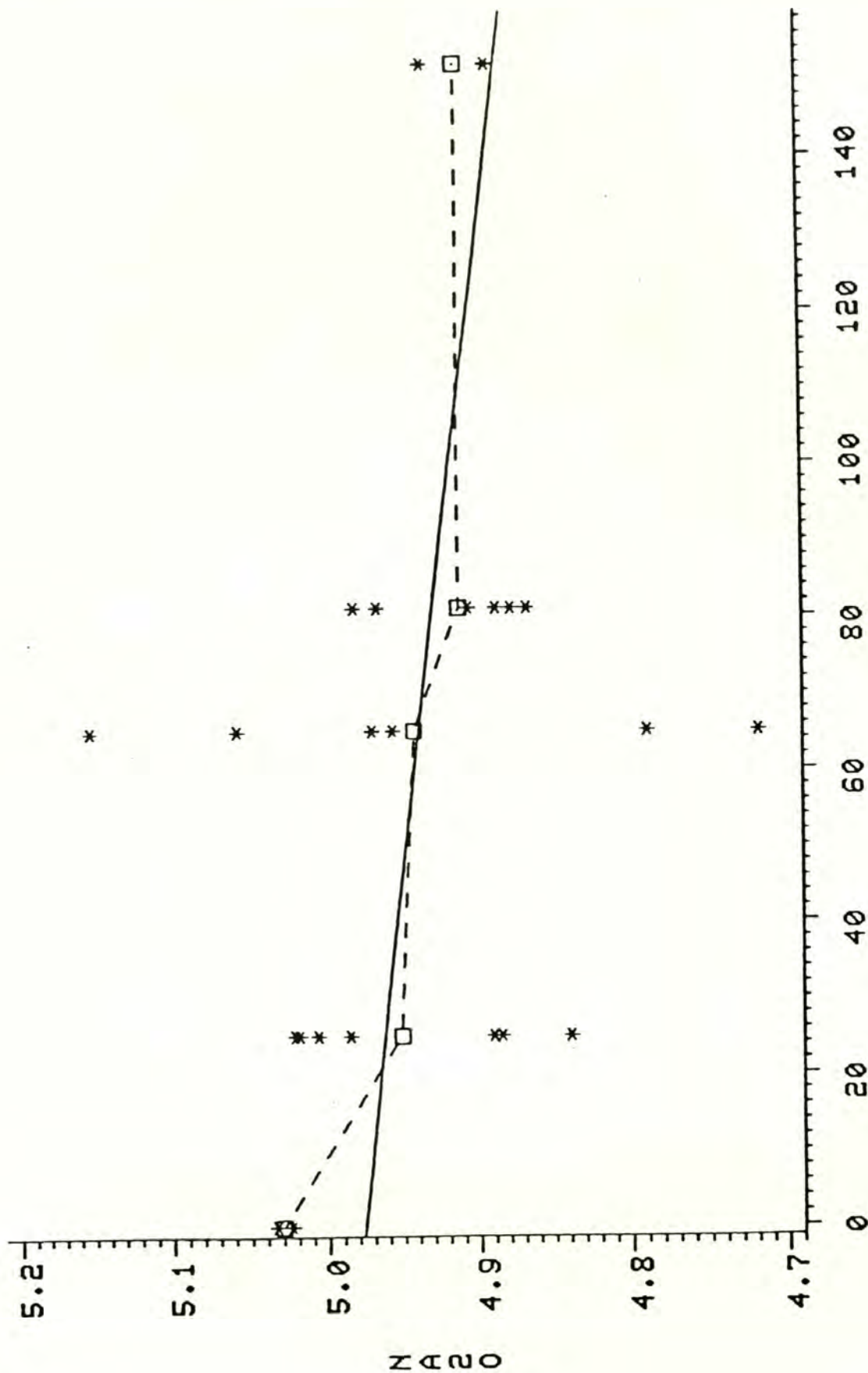
Figure 17. Na$_2$O versus time after May 18 eruption. Analyses shown by stars, means of analyses shown by boxes; dashed line connects means, solid line is linear regression. See Table 8 for R values.
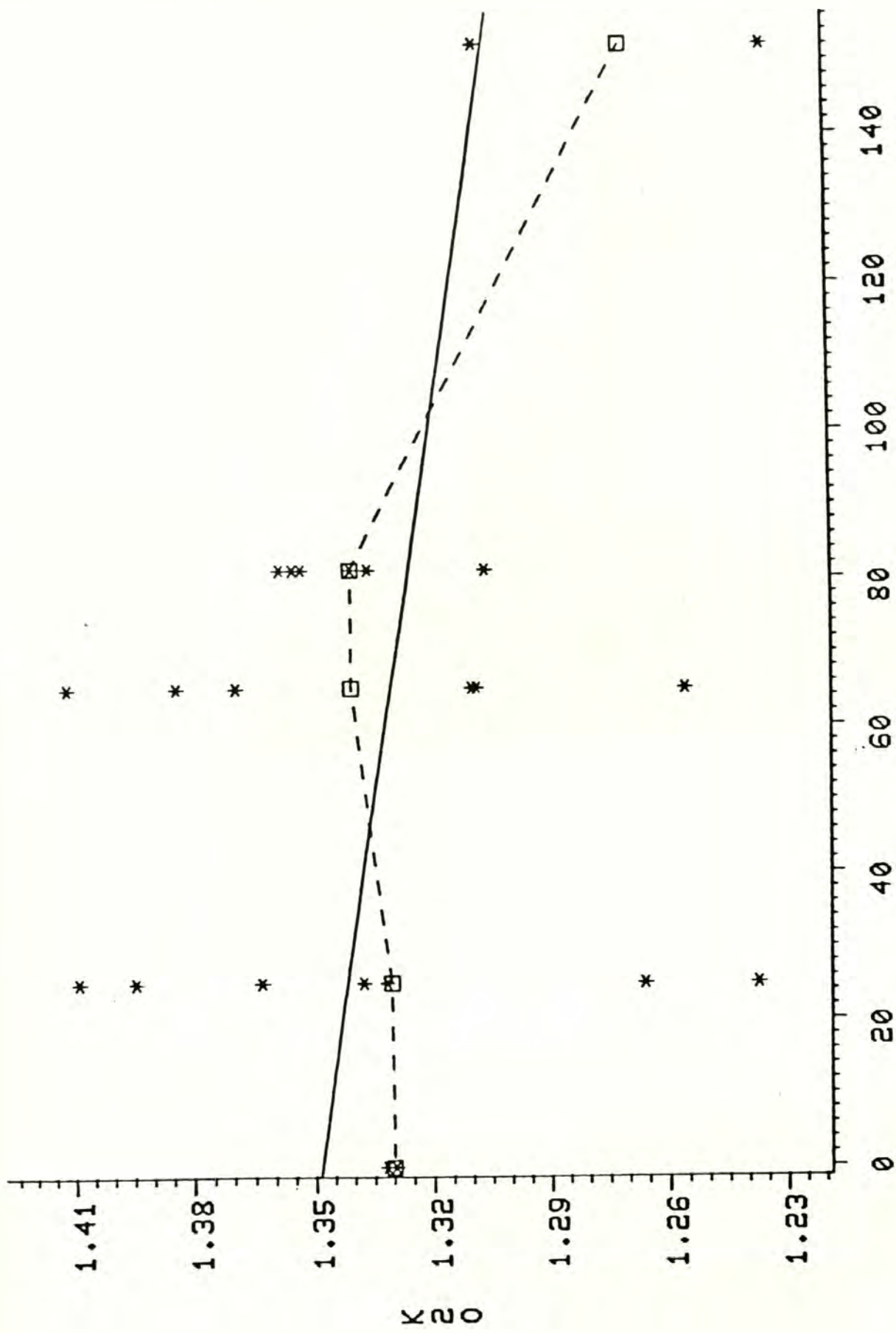
Figure 18. K$_2$O versus time after May 18 eruption. Analyses shown by stars, means of analyses shown by boxes; dashed line connects means, solid line is linear regression. See Table 8 for R values.
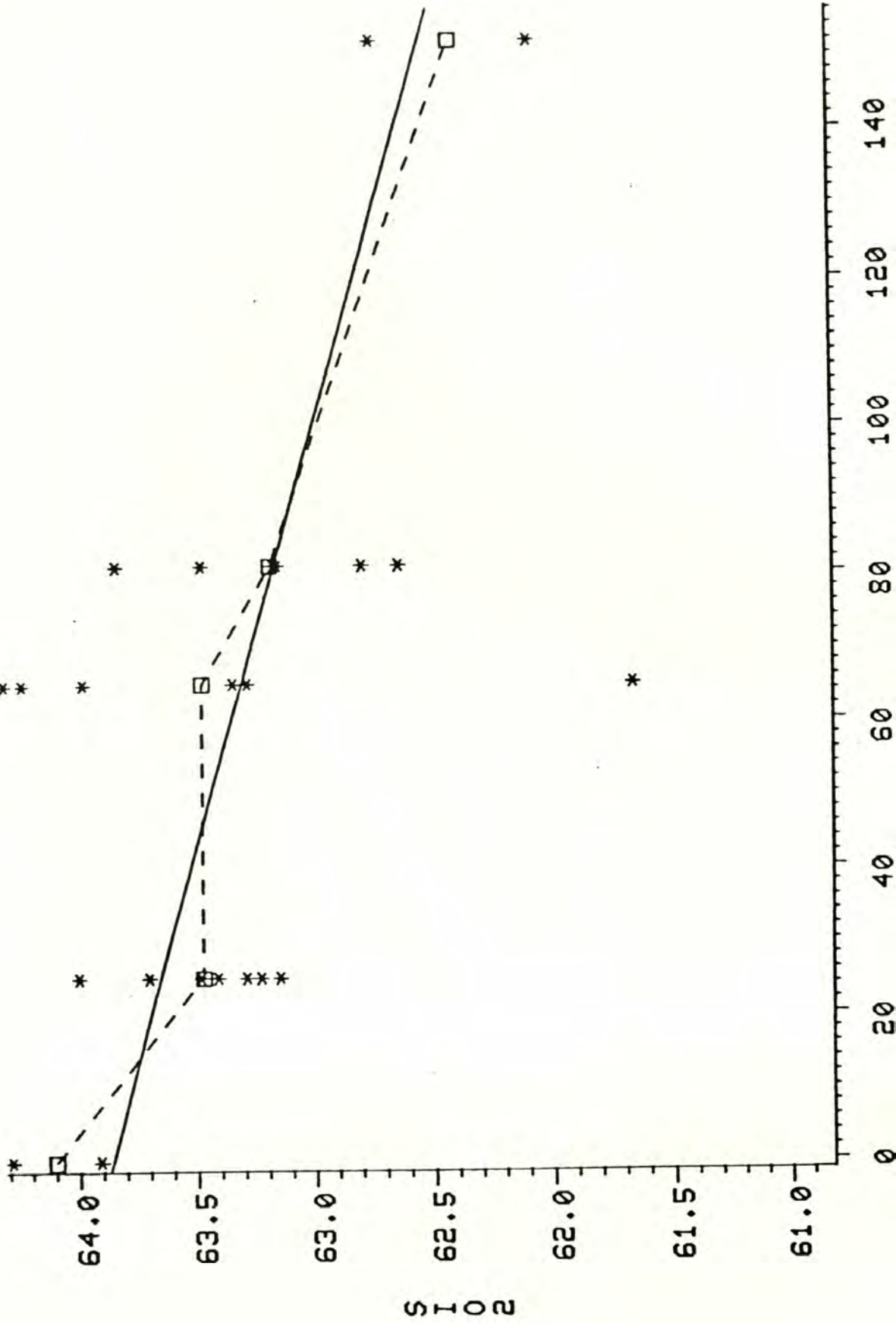
Figure 19. SiO_2 versus time after May 18 eruption. Analyses shown by stars, means of analyses shown by boxes; dashed line connects means, solid line is linear regression. See Table 8 for R values.
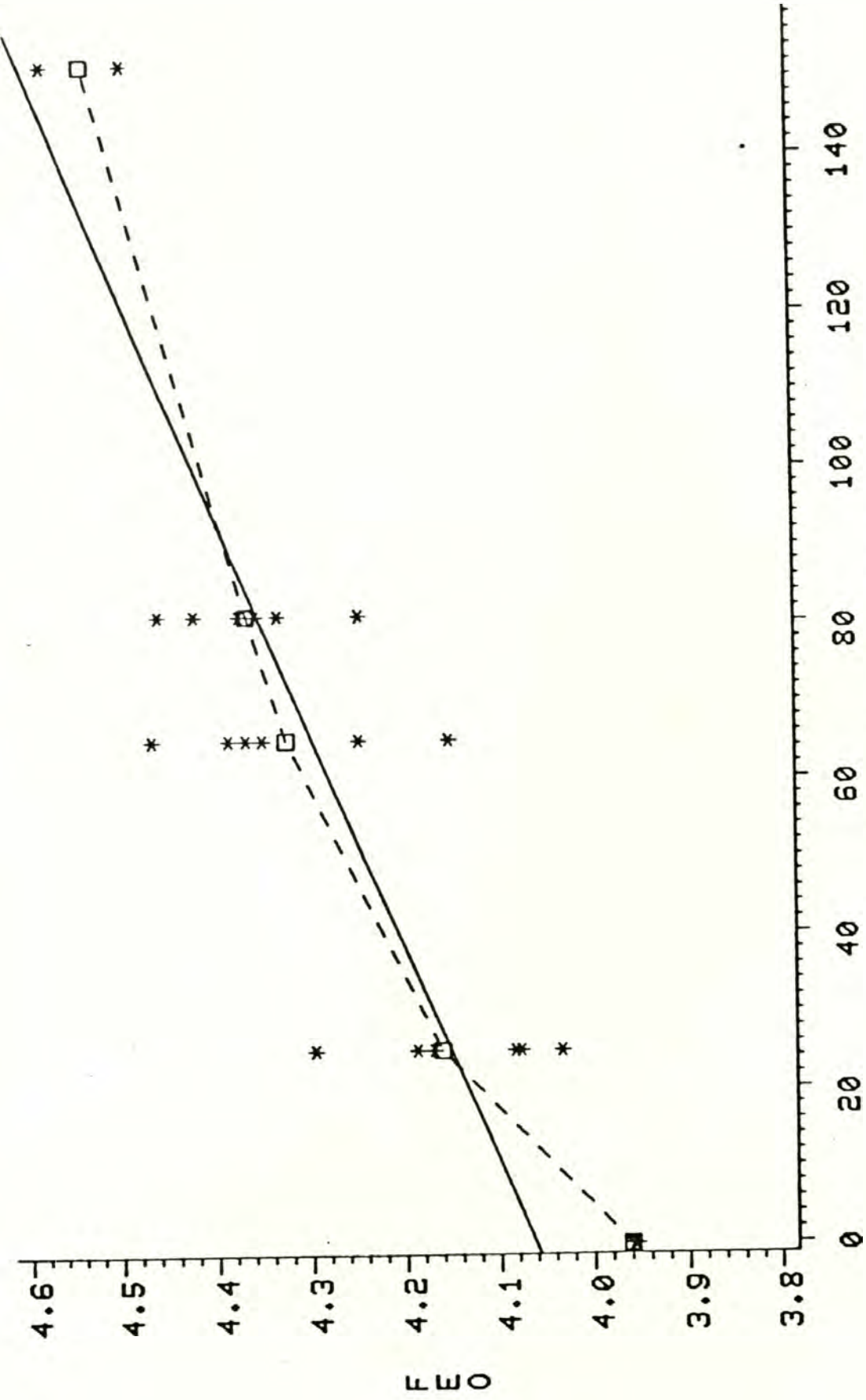
Figure 20. FeO (total) versus time after May 18 eruption. Analyses shown by stars, means of analyses shown by boxes; dashed line connects means, solid line is linear regression. See Table 8 for R values.
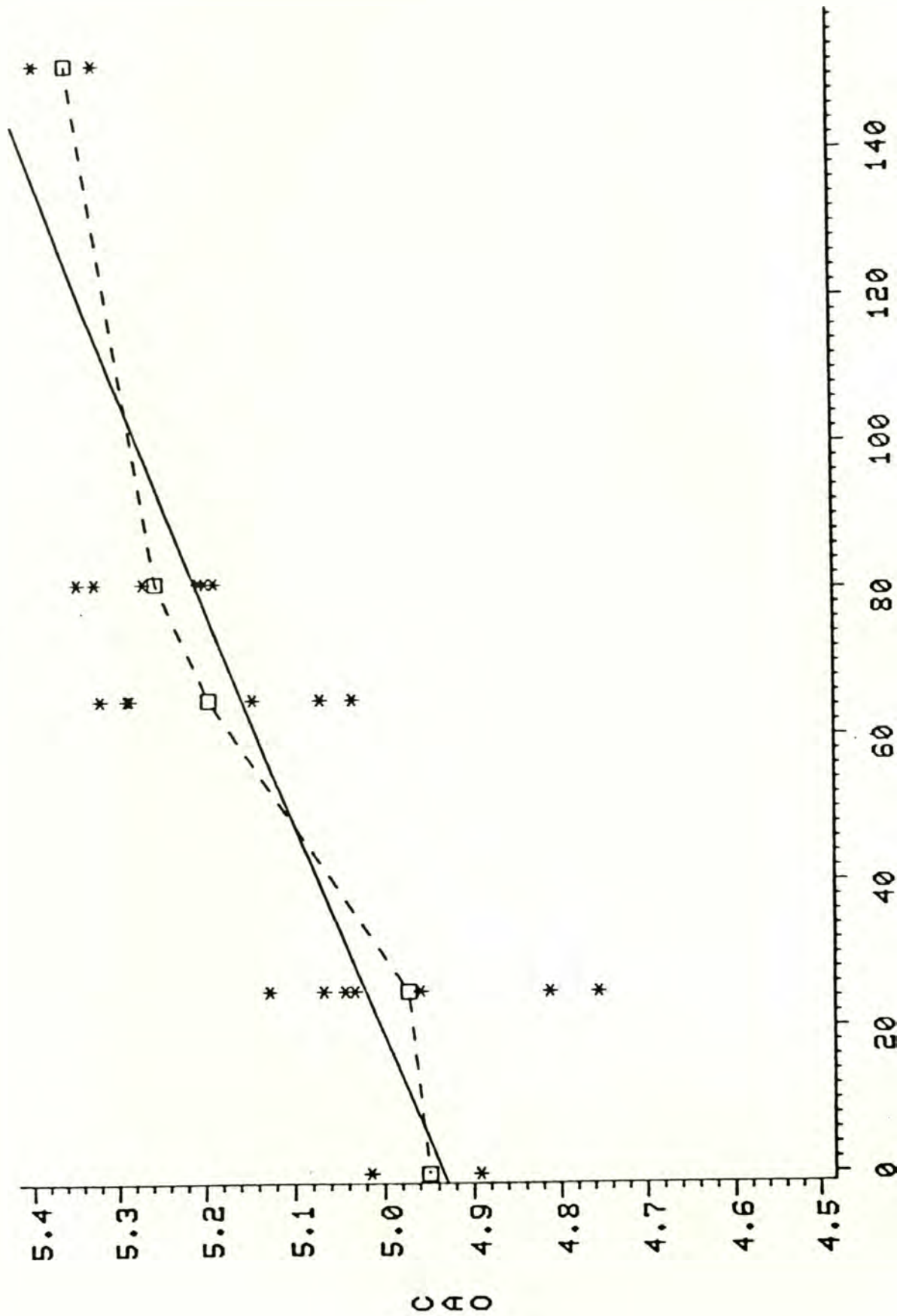
Figure 21. CaO versus time after May 18 eruption. Analyses shown by stars, means of analyses shown by boxes; dashed line connects means, solid line is linear regression. See Table 8 for R values.

Figure 22. MgO versus time after May 18 eruption. Analyses shown by stars, means of analyses shown by boxes; dashed line connects means, solid line is linear regression. See Table 8 for R values.

Figure 23. TiO₂ versus time after May 18 eruption. Analyses shown by stars, means of analyses shown by boxes; dashed line connects means, solid line is linear regression. See Table 8 for R values.

Figure 24. MnO versus time after May 18 eruption. Analyses shown by stars, means of analyses shown by boxes; dashed line connects means, solid line is linear regression. See Table 8 for R values.

Figure 25. P_2O_5 versus time after May 18 eruption. Analyses shown by stars, means of analyses shown by boxes; dashed line connects means, solid line is linear regression. See Table 8 for R values.

Figure 26. Al_2O_3 versus time after May 18 eruption. Analyses shown by stars, means of analyses shown by boxes; dashed line connects means, solid line is linear regression. See Table 8 for R values.

9 percent, TiO_2 15 percent, and MgO 23 percent, while Na_2O decreases an apparent 1.6 percent and K_2O 3.4 percent.

Scheidegger et al. (1982), using electron microprobe of selected mineral phases from May 25, June 12, July 22, and October 16-18 pumices, report that plagioclase rims are less calcic with time. But, if the bulk chemistry is becoming significantly more calcic, then reverse zoning in plagioclase should be expected. It is difficult to explain this inconsistency, but it may be the result of one or a combination of any of the following possibilities.

The average relative abundances of Na_2O and CaO change by only 4.6 percent between May 18 and October 16-18. This change may not be enough to result in strong reverse zoning in plagioclase. Furthermore, the excess CaO could be entering the augite lattice. Based on petrographic evidence, augite is the only likely phase that might accept CaO since hornblende is not an equilibrium phase. If the trend in CaO enrichment continues in the future, augite may become an increasingly abundant phase.

The increase in FeO (total) may be partially accomodated by augite, hypersthene and hornblende. Although the modal abundance of magnetite was not determined, FeO could be partitioned into this phase, which may increase in modal abundance with time. On the other hand, through continual degassing of the magma chamber, lower PH_2O should cause less of the Fe to crystallize out as magnetite, leaving hypersthene and hornblende as preferential sites for its accomodation. A review of the data presented by Scheidegger et al. (1982) shows a slight depletion of both FeO and MgO in magnetite, a

depletion of FeO in glass, and an enrichment of MnO in glass with time. The increase in MgO will be accomodated by hypersthene as well.

Trends in trace element abundances are not as apparent as those for the major and minor elements. However, Cr, Cu, Sc, and V (Figures 27-30) show slight enrichment with time, while Ba (Figure 31) shows a depletion with time. Regression coefficients for copper and vanadium are good, but are weak for chromium, barium, and scandium. La, Nb, Sr, Y, Zn, and Zr (Figures 32-37) show no apparent trends with time, based either on the low slope of their graphs or the wide scatter of data points.

The enrichment trends of Cr, Cu, Sc, and V as well as the depletion trend in Ba can be explained as normal trends toward a more andesitic magma composition. Taylor and White (1965 and 1966) have presented data on major, minor, and trace element average abundances for andesite, basalt, granite, and continental crust. Mount St. Helens pumice is depleted in V, Cr, Cu, Y and Sc relative to the average andesite. The trend toward more andesitic composition must, therefore, be toward enrichment in these elements. Barium, in the Mount St. Helens pumice, is slightly more abundant than in the average andesite values, and conversely becomes more depleted during the trend toward andesitic composition.

On the other hand, additional analysis of pumice and dome rock may show that the trends are not real but only exist because of the small number of samples analyzed in this study. However, because the trends in major and minor elements in this study corroborate data in
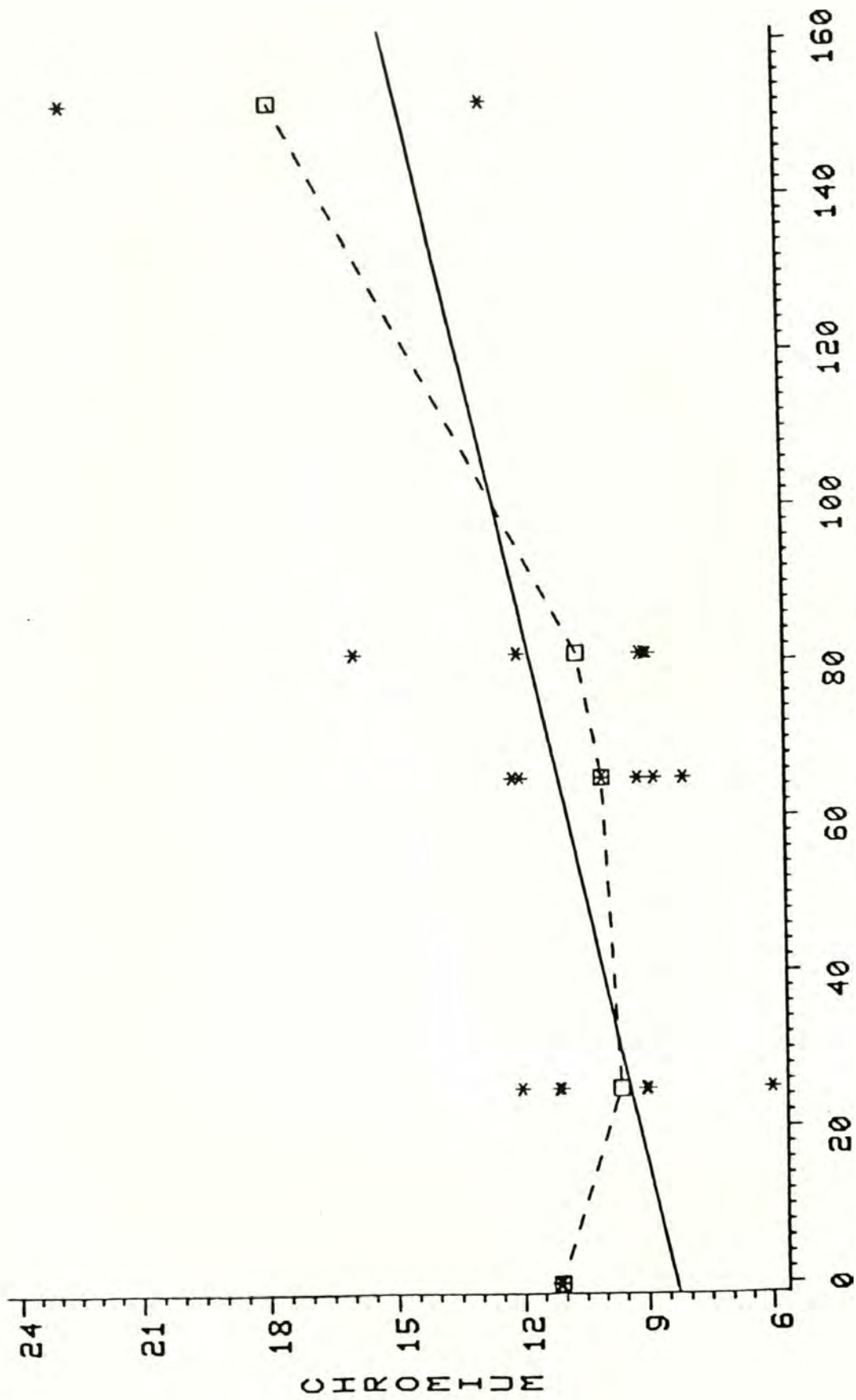
Figure 27. Cr versus time after May 18 eruption. Analyses shown by stars, means of analyses shown by boxes; dashed line connects means, solid line is linear regression. See Table 8 for R values.
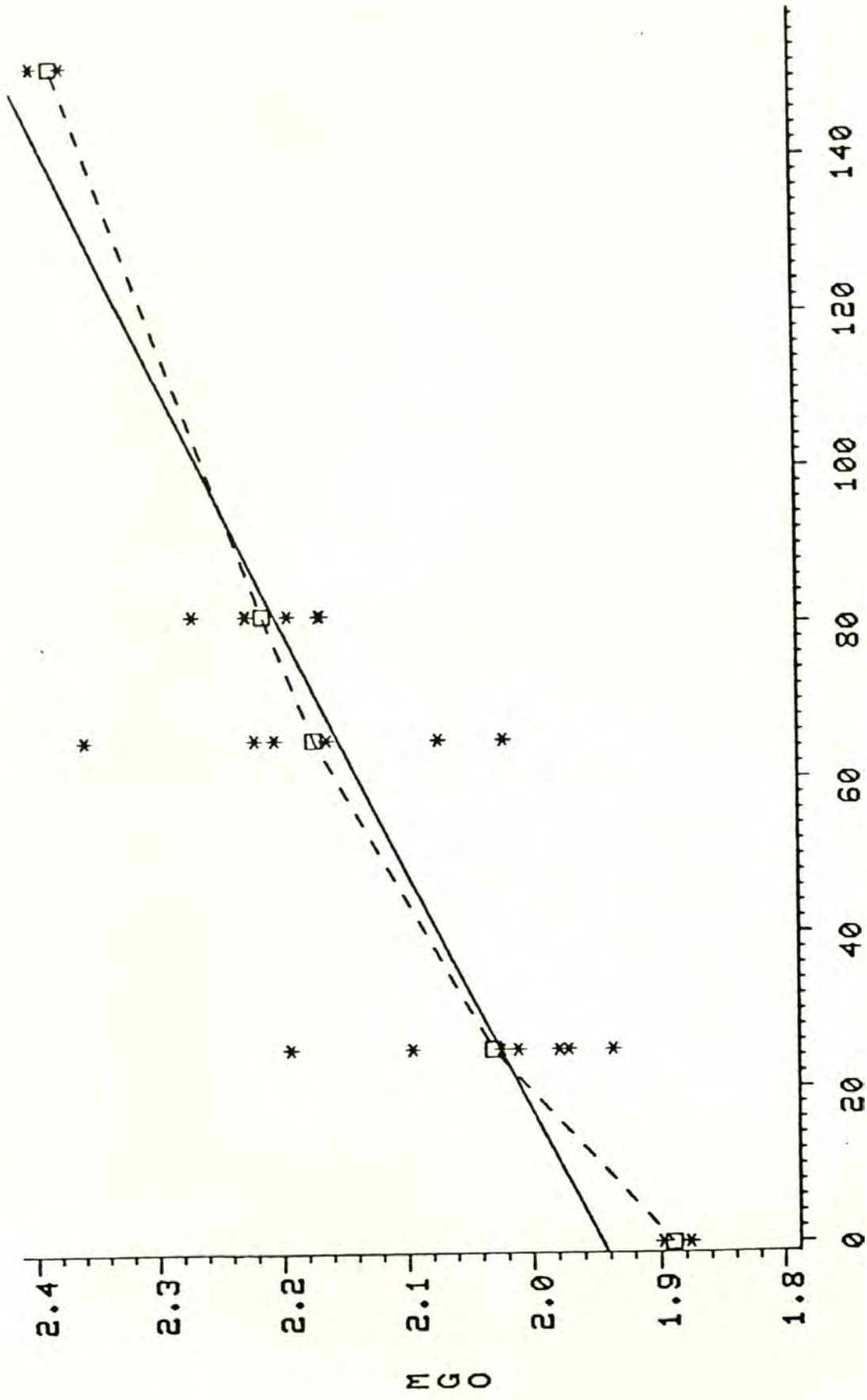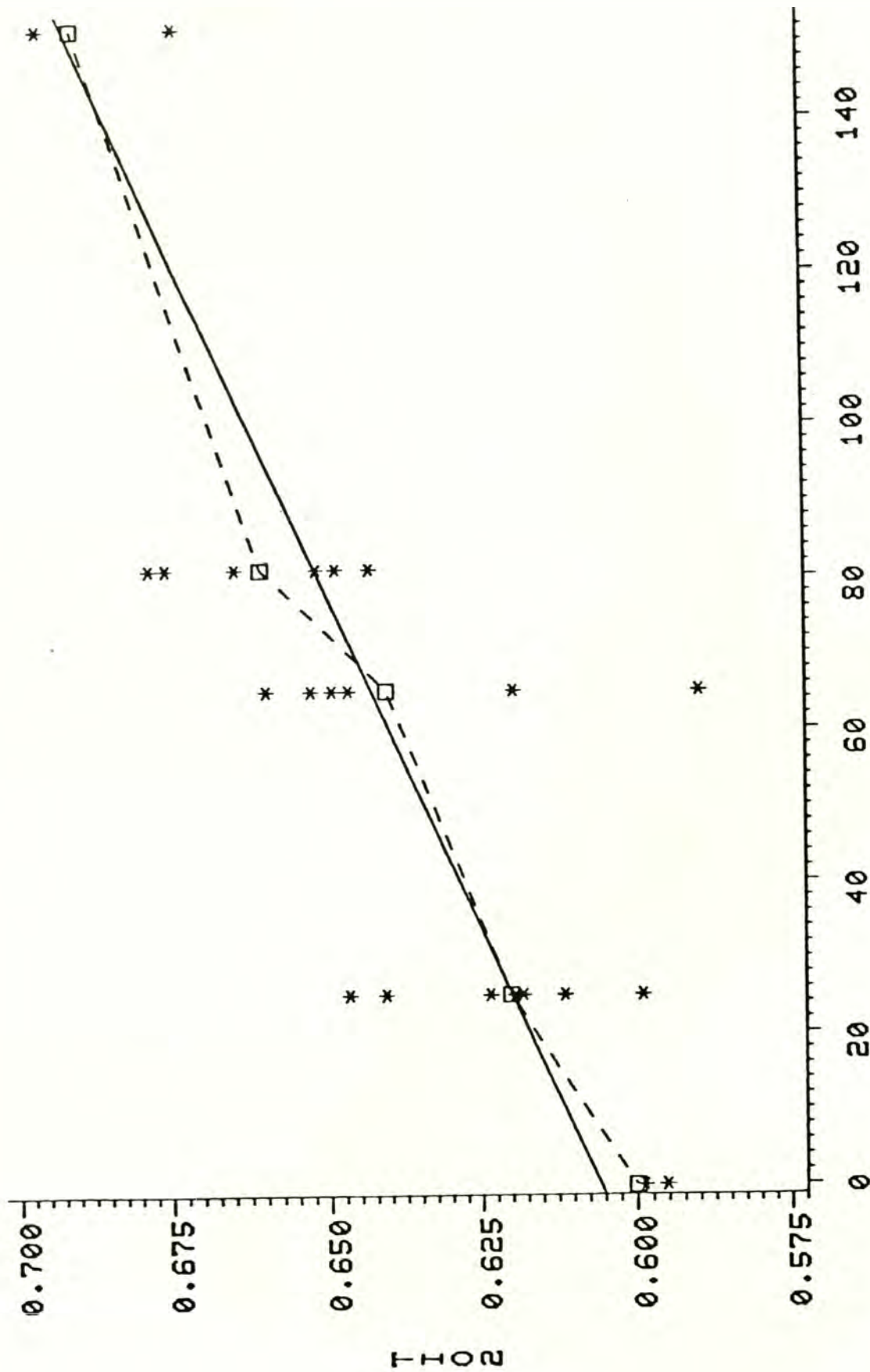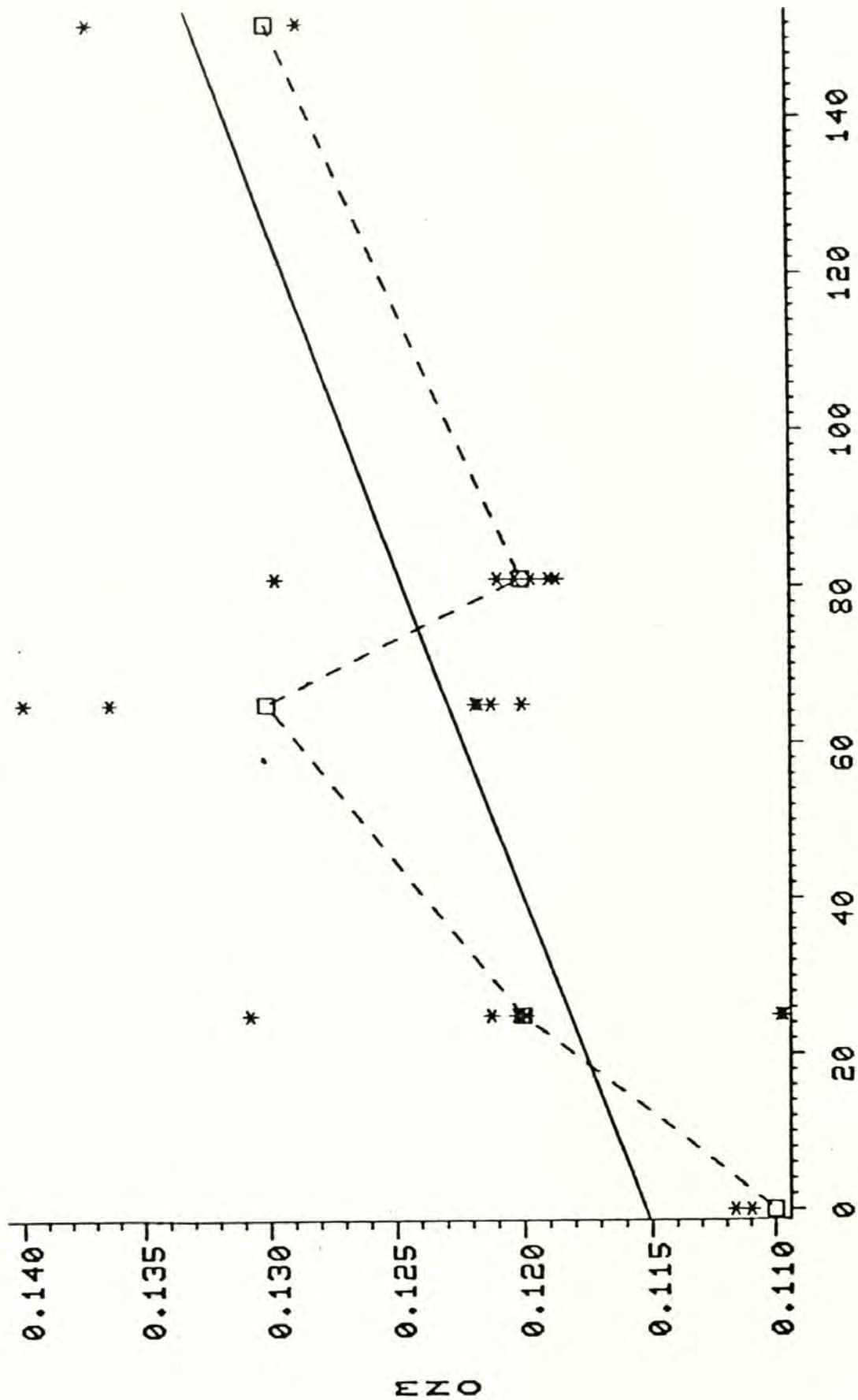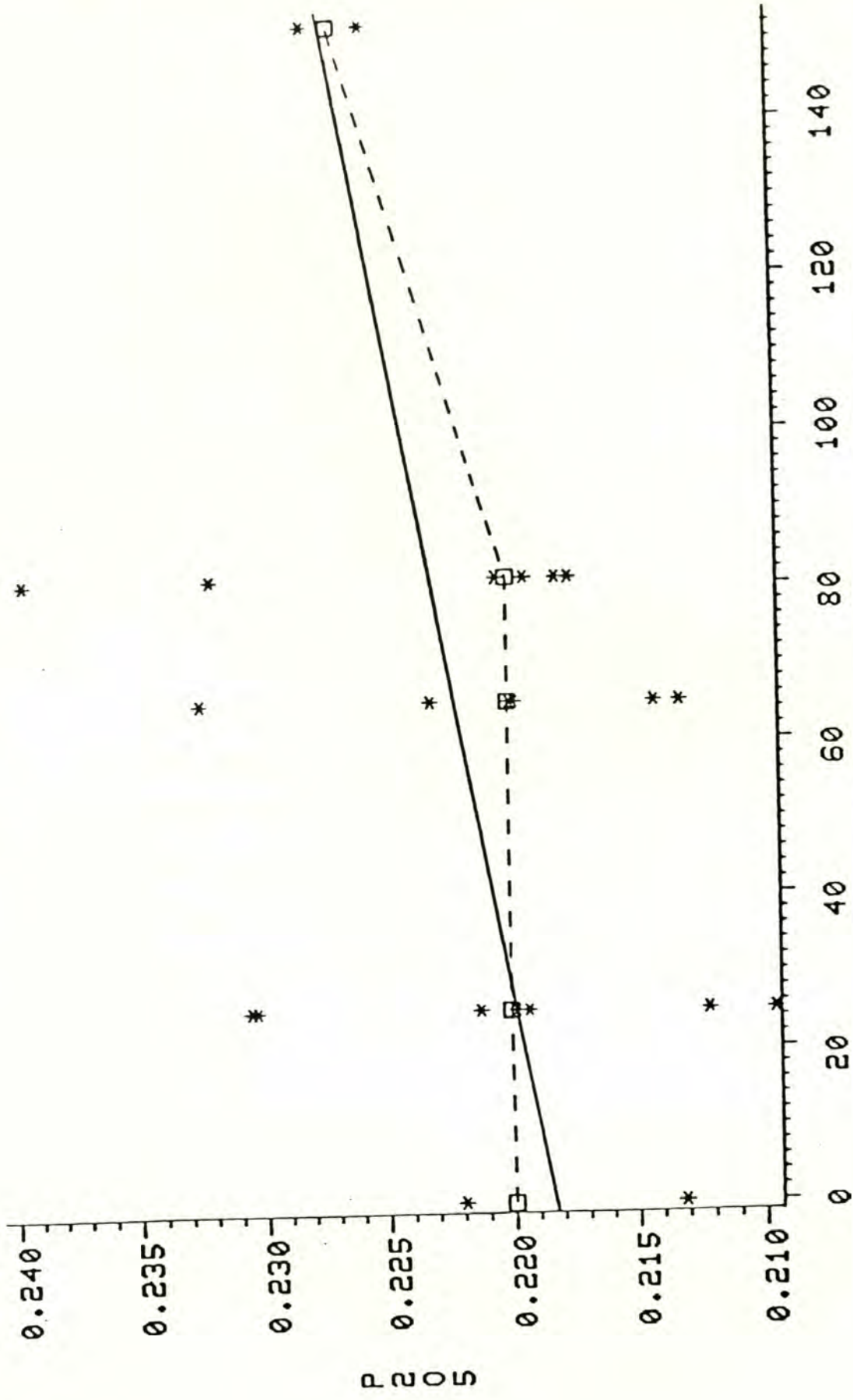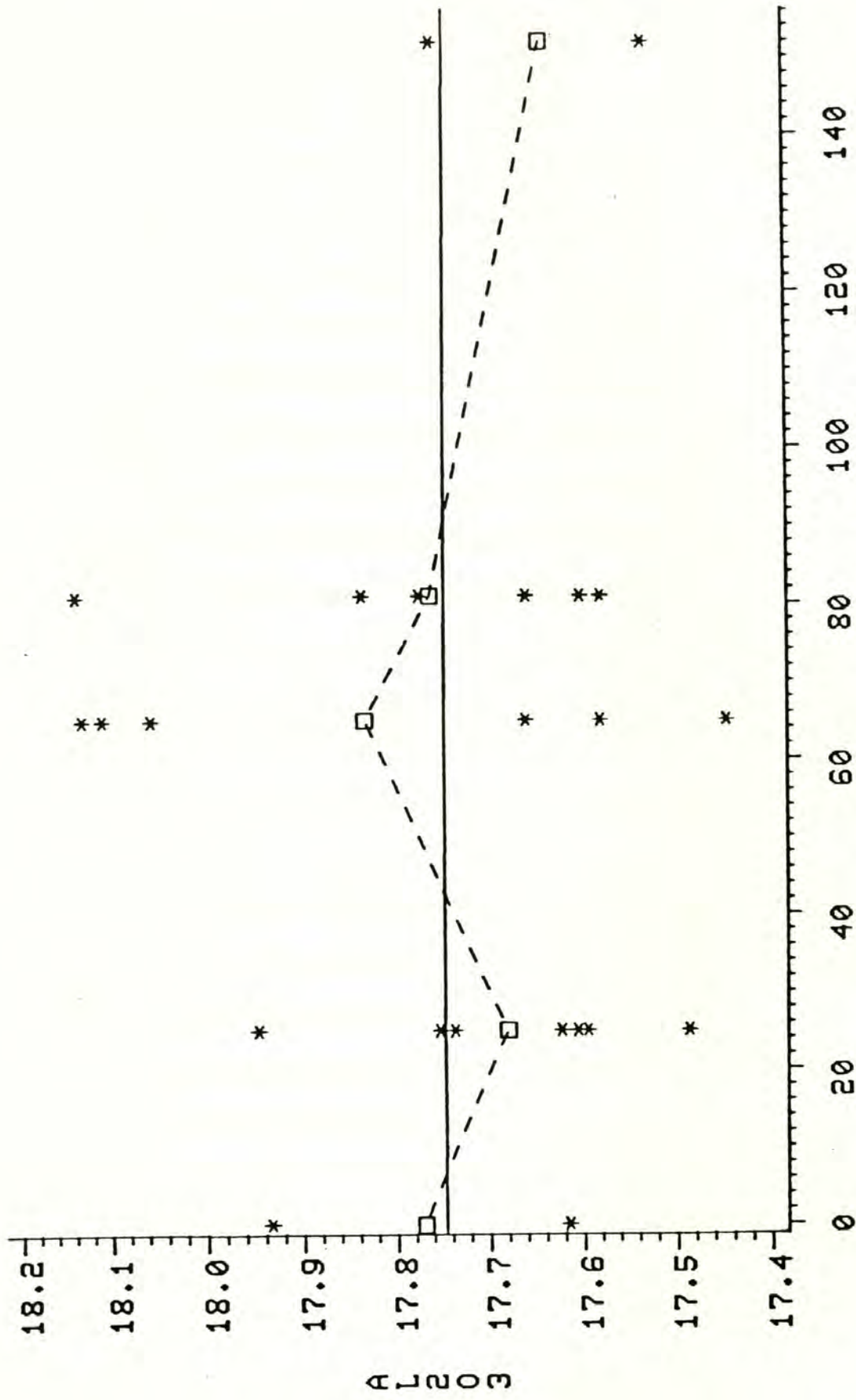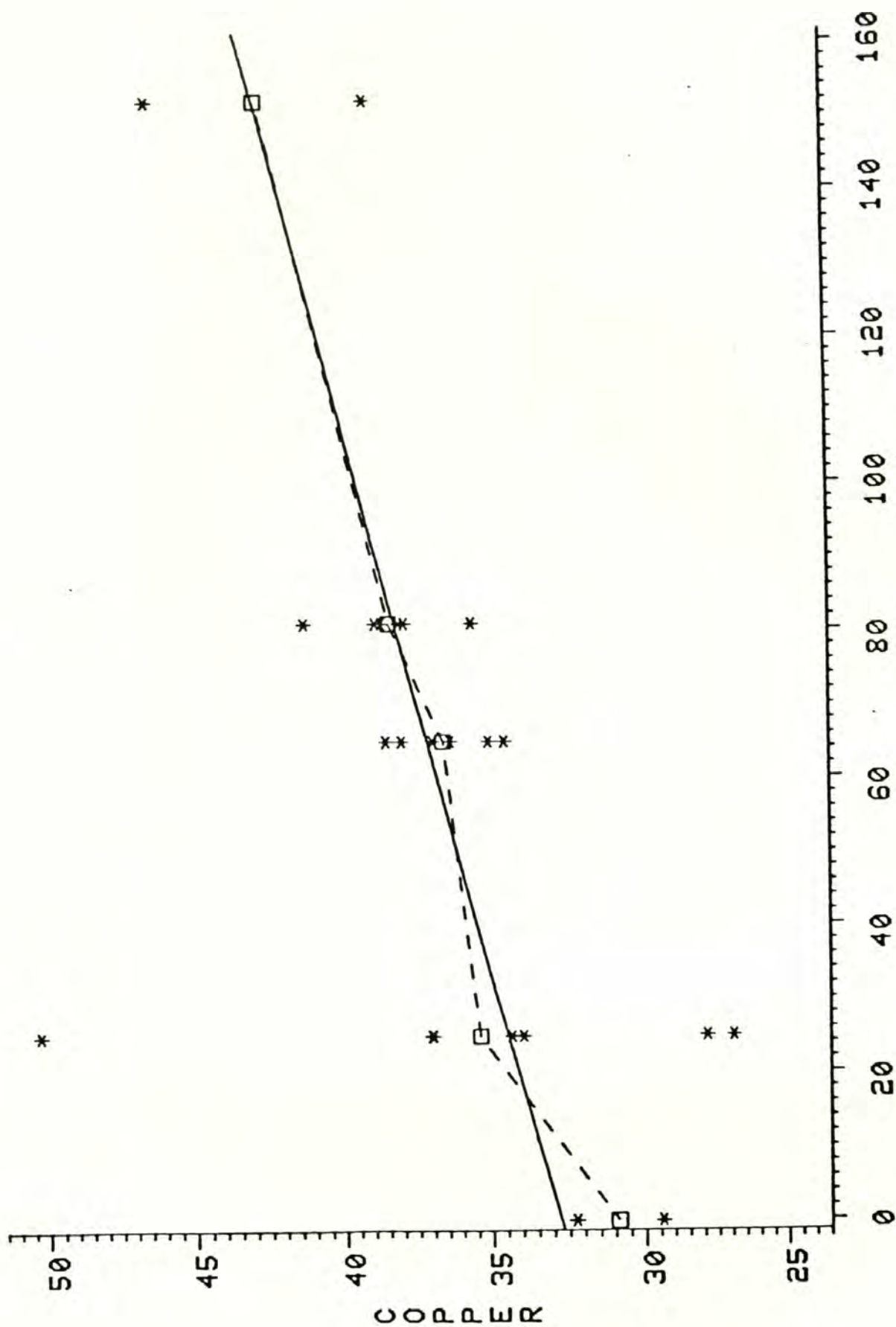
Figure 28. Cu versus time after May 18 eruption. Analyses shown by stars, means of analyses shown by boxes; dashed line connects means, solid line is linear regression. See Table 8 for R values.
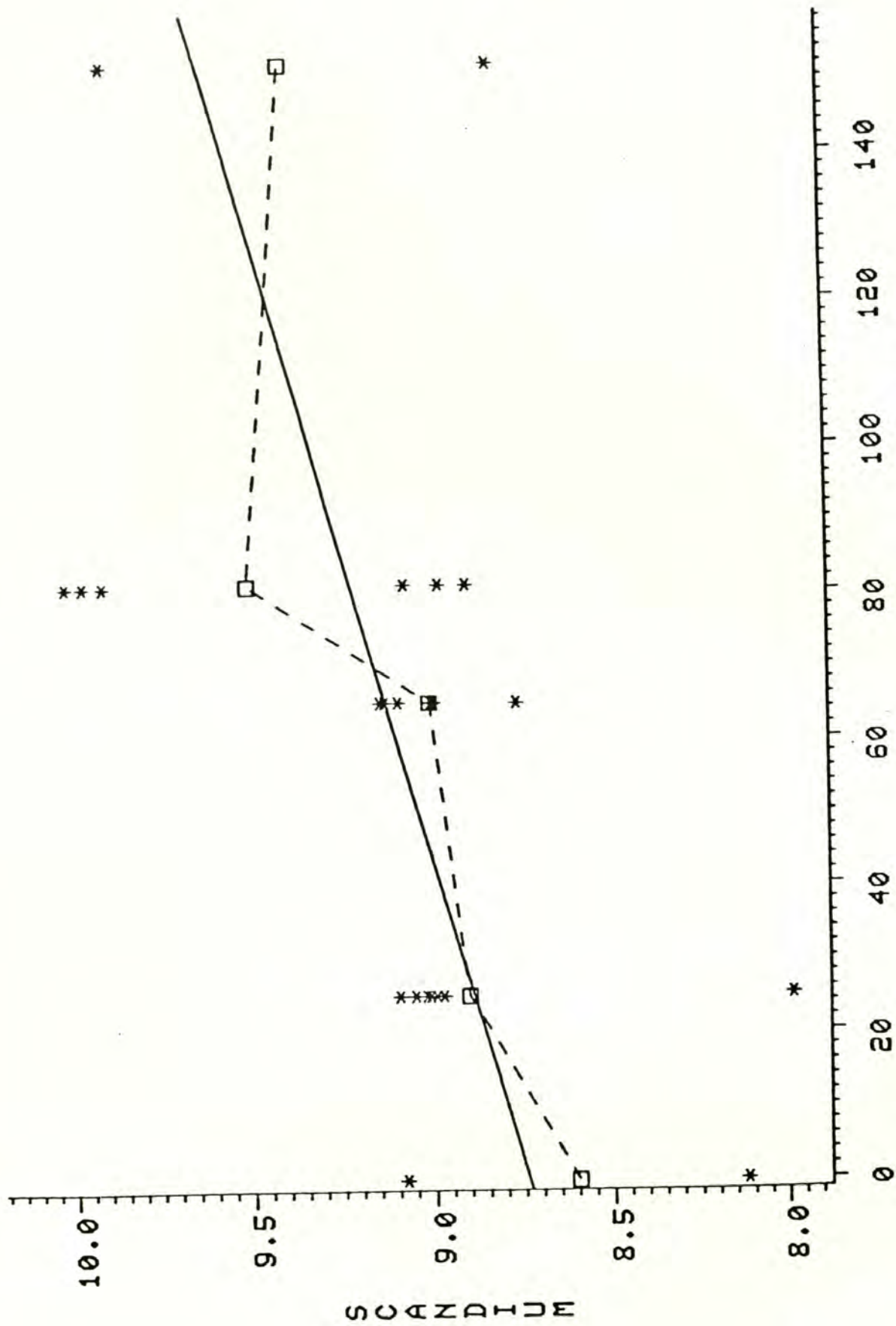
DAYS AFTER 18 MAY 1980 ERUPTION

Figure 29. Sc versus time after May 18 eruption. Analyses shown by stars, means of analyses shown by boxes; dashed line connects means, solid line is linear regression. See Table 8 for R values.
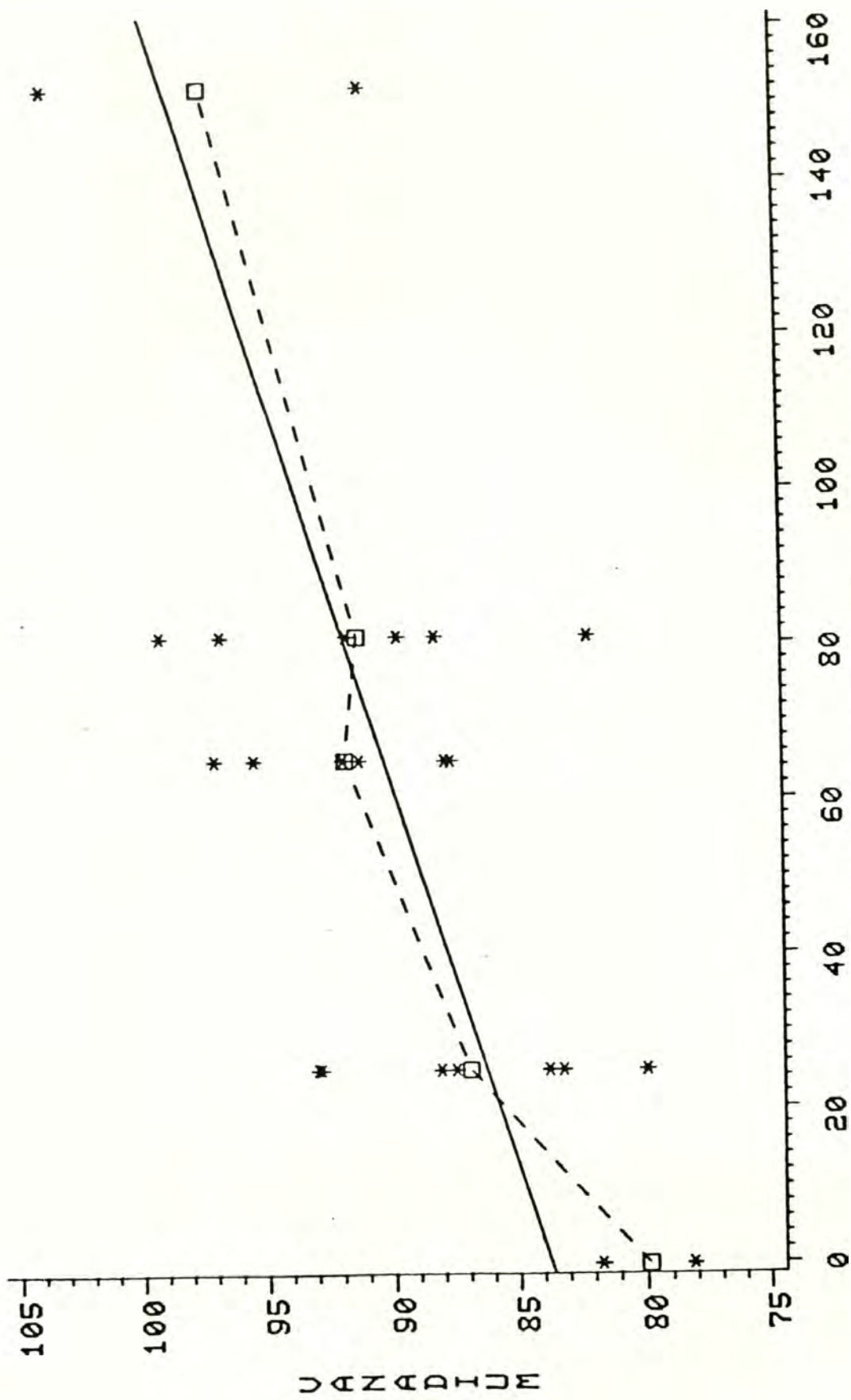
Figure 30. V versus time after May 18 eruption. Analyses shown by stars, means of analyses shown by boxes; dashed line connects means, solid line is linear regression. See Table 8 for R values.
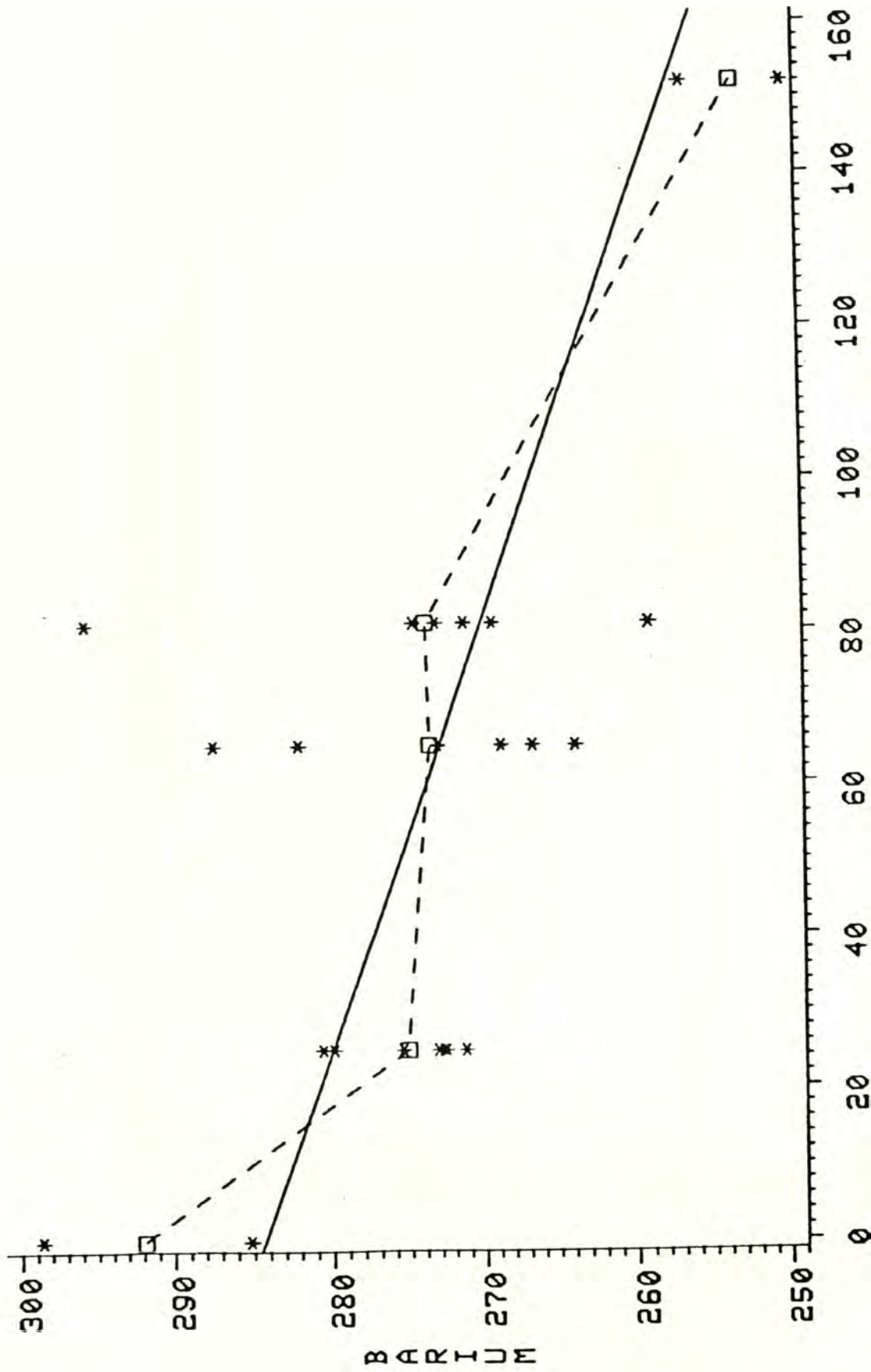
Figure 31. Ba versus time after May 18 eruption. Analyses shown by stars, means of analyses shown by boxes; dashed line connects means, solid line is linear regression. See Table 8 for R values.
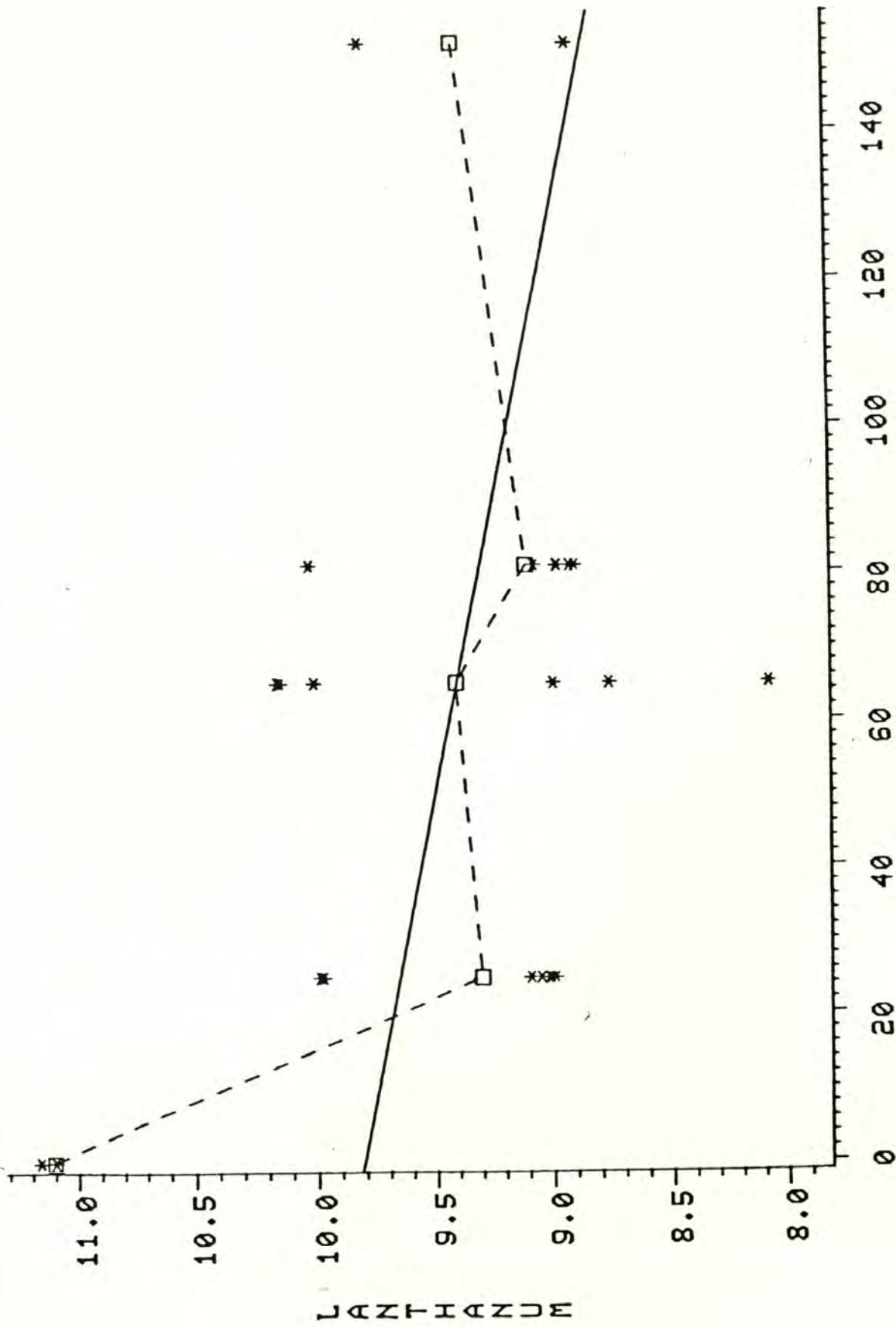
DAYS AFTER 18 MAY 1980 ERUPTION

Figure 32. La versus time after May 18 eruption. Analyses shown by stars, means of analyses shown by boxes; dashed line connects means, solid line is linear regression. See Table 8 for R values.
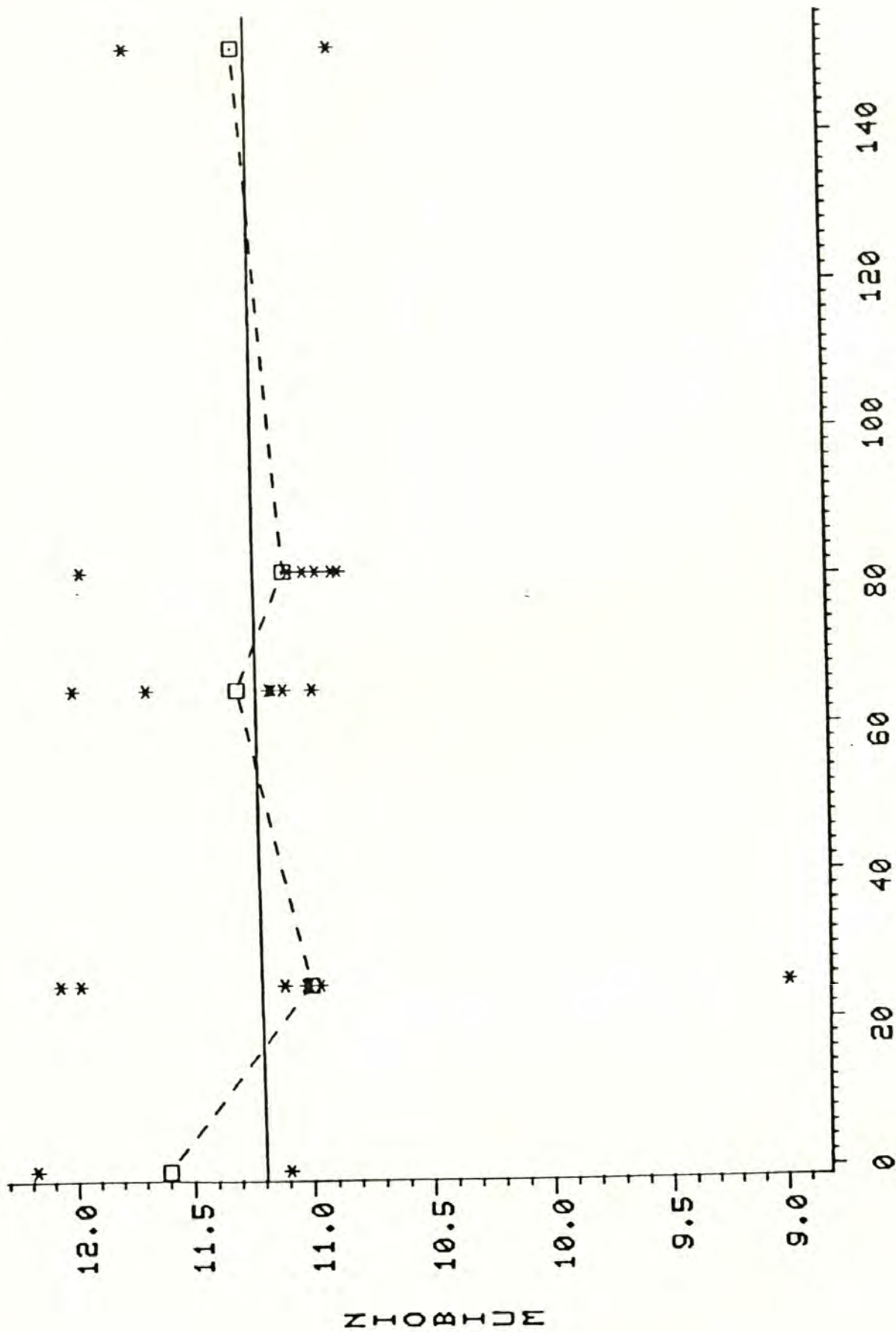
Figure 33. Nb versus time after May 18 eruption. Analyses shown by stars, means of analyses shown by boxes; dashed line connects means, solid line is linear regression. See Table 8 for R values.

Figure 34. Sr versus time after May 18 eruption. Analyses shown by stars, means of analyses shown by boxes; dashed line connects means, solid line is linear regression. See Table 8 for R values.
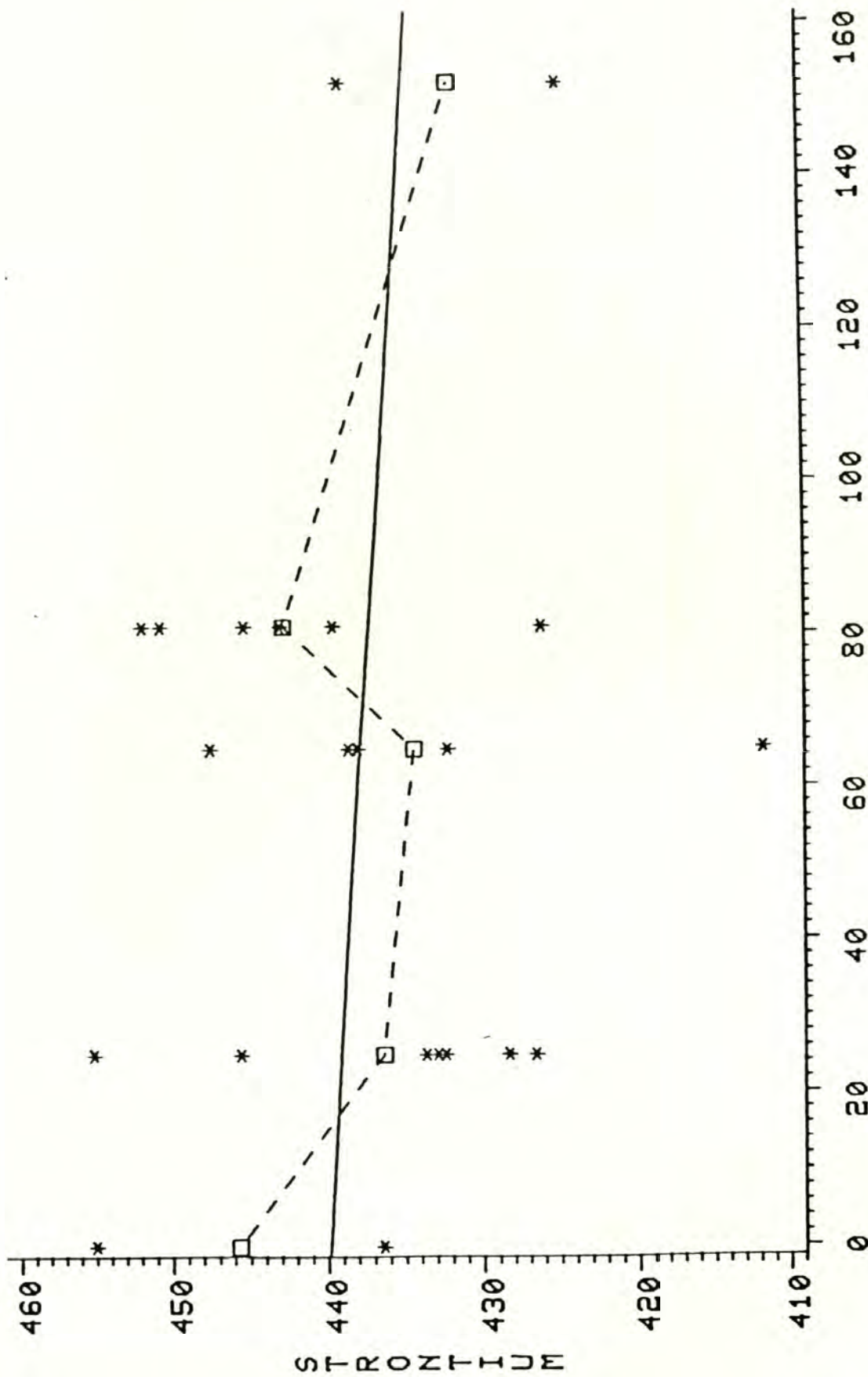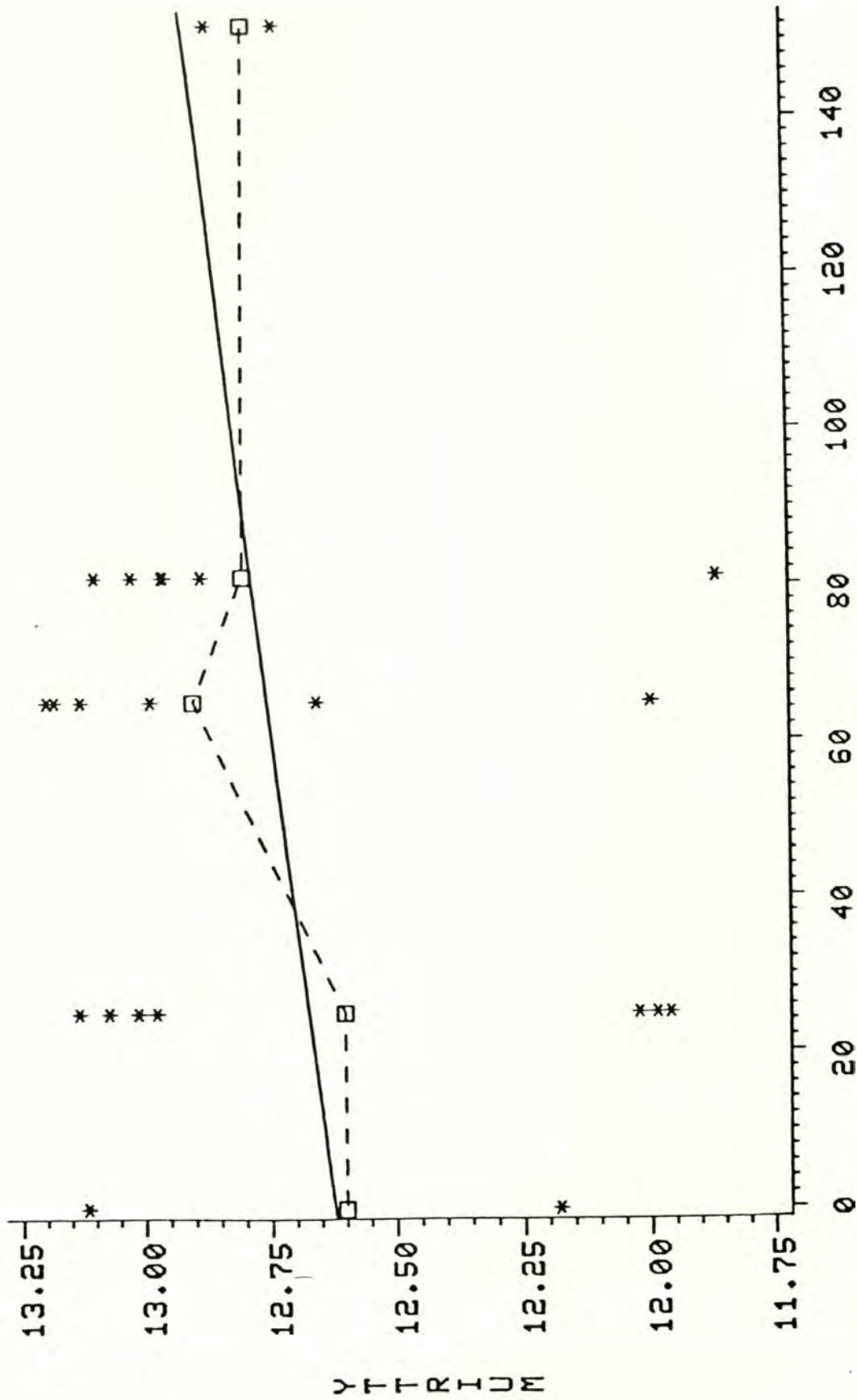
Figure 35. Y versus time after May 18 eruption. Analyses shown by stars, means of analyses shown by boxes; dashed line connects means, solid line is linear regression. See Table 8 for R values.
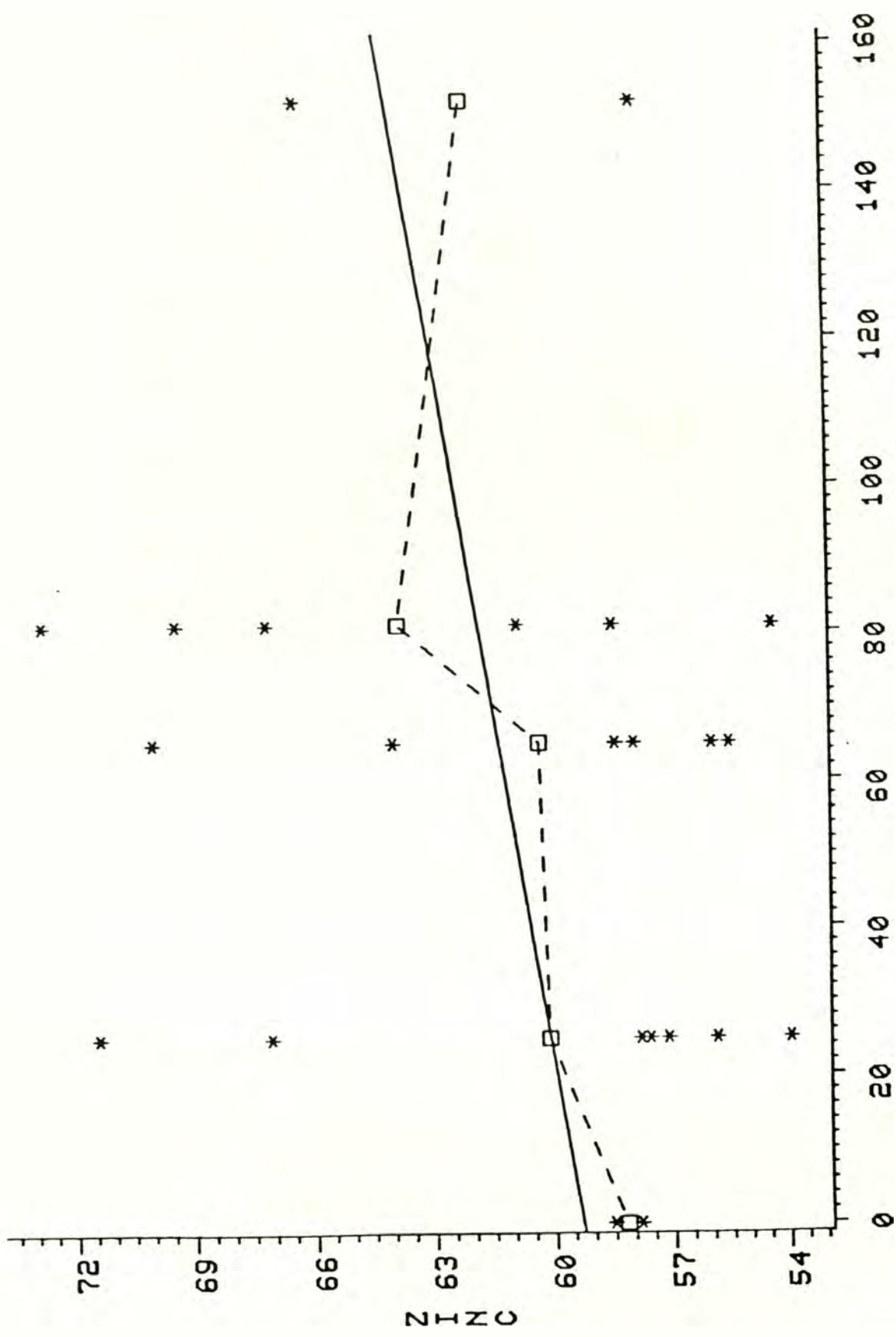
Figure 36. Zn versus time after May 18 eruption. Analyses shown by stars, means of analyses shown by boxes; dashed line connects means, solid line is linear regression. See Table 8 for R values.

Figure 37. Zr versus time after May 18 eruption. Analyses shown by stars, means of analyses shown by boxes; dashed line connects means, solid line is linear regression. See Table 8 for R values.

other similar studies (e.g., Melson et al., 1980a), there is an indication that the trends are probably real.

In order to further delineate temporal trends in pumice chemistry, harker-type silica variation diagrams were developed. Normalized major and minor element oxides have been plotted against silica and fields have been drawn around data points for each eruption date. The major and minor element oxides versus silica are presented in Figures 38-46.

All of these diagrams show a trend between the end members of May 18 and October 16-18. This trend is reflected by virtue of the relative high and low silica values of the respective end members. However, plots of the elements showing the strongest changes in abundance versus time, generally reflect those trends by grouping into distinct temporal fields.

There are some exceptions, notably, the June 12 and especially the July 22 fields are somewhat erratic in many of the graphs. Sample number 28, representing July 22 pumice, is anomalously low in silica and was not included in the July 22 field in any of the diagrams, but was, nonetheless, plotted.

With these exceptions aside, distinct trends are apparent in relative abundances of silica and TiO_2, FeO, CaO, MgO, and possibly MnO (Figures 38-42). Those oxides showing weak or no apparent trends are Al_2O_3, K_2O, Na_2O, and P_2O_5 (Figures 43-46).

Both the major and trace element data for the Mount St. Helens pumice fit the scheme of Taylor et al. (1969a) for the origin of
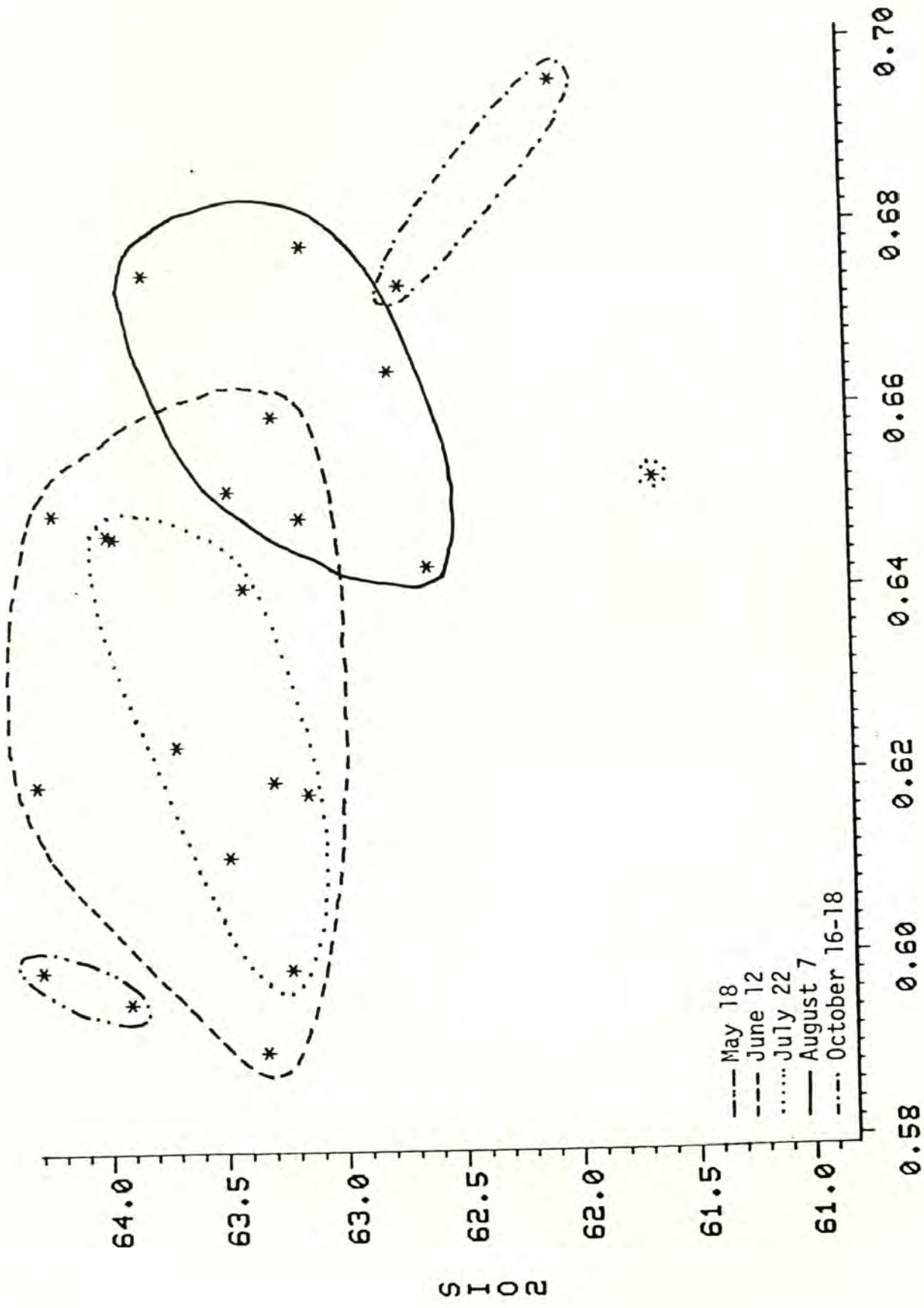
Figure 38. Harker type variation diagram: TiO_2 versus SiO_2.
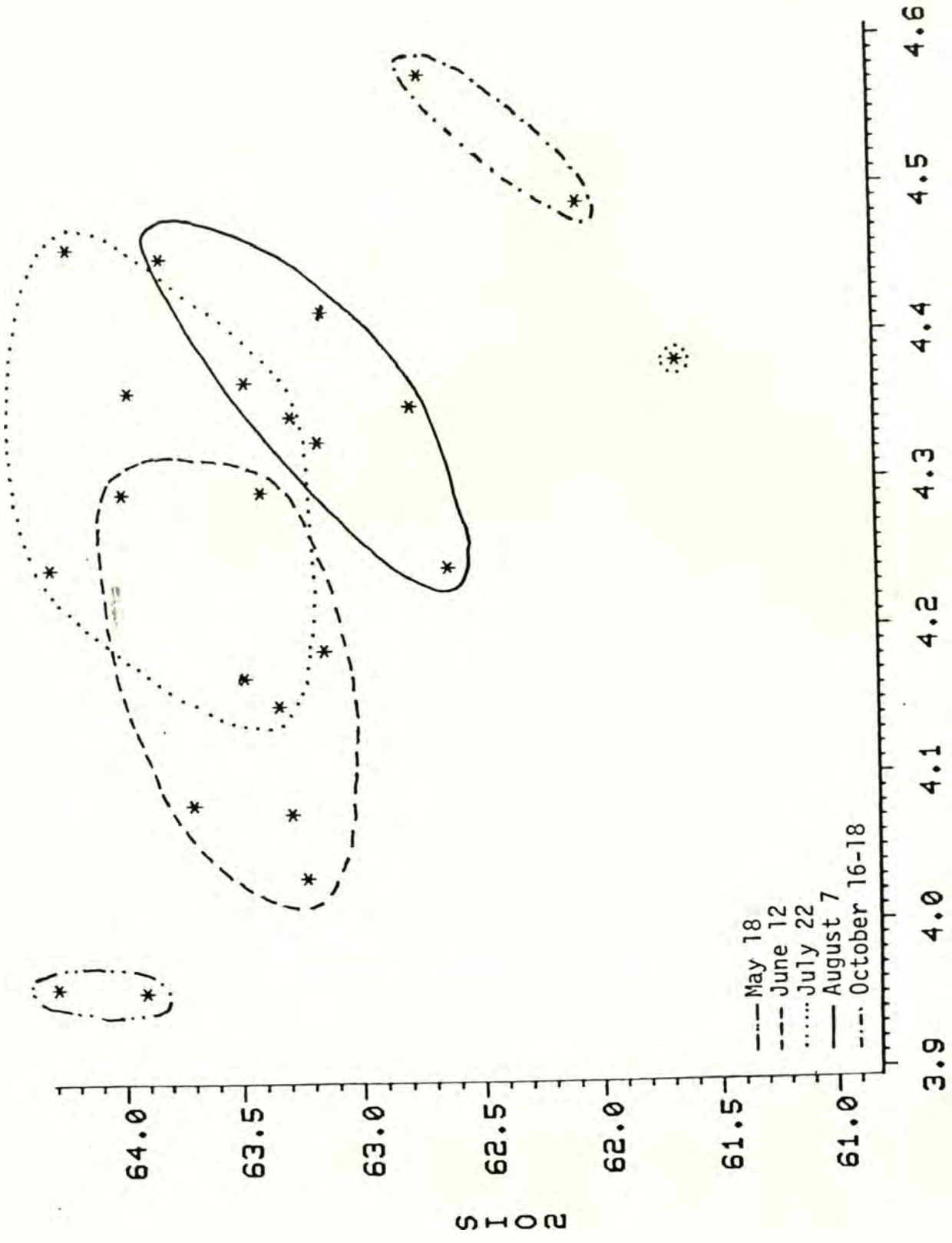
Figure 39. Harker type variation diagram: FeO versus SiO_2.
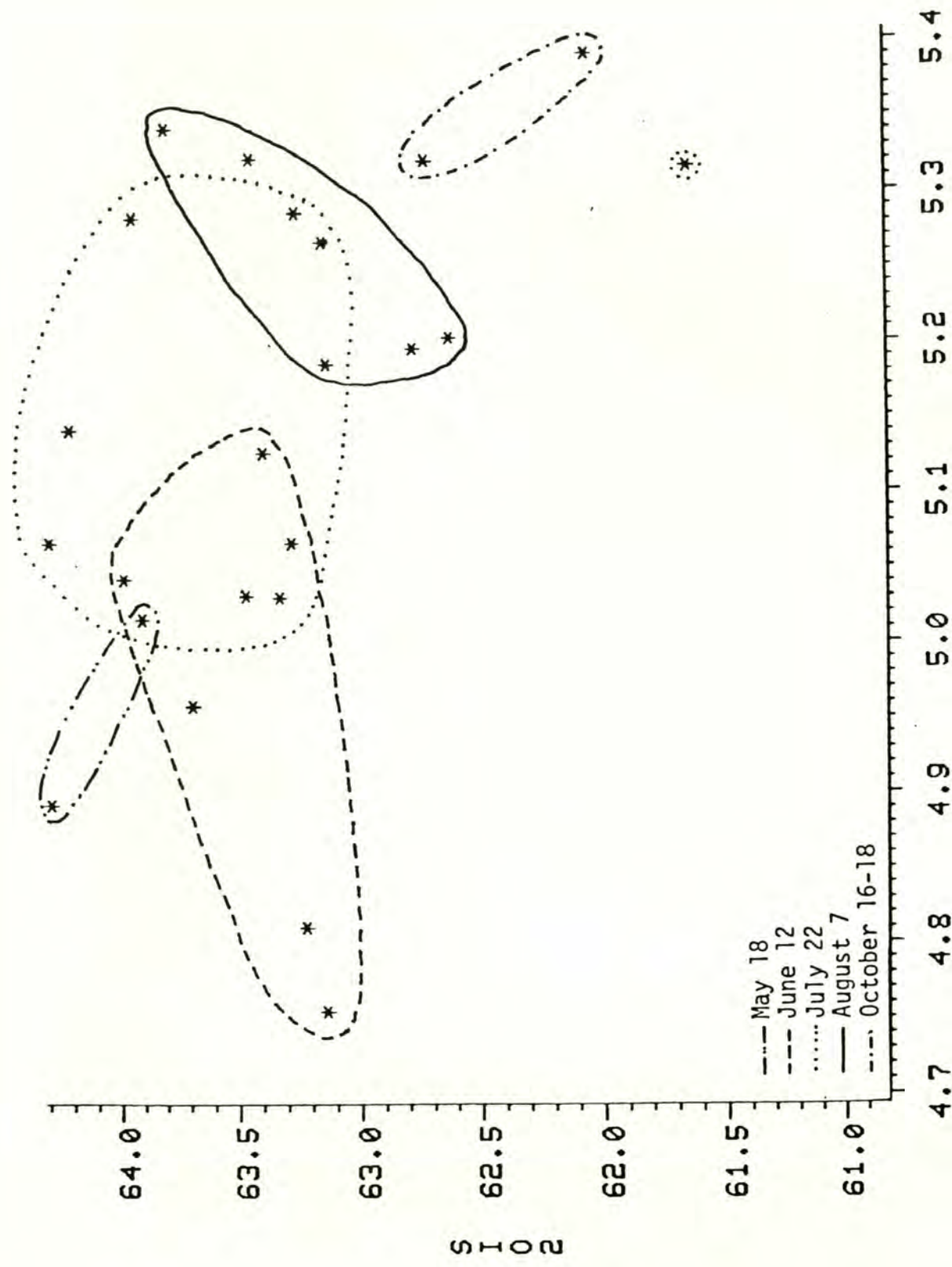
Figure 40. Harker type variation diagram: CaO versus SiO_2.
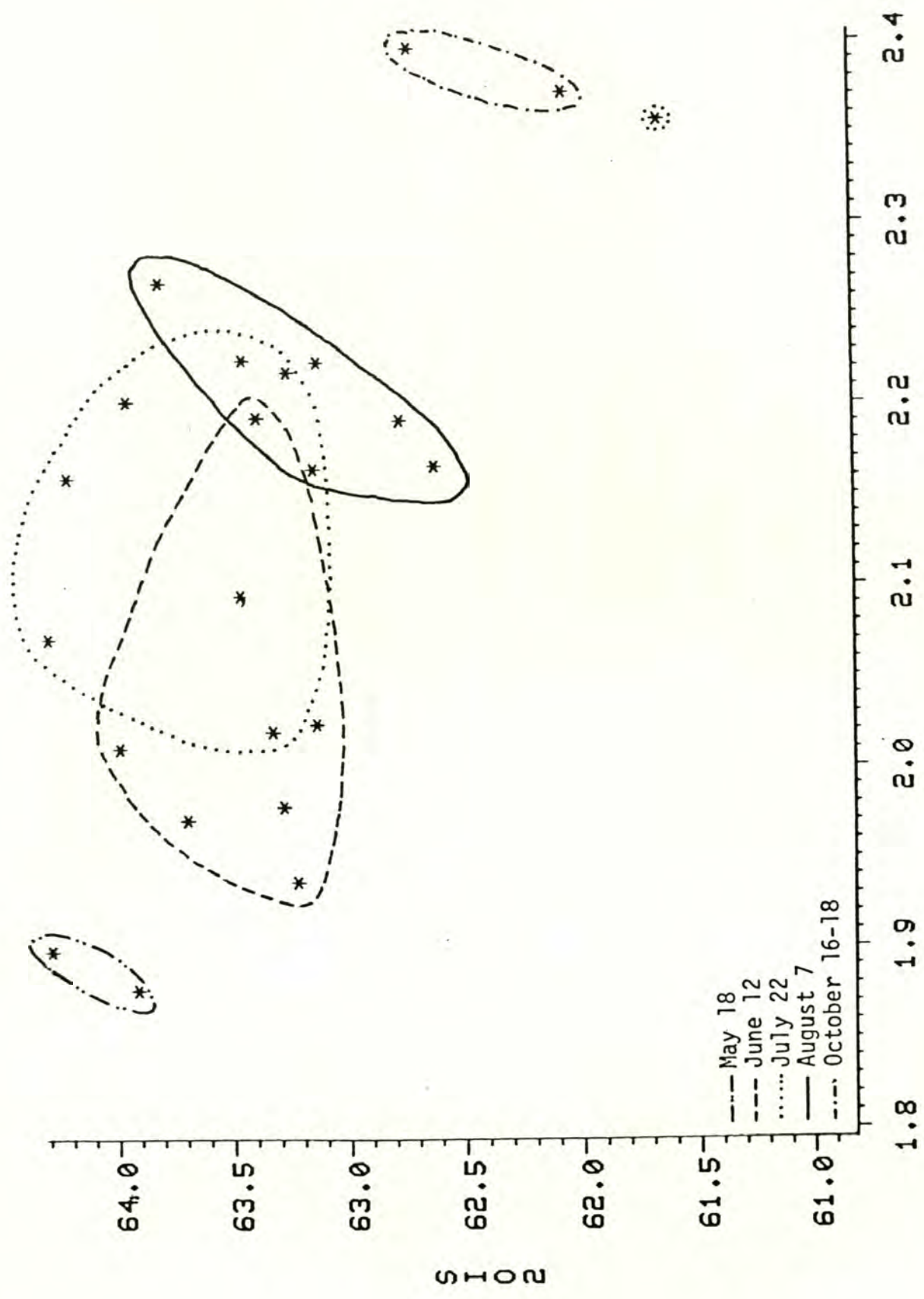
Figure 41. Harker type variation diagram: MgO versus SiO_2.
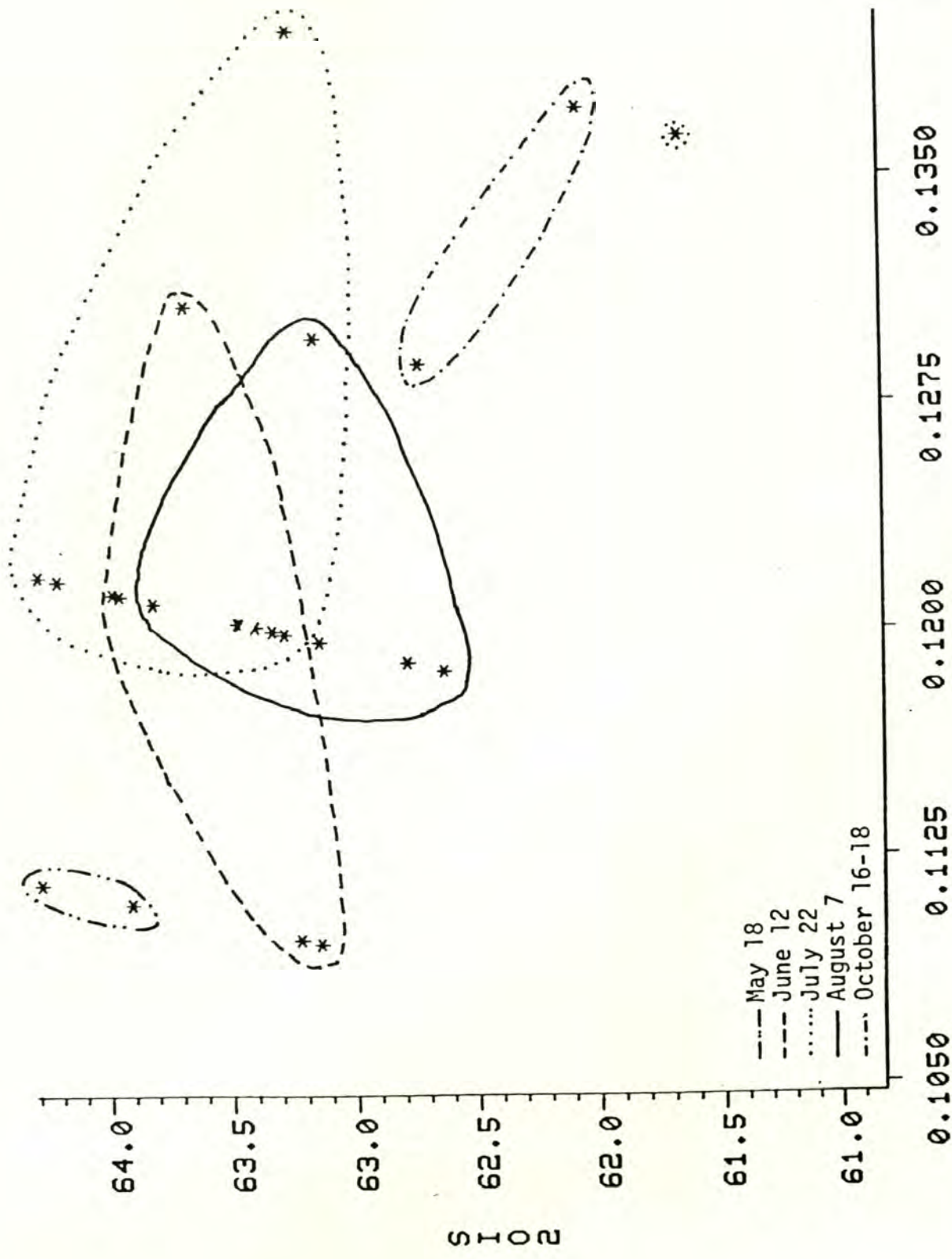
Figure 42. Harker type variation diagram: MnO versus SiO$_2$.
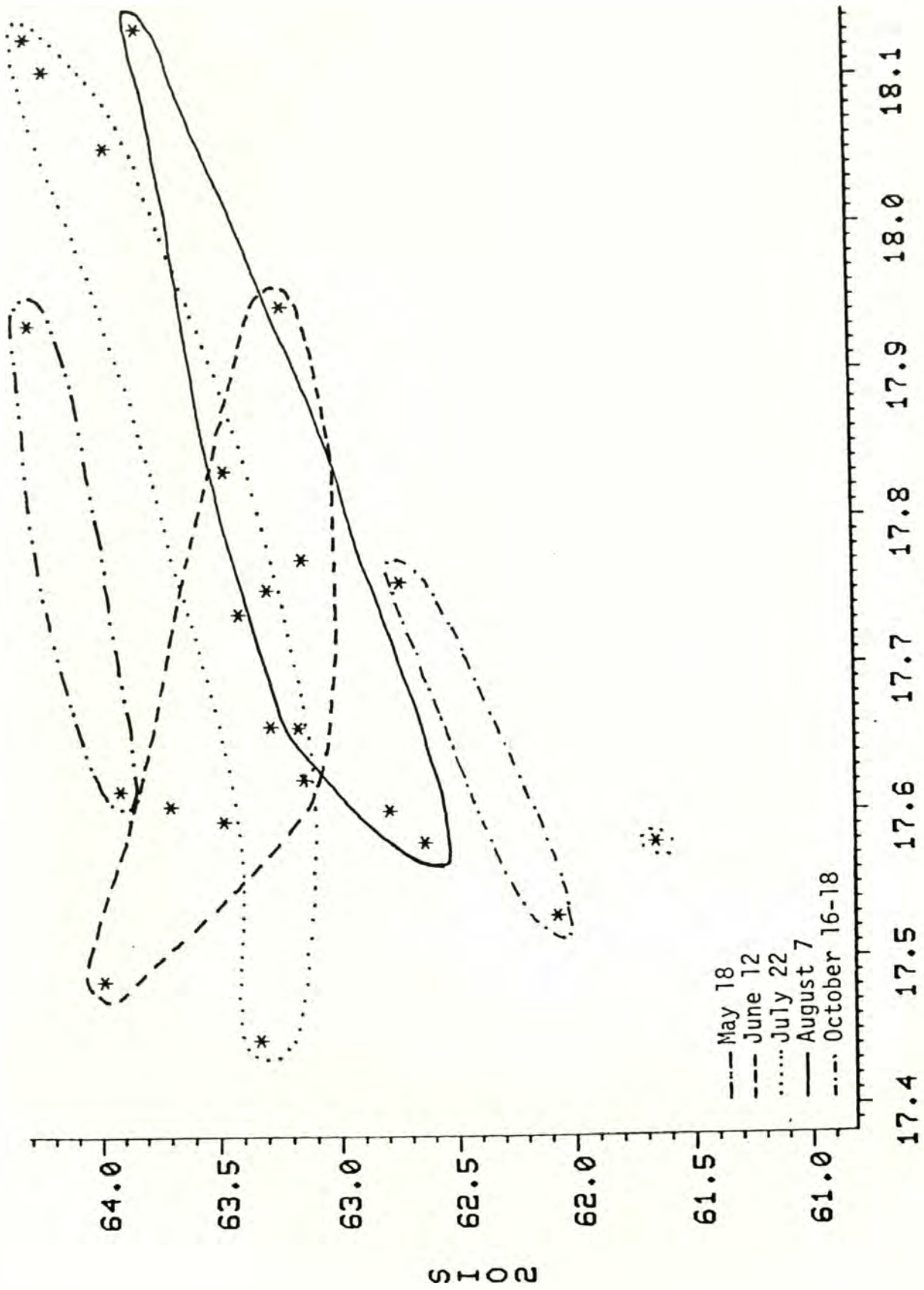
Figure 43. Harker type variation diagram: Al_2O_3 versus SiO_2.
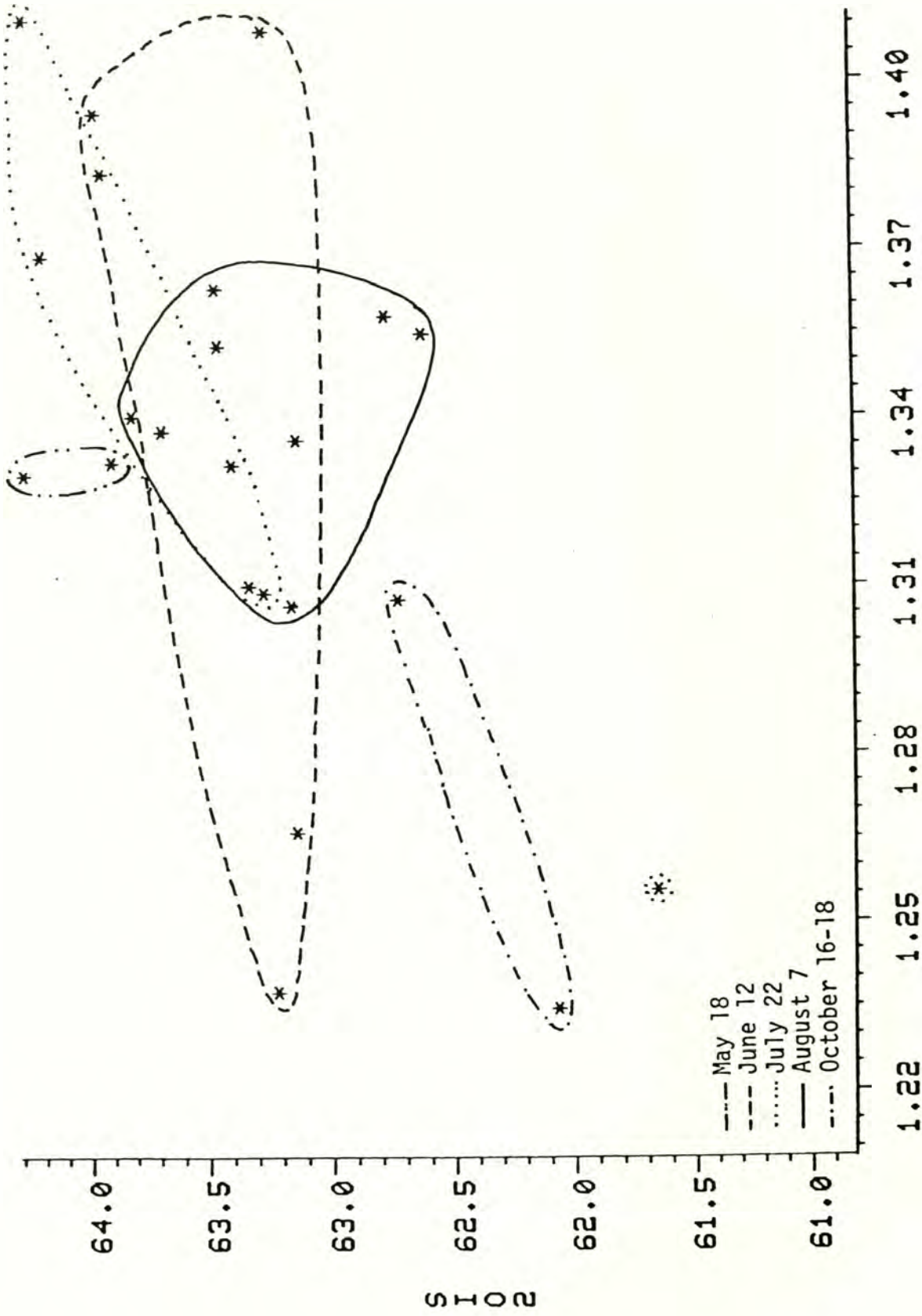
Figure 44. Harker type variation diagram: K_2O versus SiO_2.
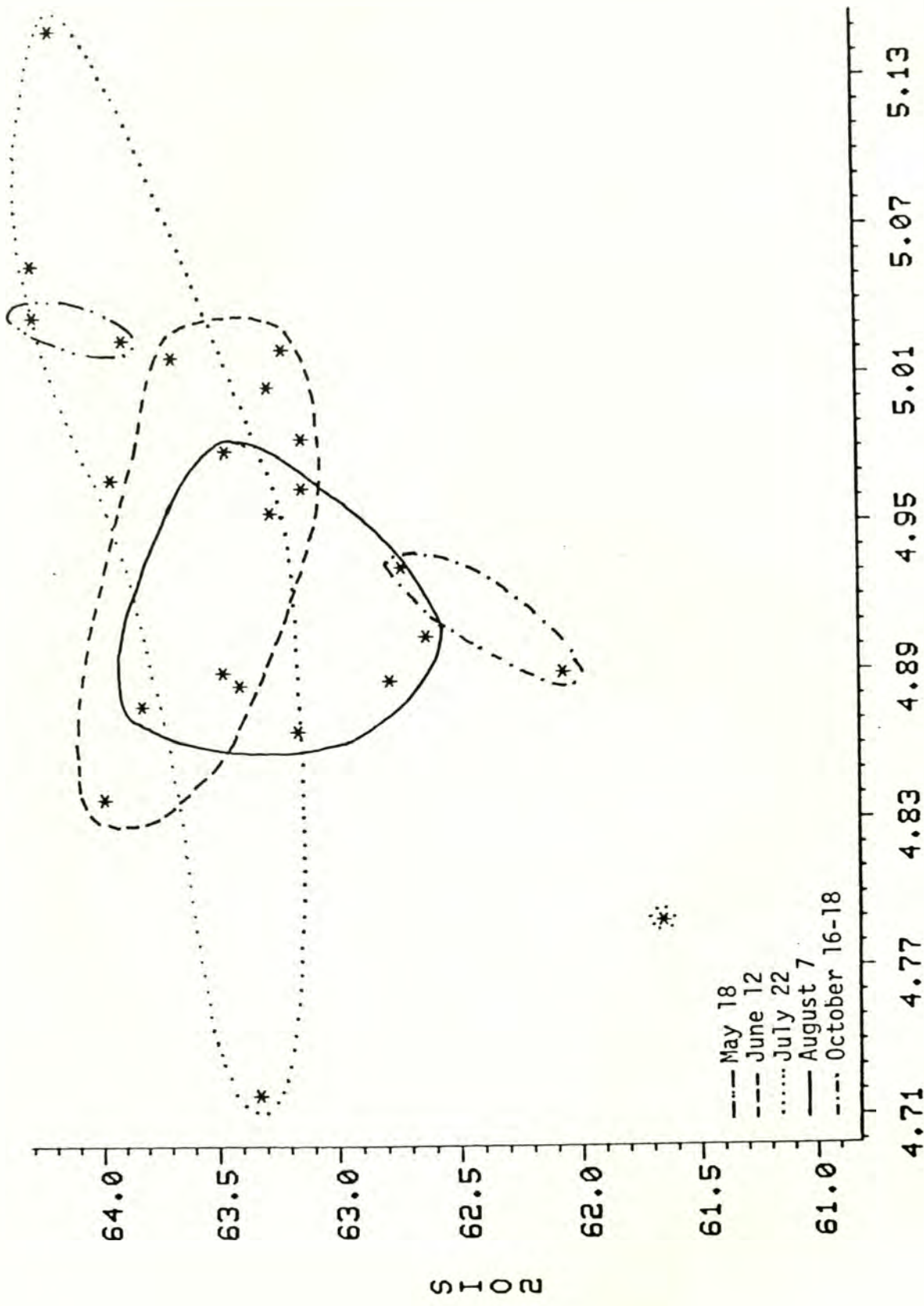
Figure 45. Harker type variation diagram: Na_2O versus SiO_2.
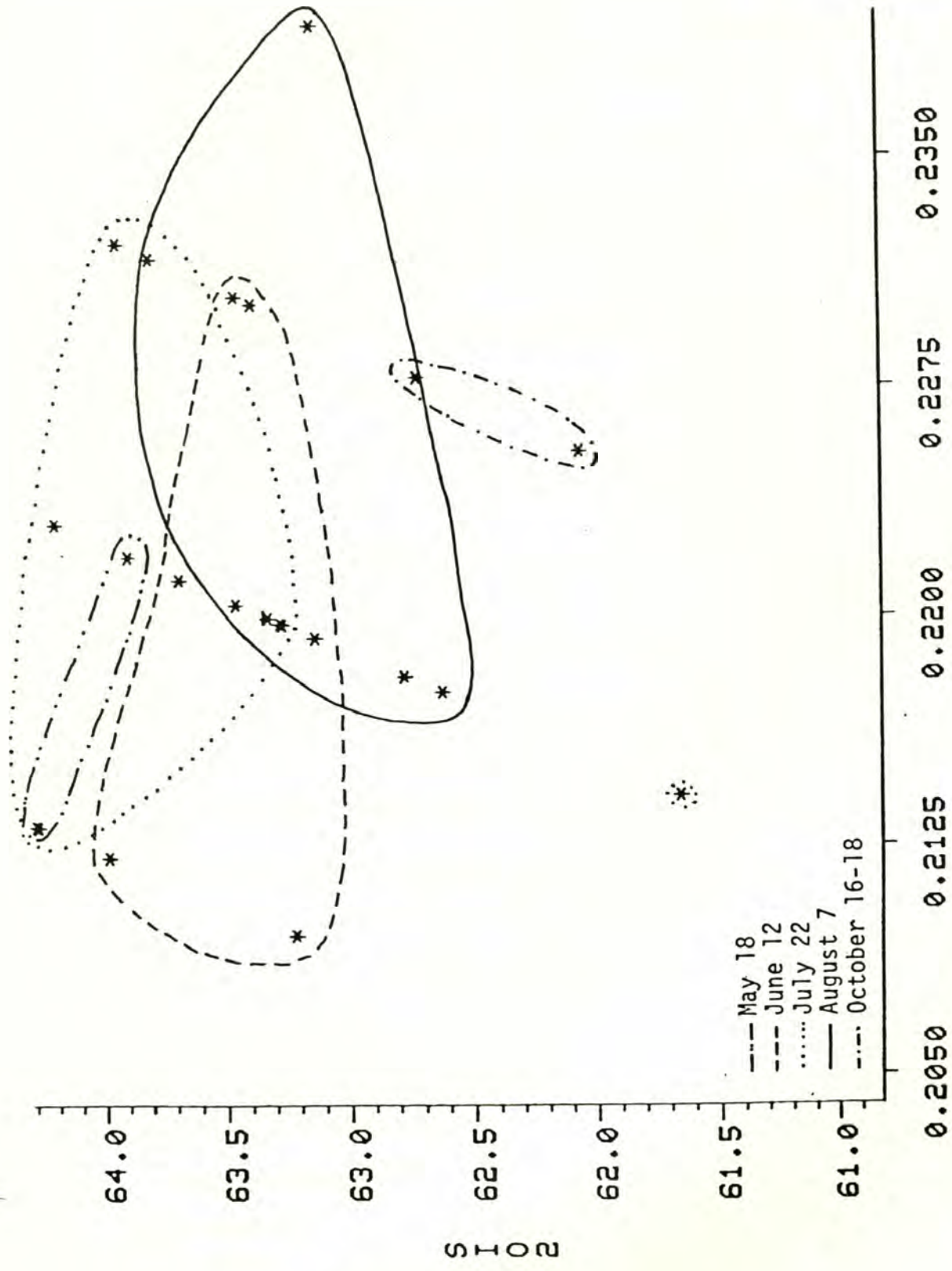
Figure 46. Harker type variation diagram: P_2O_5 versus SiO_2.

calc-alkaline association rocks. The Mount St. Helens dacite pumice probably represents an early stage of partial melting of the upper mantle, and the trend toward andesite represents the evolution of the melting process. A description of this model is presented in the discussion chapter.

DISCUSSION

Temporal trends in major and trace element chemistry of the 1980 Mount St. Helens pumice are apparent from data presented in this paper and elsewhere. The trend is toward a more andesitic, less gas-charged magma. If the trend is extended past 1980, relatively less-explosive eruptions are predicted; these actually occurred as the dome building eruptions of 1981-1983. Short term prediction of eruptive behavior of Mount St. Helens, using seismic and geodetic techniques has been successful with the exception of two unforeseen phreatomagmatic eruptions in March 1982 and February 1983. However, before short or long term predictions of eruptive activity can be made with any certaintly a better understanding of the mechanisms for generation of calc-alkaline magma is necessary.

Numerous models have been proposed for the genesis of calc-alkaline magma. These models have attempted to explain the petrologic and chemical characteristics of rocks belonging to the basalt-andesite-dacite-rhyolite association. In general, the proposed petrogenetic models include:

1. Fractional crystallization of basaltic magma (Bowen, 1956; Osborn, 1959, 1962).

2. Fractional crystallization of basaltic magma with contamination by assimilation of crustal material (Tilley, 1950; Kuno, 1950; Waters, 1955).

3. Mixing of basaltic and rhyolitic magmas (Larsen et al., 1938; Holmes, 1932; Eichelberger, 1978).

4. Partial melting of the mantle resulting in primary andesitic magma (Green and Ringwood, 1966, 1968; Hamilton, 1966; Taylor and White, 1966; and Taylor et al., 1969a).

Fractional crystallization, assimilation, mixing, and partial melting, have been popular mechanisms for explaining the formation of calk-alkaline rocks; however, these models were based primarily on major element chemistry and petrology. With the advent of more rapid and less expensive analytical techniques, trace element chemistry has become increasingly useful in unraveling the origin of orogenic andesites, primarily by providing constraints on the various petrogenetic processes mentioned above.

The calk-alkaline series rocks are typified by their intermediate-composition member, andesite, and are restricted to orogenic belts where andesite is the most abundant eruptive product. True basalts are typically absent, or present in only minor amounts, as are rhyolites and dacites, suggesting that andesite is a primary magma not derived by fractionation of parental basalt (Taylor and White, 1966; Smith and Carmichael, 1968).

Hyde (1973) reports that 85 percent of Mount St. Helen's eruptive products are dacitic to andesitic. Therefore, using the argument based on sheer volume of andesites, the abundance of intermediate products at Mount St. Helens suggests that fractional crystallization of basalt does not play an important role in the production of Mount St. Helens magma.

Further evidence against fractional crystallization of a parent basalt to produce andesites lies in the V and Ni contents of these rocks. Ni values ranging from a minimum of six to a maximum of 27 ppm in the May 18, 1980 ash were reported by Sarna-Wojcicki et al. (1981); Taylor and Lichte (1980); and Fruchter et al. (1980). These values are similar to the 25 ppm reported for average high-alumina basalts (Taylor et al., 1969b). Taylor et al. (1969b) suggested that Ni, which shows strong preference for the abundant octahedral lattice sites in ferromagnesian minerals, would be much lower in andesites if they were derived by fractionation of high-alumina basalts.

In rebuttal to Osborn (1959, 1962) who suggested early crystalli- zation of magnetitie during andesite production, Taylor et al. (1969b) pointed out that V is very rapidly depleted from the parent basalt by removal of a small amount of ferromagnesian minerals, espe- cially magnetite. However, the difference in Fe content between average andesite and average basalt of all classes is too great to allow for the similar abundances of V found in both, i.e., 250 ppm in basalt and 175 ppm in andesite.

Taylor and White (1966) and Ewart et al. (1968) have shown that whole rock V abundances in more silicic calc-alkaline rocks are

slightly lower than in more basic members. The V abundance in 1980 Mount St. Helens pumice (78 ppm May 18, 104 ppm October 16-18) is close to that of the average andesite and is trending toward the andesite value with time, indicating that the Mount St. Helens pumice is close in V values to those of average calc-alkaline rocks. Therefore, the Mount St. Helens pumice was probably not produced by fractional crystallization.

Assimilation of crustal materials by alkali or tholeiitic basalt will not produce the relative abundances of Ni and V that are found in average andesites or Mount St. Helens pumice. Average alkali or tholeiitic basalts contain 120 ppm Ni and 200 ppm V, whereas average 1980 Mount St. Helens ash contains only about 15 ppm Ni and 90 ppm V, requiring a very large dilution of silicic material to lower the Ni content sufficiently. This large dilution would also reduce the amount of V in Mount St. Helens rocks far below its present value. Because of the similarities in Ni and V content of high alumina basalt and Mount St. Helens pumice, assimilation of silica-rich material by high-alumina basalt would severely limit the amount of silicic material that could be assimilated. This would not be sufficient to account for the amount of silica present in Mount St. Helens rocks. Furthermore, Bowen (1956) has shown that assimilation of solid crustal material by a magma can occur only on a very small scale due to lack of available heat that is needed to overcome the solution heats of silicates.

A mixing model as proposed by Eichelberger (1978) would require extensive basaltic magmas beneath stratovolcanoes yet a gravitational low is associated with Mount St. Helens (Danes and Phillips, 1983). On the other hand, this model does address the fact that most andesites contain phenocrysts completely out of phase with the melt.

Partial melting of eclogites in the mantle as proposed by Green and Ringwood (1966) would not produce Ni/Co and V/Ni ratios appropriate for andesites, nor would single stage partial melting of pyrolite produce appropriate concentrations of Ni and Cr or Ni/Co ratios (Taylor et al., 1969b). However, Taylor et al. (1969a) have proposed a two-stage partial melting process which is compatible with the observed andesite and Mount St. Helens petrochemistry. This process involves partial melting of pyrolite below mid-ocean ridges, producing oceanic crust that is transported together with the underlying lithosphere to subduction zones where they are converted to amphibolite. A remelting of the amphibolite forms rocks of the calc-alkaline series, the members of which represent different stages of partial melting. Trace element chemistries of the calc-alkaline series are compatible with this process, but it requires contamination by deep sea sediments to account for the paucity of K, Rb, and Ba in the low-K tholeiites of the parent oceanic crust. Variations in large cation content (K, Rb, Ba) and Sr isotope ratios are accounted for by various amounts of contamination from deep sea or continental sediments.

The chemistry and petrology of the Mount St. Helens pumice fits nicely into the Taylor et al. (1969a) model. The temporal trend

toward a more andesitic composition could be the result of either of two separate processes, or a combination.

1. The early more dacitic ejecta probably represents the first stages of partial melting of source area material. The more siliceous material, being the first to melt, spearheads the rise of the magma to the surface where it is extruded. It is followed by more andesitic primary melt in the later stages.

2. The primary andesitic melt moved to a shallow magma chamber where mixing by thermogravitational convection as described by Hildreth (1979) could account for such features as minor magma inhomogeneity and reverse and oscillatory zoning in plagioclase. Weak stratification or differentiation within the magma chamber due to gaseous exsolution is also a possibility.

REFERENCES

Abbey, S., 1980, Studies in "standard samples" for use in the general analysis of silicate rocks and minerals; part 6, 1979 issue of "usable" values: Geological Survey of Canada, paper 80-14, 30 p.

Banks, N. G.; Hoblitt, R. P., 1981, Summary of temperature studies of 1980 deposits. In Lipman, P. W.; Mullineaux, D. R., editors, 1981, The 1980 eruptions of Mount St. Helens, Washington: U.S. Geological Survey Professional Paper 1250, p. 295-313.

Borchardt, G. A.; Harward, M. E.; Schmitt, R. A., 1971, Correlation of volcanic ash deposits by activation analysis of glass separates: Quaternary Research, v. 1, no. 2, p. 247-260.

Bowen, N. L., 1956, The evolution of the igneous rocks: Dover Publications, 332 p.

Carmichael, I. S. E.; Turner, F. J.; Verhoogen, John, 1974, Igneous petrology: McGraw-Hill Book Company, 739 p.

Carithers, Ward, 1946, Pumice and pumicite occurrences of Washington: Washington Division of Mines and Geology Report of Investigations 15, 78 p.

Danes, Z. F.; Phillips, W. M., 1983, Complete Bouguer gravity anomaly map of the Cascade Mountains, Washington: Washington Division of Geology and Earth Resources Geologic Map GM-27, 2 sheets, scale 1:250,000.

Dudas, M. J.; Harward, M. E.; Schmitt, R. A., 1973, Identification of dacitic tephra by activation analysis of their primary mineral phenocrysts: Quaternary Research, v. 3, no. 2, p. 307-315.

Eichelberger, J. C., 1978, Andesitic volcanism and crustal evolution: Nature, v. 275, no. 5674, p. 21-27.

Erdmann, C. E.; Warren, Walter, 1938, Geology of three dam sites on the Toutle River, Washington: U.S. Geological Survey Open-File Report, 116 p.

Ewart, A.; Taylor, S. R., 1969, Trace element geochemistry of the rhyolitic volcanic rocks, central North Island, New Zealand, phenocryst data: Contributions to Mineralogy and Petrology, v. 22, p. 127-146.

Ewart, A.; Taylor, S. R.; Capp, A. C., 1968, Trace and minor element chemistry of the rhyolitic volcanic rocks, central North Island, New Zealand: Contributions to Mineralogy and Petrology, v. 18, p. 76-104.

Folsom, M. M., 1970, Volcanic eruptions; the pioneers' attitude on the Pacific Coast from 1800 to 1875: Ore Bin, v. 32, no. 4, p. 61-71.

Fruchter, J. S.; Robertson, D. E.; Evans, J. C.; and others, 1980, Mount St. Helens ash from the 18 May 1980 eruption; chemical, physical, mineralogical, and biological properties: Science, v. 209, no. 4461, p. 1116-1125.

Greeley, Ronald; Hyde, J. H., 1972, Lava tubes of the cave basalt, Mount St. Helens, Washington: Geological Society of America Bulletin, v. 83, no. 8, p. 2397-2418.

Green, T. H.; Ringwood, A. E., 1966, Origin of the calc-alkaline igneous rock suite: Earth and Planetary Science Letters, v. 1, p. 307-316.

Green, T. H.; Ringwood, A. E., 1968, Genesis of the calc-alkaline igneous rock suite: Contributions to Mineralogy and Petrology, v. 8, p. 105-162.

Hamilton, Warren, 1966, Origin of the volcanic rocks of eugeosynclines and island arcs. In Poole, W. H., editor, 1966, Continental margins and island arcs: Geological Survey of Canada Paper 66-15, p. 348-355.

Heiken, G.; Eichelberger, J. C., 1980, Eruptions of Chaos Crags, Lassen Volcanic National Park, California: Journal of Volcanology and Geothermal Research, v. 7, no. 3-4, p. 443-481.

Hildreth, W., 1979, The Bishop Tuff; evidence for the origin of compositional zonation in silicic magma chambers. In Chapin, C. E.; Elson, W. E., editors, 1979, Ash-flow tuffs: Geological Society of America Special Paper 180, p. 43-75.

Hoblitt, R. P., 1980, Observations of pyroclastic flows of July 22 and August 7, 1980, Mount St. Helens, Washington [abstract]: Eos (American Geophysical Union Transactions), v. 61, no. 46, p. 1137-1138.

Hoblitt, R. P.; Banks, N. G.; Ryan, M. P.; Rosenbaum, J. G.; Davis, M. J., 1980, Emplacement temperatures of Mount St. Helens eruptive products [abstract]: Geological Society of America Abstracts with Programs, v. 12, no. 7, p. 447.

Holmes, Arthur, 1932, The origin of igneous rocks: Geology Magazine, v. 69, p. 543-558.

Holmes, K. L., 1955, Mount St. Helens' recent eruptions: Oregon Historical Quarterly, v. 56, p. 197-210.

Hooper, P. R.; Herrick, I. W.; Laskowski, E. R.; Knowles, C. R., 1980, Composition of the Mount St. Helens ashfall in the Moscow-Pullman area on 18 May 1980: Science, v. 209, no. 4461, p. 1125-1126.

Hopson, C. A., 1971, Eruptive sequence at Mount St. Helens, Washington [abstract]: Geological Society of America Abstracts with Programs, v. 3, no. 2, p. 138.

Hopson, C. A., 1980, [Preliminary geologic map of Mount St. Helens]: U.S. Geological Survey unpublished map, 1 sheet.

Hopson, C. A.; Melson, W. G., 1980, Mount St. Helens eruptive cycles since 100 A. D. [abstract]: Eos (American Geophysical Union Transactions), v. 61, no. 46, p. 1132-1133.

Hughes, J. M.; Stoiber, R. E.; Car, M. J., 1980, Segmentation of the Cascade volcanic chain: Geology, v. 8, no. 1, p. 15-17.

Hughes, S. S., 1981, Trace element analyses of Mount St. Helens pumice and separated phases [abstract]: Eos (American Geophysical Union Transactions), v. 62, no. 6, p. 62.

Huntsberger, D. V.; Billingsley, Patrick, 1973, Elements of statistical inference; third edition: Allyn and Bacon, Inc., 349 p.

Hyde, J. H., 1970, Geologic setting of Merrill Lake and evaluation of volcanic hazards in the Kalama River Valley near Mount St. Helens, Washington: U.S. Geological Survey Open-File Report 70-169, 17 p.

Hyde, J. H., 1973, Late Quaternary volcanic stratigraphy, south flank of Mount St. Helens, Washington: University of Washington Doctor of Philosophy thesis, 114 p.

Hyde, J. H.; Crandell, D. R., 1972, Potential volcanic hazards near Mount St. Helens in southwestern Washington [abstract]: Northwest Scientific Association, 45th Annual Meeting, Abstracts of Papers, p. 7.

Irving, A. J.; Rhodes, J. M.; Sparks, J. W., 1980, Mount St. Helens lava dome, pyroclastic flow and ash samples; major and trace element chemistry [abstract]: Eos (American Geophysical Union Transactions), v. 61, no. 46, p. 1138.

Jillson, W. R., 1917, New evidence of a recent volcanic eruption on Mount St. Helens, Washington: American Journal of Science, v. 44, no. 259, p. 59-62.

Krumbein, W. C.; Graybill, F. A., 1965, An introduction to statistical models in geology: McGraw-Hill Book Company, 574 p.

Kuno, Hisashi, 1950, Petrology of Hakone volcano and the adjacent areas, Japan: Geological Society of America Bulletin, v. 61, p. 957-1014.

Kuntz, M. A.; Rowley, P. D.; MacLeod, N. S.; Reynolds, R. L.; McBroome, L. A.; Kaplan, A. M.; Lidke, D. J., 1981, Petrography and particle-size distribution of pyroclastic-flow, ash-cloud, and surge deposits. In Lipman, P. W.; Mullineaux, D. R., editors, 1981, The 1980 eruptions of Mount St. Helens, Washington: U.S. Geological Survey Professional Paper 1250, p. 525-539.

Larsen, E. S.; Irving, John; Gonyer, F. A., 1938, Petrologic results of a study of the minerals from the Tertiary volcanic rocks of the San Juan region, Colorado: American Mineralogist, v. 23, no. 7, p. 417-429.

Lawrence, D. B., 1938, Trees on the march: Mazama, v. 20, no. 12, p. 49-54.

Lawrence, D. B., 1939, Continuing research on the flora of Mount St. Helens: Mazama, v. 21, no. 12, p. 49-54.

Lawrence, D. B., 1941, The "Floating Island" lava flow of Mount St. Helens: Mazama, v. 23, no. 12, p. 56-60.

Lawrence, D. B., 1954, Diagrammatic history of the northeast slope of Mount St. Helens, Washington: Mazama, v. 36, no. 13, p. 41-44.

Lipman, P. W.; Norton, D. R.; Taggart, J. E., Jr.; Brandt, E. L.; Engleman, E. E., 1981, Compositional variations in 1980 magmatic deposits. In Lipman, P. W.; Mullineaux, D. R., editors, 1981, The 1980 eruptions of Mount St. Helens, Washington: U.S. Geological Survey Professional Paper 1250, p. 631-640.

Logan, R. L., 1981, Some petrographic characteristics of pumice from the 1980 Mount St. Helens pyroclastic flows: Washington Geologic Newsletter, v. 9, no. 4, p. 1-4.

McBirney, A. R., 1968, Petrochemistry of the Cascade andesite volcanoes. In Dole, H. M., editor, 1968, Andesite conference guidebook--International Upper Mantle Project Scientific Report 16-S: Oregon Department of Geology and Mineral Industries Bulletin 62, p. 101-107.

Melson, W. G., and others, 1980a, Volcanic events, Mount St. Helens volcano: SEAN Bulletin, v. 5, no. 11, p. 2-3.

Melson, W. G., and others, 1981, Volcanic activity, Mount St. Helens volcano: SEAN Bulletin, v. 6, no. 2, p. 2-3.

Melson, W. G.; Hopson, C. A., 1981, Preeruption temperatures and oxygen fugacites in the 1980 eruptive sequence. In Lipman, P. W.; Mullineaux, D. R., editors, 1981, the 1980 eruptions of Mount St. Helens, Washington: U.S. Geological Survey Professional Paper 1250, p. 641-648.

Melson, W. G.; Hopson, C. A.; Kienle, C. F., 1980b, Petrology of tephra from the 1980 eruptions of Mount St. Helens [abstract]: Geological Society of America Abstracts with Programs, v. 12, no. 7, p. 482.

Moyer, T. C.; Self, S.; Sykes, M. L.; Neal, C. A., 1982, Pyroclastic flow deposits of Mount St. Helens, 1980-82; an evaluation of emplacement mechanisms [abstract]: Geological Society of America Abstracts with Programs, v. 14, no. 7, p. 572.

Mullineaux, D. R., 1964, Extensive recent pumice lapilli and ash layers from Mount St. Helens volcano, southern Washington [abstract]: Geological Society of America Special Paper 76, p. 285.

Mullineaux, D. R.; Crandell, D. R., 1962, Recent lahars from Mount St. Helens, Washington: Geological Society of America Bulletin, v. 73, no. 7, p. 855-869.

Mullineaux, D. R.; Hyde, J. H.; Rubin, Meyer, 1972, Preliminary assessment of upper Pleistocene and Holocene pumiceous tephra from Mount St. Helens, southern Washington [abstract]: Geological Society of America Abstracts with Programs, v. 4, no. 3, p. 204-205.

Mullineaux, D. R.; Hyde, J. H.; Rubin, Meyer, 1975, Widespread late glacial and postglacial tephra deposits from Mount St. Helens volcano, Washington: U.S. Geological Survey Journal of Research, v. 3, no. 3, p. 329-335.

Okazaki, Rose; Smith, H. W.; Gilkeson, R. A.; Franklin, Jerry, 1972, Correlation of West Blacktail ash with pyroclastic Layer T from the 1800 A. D. eruption of Mount St. Helens: Northwest Science, v. 46, no. 2, p. 77-89.

Osborn, E. F., 1959, Role of oxygen pressure in the crystallization and differentiation of basaltic magma: American Journal of Science, v. 257, p. 609-647.

Osborn, E. F., 1962, Reaction series for subalkaline igneous rocks based on different oxygen pressure conditions: American Mineralogist, v. 47, nos. 3-4, p. 211-226.

Paine, J. G., 1982, Crustal structure of volcanic arcs based on physical properties of andesites, volcaniclastic rocks, and inclusions in the Mount St. Helens lava dome: University of Washington Masters of Science thesis, 138 p.

Pevear, D. R.; Dethier, D. P.; Frank, D., 1982, Clay minerals in the 1980 deposits from Mount St. Helens: Clays and Clay Minerals, v. 30, no. 4, p. 241-252.

Raedeke, L. D.; Mathez, E. A.; Irving, A. J., 1980, Mount St. Helens lava dome; petrography and mineral chemistry [abstract]: Eos (American Geophysical Union Transactions), v. 61, no. 46, p. 1138.

Randle, Keith; Goles, G. G.; Kittleman, L. R., 1971, Geochemical and petrological characterization of ash samples from Cascade Range volcanoes: Quaternary Research, v. 1, no. 2, p. 261-282.

Rice, Alan, 1981, Convective fractionation; a mechanism to provide cryptic zoning (macrosegregation), layering, crescumulates, banded tuffs and explosive volcanism in igneous processes: Journal of Geophysical Research, v. 86, no. B1, p. 405-417.

Rowley, P. D.; Kuntz, M. A.; MacLeod, N. S., 1981, Pyroclastic-flow deposits. In Lipman, P. W.; Mullineaux, D. R., editors, 1981, The 1980 eruptions of Mount St. Helens, Washington: U.S. Geological Survey Professional Paper 1250, p. 489-512.

Sarna-Wojcicki, A. M.; Waitt, R. B., Jr.; Woodward, M. J.; Shipley, Susan; Rivera, Jose, 1981, Premagmatic ash erupted from March 27 through May 14, 1980--Extent, mass, volume, and composition. In Lipman, P. W.; Mullineaux, D. R., editors, 1981, The 1980 eruptions of Mount St. Helens, Washington: U.S. Geological Survey Professional Paper 1250, p. 569-575.

Scarfe, C. M.; Fujii, T.; Harris, D. M., 1982, Mineralogy and geochemistry of pumice from 19 March 1982 eruption of Mount St. Helens [abstract]: Geological Society of American Abstracts with Programs, v. 14, no. 7, p. 608.

Scheidegger, K. F.; Federman, A. N.; Tallman, A. M., 1981 Compositional heterogeneity of tephras from the 1980 eruptions of Mount St. Helens [abstract]: Eos (American Geophysical Union Transactions), v. 63, no. 41, p. 809-810.

Scheidegger, K. F.; Federman, A. N.; Tallman, A. M., 1982, Compositional heterogeneity of tephras from the 1980 eruptions of Mount St. Helens: Journal of Geophysical Research, v. 87, no. B13, p. 10,861-10,881.

Smith, A. L.; Carmichael, I. S. E., 1968, Quaternary lavas from the southern Cascades, western U.S.A.: Contributions of Mineralogy and Petrology, v. 19, no. 3, p. 212-238.

Smith, D. G. W.; Westgate, J. A., 1969, Electron probe technique for Characterizing pyroclastic deposits: Earth and Planetary Science Letters, v. 5, no. 5, p. 313-319.

Smith, D. R., 1980, The mineralogy and phase chemistry of silicic tephras erupted from Mount St. Helens volcano, Washington: Rice University Master of Arts thesis, 202 p.

Smith, D. R.; Leeman, W. P., 1980, Mineralogy of high-temperature pumiceous tephras from Mount St. Helens [abstract]: Geological Society of America Abstracts with Programs, v. 12, no. 7, p. 524.

Smith, D. R.; Leeman, W. P., 1982, Petrochemistry of pre-1980 volcanic rocks of Mount St. Helens [abstract]: Geological Society of America Abstracts with Programs, v. 14, no. 2, p. 234.

Smith, H. W.; Okazaki, Rose, Knowles, C. R., 1977, Electron microprobe analysis of glass shards from tephra assigned to Set W, Mount St. Helens, Washington: Quaternary Research, v. 7, no. 2, p. 207-217.

Sykes, M. L.; Self, S., 1981, Pyroclastic flows of Mount St. Helens, Washington, May-July, 1980 [abstract]: Eos (American Geophysical Union Transactions), v. 62, no. 45, p. 1088-1089.

Taylor, H. E.; Lichte, F. E., 1980, Chemical composition of Mount St. Helens volcanic ash: Geophysical Research Letters, v. 7, no. 11, p. 949-952.

Taylor, S. R.; Capp, A. C.; Graham, A. L.; Blake, D. H., 1969a, Trace element abundances in andesites; II, Saipan, Bougainville and Fiji: Contributions to Mineralogy and Petrology, v. 23, p. 1-26.

Taylor, S. R.; Kaye, Maureen; White, A. J. R.; Duncan, A. R.; Ewart, A., 1969b, Genetic significance of Co, Cr, Ni, Sc and V content of andesites: Geochimica et Cosmochimica Acta, v. 33, p. 275-286.

Taylor, S. R.; Kaye, Maureen; White, A. J. R.; Duncan, A. R.; Ewart, A., 1969c, Genetic significance of V and Ni content of andesites; reply to Prof. E. F. Osborn: Geochemica et cosmochimica Acta, v. 33, no. 12, p. 1555-1557.

Taylor, S. R.; White, A. J. R., 1966, Trace element abundances in andesites: Bulletin Volcanologique, v. 29, p. 177-194.

Tilley, C. E., 1960, Some aspects of magmatic evolution: Geological Society of London Quarterly Journal, v. 106, Pt. 1, no. 421, p. 37-61.

Tong, L. S., 1972, Boiling crisis and critical heat flux: U.S. Atomic Energy Commission Critical Review Series TD-25887, 82 p.

Verhoogen, Jean, 1937, Mount St. Helens; a recent Cascade volcano: University of California Publications in Geological Sciences, v. 24, no. 9, p. 263-302.

Voight, Barry; Glicken, Harry; Janda, R. J.; Douglass, P. M., 1981, Catastrophic rockslide avalanche of May 18. In Lipman, P. W.; Mullineaux, D. R., editors, 1981, The 1980 eruptions of Mount St. Helens, Washington: U.S. Geological Survey Professional Paper 1250, p. 347-377.

Waters, A. C., 1955, Volcanic rocks and the tectonic cycle. In Poldervaart, A., editor, 1955, Crust of the earth--A symposium: Geological Society of America Special Paper 623, p. 703-722.

Wilson, Lionel; Head, J. W., 1981, Morphology and rheology of pyroclastic flows and their deposits, and guidelines for future observations. In Lipman, P. W.; Mullineaux, D. R., editors, 1981, The 1980 eruptions of Mount St. Helens, Washington: U.S. Geological Survey Professional Paper 1250, p. 513-524.

Wozniak, K. C.; Hughes, S. S.; Taylor, E. M., 1980, Chemical analyses of Mount St. Helens pumice and ash: Oregon Geology, v. 42, no. 7, p. 130.

APPENDIX A

Sample Localities and Petrographic Descriptions of Analyzed Rocks

All thin sections analyzed are hornblende hypersthene dacites with glassy, highly vesiculated groundmass containing varying amounts of microlites. The abundance of crystal phases generally increases with time after May 18, 1980.

Sample

1. Locality: Western distal August 7, pyroclastic flow.

   Plagioclase: Reaches maximum size of 1.13mm; exhibits common carlsbad and carlsbad/albite polysynthetic twinning and one pericline twinned phenocryst; normal, oscillatory and reverse zoning present; corroded cores with pink glass inclusions. Euhedral or broken crystals.
   Hypersthene: Pleochroic, colorless/very light green to pink, to 0.75mm, euhedral.
   Hornblende: Pleochroic, light brown to dark olive, euhedral, irregular inclusions, embayed, common twinning, reaction rims of magnetite and colorless hypersthene.
   Opaque Minerals: Disseminated in groundmass, inclusions in hypersthene and plagioclase.

2. Locality: Central distal August 7 pyroclastic flow.

   Plagioclase: Phenocrysts up to 1.9mm, An_{57} and An_{56}; some corroded cores; pink glass inclusions; euhedral and broken crystals; normal, reverse and oscillatory zoning; carlsbad, polysynthetic and pericline twinning in phenocrysts.
   Hypersthene: Euhedral; light green to pink pleochroism.
   Hornblende: Partially resorbed with microlite rims light brown to olive green pleochroism.
   Opaque Minerals: As inclusions in feldspar and hyperthene phenocrysts and disseminated throughout groundmass.
   Apatite: As acicular inclusions in feldspar phenocrysts.

3. Locality: Eastern distal August 7 pyroclastic flow.

   Plagioclase: Euhedral phenocrysts and microlites; some corroded cores; pink glass inclusions; normal, reverse and oscillatory zoning; carlsbad and polysynthetic twinning.
   Hypersthene: Euhedral, pale pink to colorless pleochroism.
   Hornblende: Up to 1.7mm; yellow-green and olive green to dark brown; some partially recrystallized boundaries; some phenocrysts have irregularly shaped inclusions.
   Opaque Minerals: As inclusions in feldspar and hypersthene phenocrysts and in xenolith.

Sample

3. Locality: Eastern distal August 7 pyroclastic flow (Cont.)

Xenolith: Colorless to very light green clinopyroxene 75%; plagioclase 20%, opaque minerals 5%.

4. Locality: Eastern proximal July 22 pyroclastic flow, main trunk.

Plagioclase: Euhedral phenocrysts; pink glass inclusions some parallel to zoning surfaces; normal reverse and oscillatory zoning; carlsbad most common twinning, poly-synthetic and pericline twinning also apparent.
Hypersthene: Euhedral to subhedral, pale pink to colorless pleochroism.
Hornblende: Some euhedral without reaction rims; some light brown to dark olive others light yellow to brown pleochroism; reaction rims of hypersthene and/or magnetite on some phenocrysts; inclusions on clinopyroxene in two hornblende phenocrysts.
Opaque Minerals: As inclusions in phenocrysts and dissemi-nated in groundmass.
Clinopyroxene: Occurs as inclusions in hornblende and rare microphenocrysts in groundmass.

5. Locality: Central proximal July 22 pyroclastic flow, main trunk.

Plagioclase: Abundant large phenocrysts many containing abundant glassy inclusions; some inclusions parallel to zoning surfaces, euhedral; normal, reverse, and oscillatory zoning; carlsbad and polysynthetic twinning common pericline less so.
Hypersthene: Light green to pink pleochroism; euhedral.
Hornblende: Light yellow to brown; light yellow to green pleochroism; anhedral to euhedral; resorbed as well as sharp crystal boundaries.
Opaque Minerals: As inclusions in phenocrysts and dissemi-nated in groundmass.
Clinopyroxene: Occasional small euhedral phenocrysts with twinning parallel to 100; as inclusion in large hornblende phenocryst.

Sample

6. Locality: Western proximal July 22 pyroclastic flow, main
      trunk.

   Plagioclase: Large euhedral phenocrysts, most having abun-
   dant glassy inclusions in their cores; reverse and oscilla-
   tory zoning more common than normal zoning; carlsbad and
   polysynthetic twinning common.
   Hypersthene: Light pink to colorless pleochroism; mostly
   euhedral phenocrysts.
   Hornblende: Anhedral to euhedral phenocrysts; some sharp
   boundaries others partially recrystallized.
   Opaque Minerals: As inclusions in phenocrysts and dissemi-
   nated in groundmass.
   Clinopyroxene: One large anhedral light green phenocryst.

7. Locality: Western proximal August 7 pyroclastic flow.

   Plagioclase: Abundant large phenocrysts and microlites;
   pink glass inclusions in cores and throughout phenocrysts;
   normal, reverse and oscillatory zoning; carlsbad and poly-
   synthetic twinning common.
   Hypersthene: Colorless to pale pink pleochroism, euhedral.
   Hornblende: Reaction rims of hypersthene microlites, opa-
   que inclusions smaller phenocrysts nearly totally
   recrystallized.
   Opaque Minerals: As inclusions in phenocrysts and dissemi-
   nated in groundmass.

8. Locality: Western central October 16-19 pyroclastic flow
      deposits.

   Plagioclase: Abundant large phenocrysts, microlites; pink
   glass inclusions in phenocryst cores; oscillatory zoning
   most common; carlsbad and polysynthetic twinning common
   pericline less so.
   Hypersthene: Abundant phenocrysts; colorless to pale pink
   pleochroism.
   Hornblende: Nearly all phenocrysts have reaction rims of
   hypersthene microlites, some grains are completely
   recrystallized; yellow-brown-green pleochroism.
   Opaque Minerals: As inclusions in plagioclase and
   hypersthene, in hornblende reaction rims, and disseminated
   in groundmass.

Sample

9. Locality: Eastern central October 16-19 pyroclastic flow
            deposits.

    Groundmass: Subtrachytic.
    Plagioclase: Abundant phenocrysts to 2.5mm, microlites;
    pink glass inclusions; normal reverse and oscillatory
    zoning; carlsbad, polysynthetic and pericline twinning.
    Hypersthene: Relatively strong pink to green pleochroism;
    phenocrysts seem significantly more abundant and larger (up
    to 1.6mm) than in previous thin sections; large and
    euhedral.
    Hornblende: Abundant large (2.1mm) phenocrysts many with
    reaction rims, but some with sharp boundaries.
    Opaque Minerals: As inclusions in phenocrysts and dissemi-
    nated in groundmass.
    Clinopyroxene: One plae green phenocryst.
    Note: Phenocrysts are larger and more abundant than in
    Samples 1-8.

10. Locality: Eastern medial August 7 pyroclastic flow deposit.

    Plagioclase: Large phenocrysts, microlites; glass inclu-
    sions in larger phenocrysts; normal, reverse and oscilla-
    tory zoning; carlsbad and polysynthetic twinning.
    Hypersthene: As pleochroic pink to green euhedral phe-
    nocrysts and as microlites.
    Hornblende: Yellow to dark brown and dark green to dark
    brown phenocrysts with reaction rims of hypersthene
    microlites.
    Opaque Minerals: As inclusions, and disseminated.

11. Locality: Central medial August 7 pyroclastic flow deposit.

    Groundmass: Locally subtrachytic.
    Plagioclase: Large phenocrysts, some with glassy
    inclusions; normal, reverse and oscillatory zoning; carls-
    bad and polysynthetic twinning most common; microlites.
    Hypersthene: As euhedral pale pink to pale green
    phenocrysts.
    Hornblende: Small phenocrysts mostly resorbed except in
    xenolith; some twinning.
    Opaque Minerals: As inclusions and disseminated in
    groundmass.
    Xenolith: 3.2mm in diameter, large intergrown plagioclase
    and hornblende.

Sample

13. Locality: Western distal June 12 pyroclastic flow deposits;
    eastern lobe.

    Groundmass: Significantly more glass in groundmass than in
    samples (1-11).
    Plagioclase: As phenocrysts and microlites; glassy inclu-
    sions in cores of phenocrysts; normal, reverse and oscilla-
    tory zoning; carlsbad twinning most common, polysynthetic
    and pericline less so.
    Hypersthene: As euhedral pale pink to pale green phe-
    nocrysts.
    Hornblende: Colorless to green pleochroism, mostly clean
    boundaries on eu-subhedral phenocrysts.
    Opaque Minerals: As inclusions and disseminated in
    groundmass.

14. Locality: Western distal June 12 pyroclastic flow deposit;
    eastern lobe.

    Plagioclase: Phenocrysts and microlites; glassy inclusions
    in cores of phenocrysts and parallel to zoning; reverse
    zoning most common but also normal and oscillatory; carls-
    bad and polysynthetic twinnning.
    Hypersthene: Euhedral, pale pink to pale green
    pleochroism.
    Hornblende: Commonly twinned, pale brown to brown to green
    pleochroism; occasional reaction rims.
    Opaque Minerals: As inclusions and disseminated in
    groundmass.

15. Locality: Eastern distal June 12 pyroclastic flow deposit;
    eastern lobe.

    Plagioclase: Phenocrysts and microlites; glassy inclusions
    in cores of phenocrysts and parallel to zoning; reverse
    zoning most common but also normal and oscialltory; carls-
    bad and polysynthetic twinning.
    Hypersthene: Euhedral, pale pink to pale green
    pleochroism.
    Hornblende: Very light brown to olive green pleochroism,
    occasional reaction rims; 2.6mm phenocryst.

Sample

16. Locality: Eastern distal June 12 pyroclastic flow deposit;
                eastern lobe.

    Plagioclase: Phenocrysts and microlites; glass inclusions
in cores of phenocrysts; normal, reverse and oscillatory
zoning, carlsbad and polysynthetic twinning.
Hypersthene: Euhedral, pale pink to pale green
pleochroism.
Hornblende: Commonly twinned, pale brown to brown to green
pleochroism; occasional reaction rims.
Opaque Minerals: As inclusions and disseminated in
groundmass.

17. Locality: Eastern medial June 12 pyroclastic flow deposit;
                eastern lobe.

    Plagioclase: Phenocrysts and microlites; glass inclusions
in cores of phenocrysts; normal, reverse and oscillatory
zoning; carlsbad and polysynthetic twinning.
Hypersthene: Euhedral, pale pink to pale green
pleochroism.
Hornblende: Commonly twinned, pale brown to brown to green
pleochroism, occasional reaction rims.
Opaque Minerals: As inclusions and disseminated in
groundmass.

18. Locality: Western mdedial June 12 pyroclastic flow deposit;
                eastern lobe.

    Plagioclase: Phenocrysts and microlites; glass inclusions
in cores of phenocrysts; normal, reverse and oscillatory
zoning; carlsbad polysynthetic and pericline twinning.
Hypersthene: Euhedral, pale pink to pale green
pleochroism.
Hornblende: Commonly twinned, pale brown to brown to green
pleochroism, occasional reaction rims.
Opaque Minerals: As inclusions and disseminated in
groundmass.
Xenolith: Hornblende and plagioclase.

<u>Sample</u>

19. Locality: Center medial June 12 pyroclastic flow deposit; eastern lobe.

Plagioclase: Phenocrysts and microlites; glass inclusions in cores of phenocrysts; normal, reverse and oscillatory zoning; carlsbad and polysynthetic twinning An_{30}.
Hypersthene: Euhedral, pale pink to pale green pleochroism.
Hornblende: Commonly twinned, pale brown to brown to green pleochroism, occasional reaction rims.
Opaque Minerals: As inclusions and disseminated in groundmass.

20. Locality: Distal June 12 pyroclastic flow deposit; eastern lobe.

Plagioclase: Phenocrysts and microlites; glass inclusions in cores of phenocrysts; normal, reverse and oscillatory zoning; carlsbad and polysynthetic twinning.
Hypersthene: Euhedral, pale pink to pale green pleochroism.
Hornblende: Commonly twinned, pale brown to brown to green pleochroism, occasional reaction rims.
Opaque Minerals: As inclusions and disseminated in groundmass.
Clinopyroxene: Twinned, colorless, euhedral.

21. Locality: Western proximal June 12 pyroclastic flow deposit; eastern lobe.

Plagioclase: Phenocrysts and microlites; glass inclusions in cores of phenocrysts; normal, reverse and oscillatory zoning; carlsbad and polysynthetic twinning.
Hypersthene: Euhedral, pale pink to pale green pleochroism.
Hornblende: Commonly twinned, pale brown to brown to green pleochroism; occasional reaction rims.
Opaque Minerals: As inclusions and disseminated in groundmass.

Sample

22. Locality: Central proximal June 12 pyroclastic flow deposit; eastern lobe.

Plagioclase: Phenocrysts and microlites; glass inclusions in cores of phenocrysts; normal, reverse and oscillatory zoning; carlsbad and polysynthetic twinning.
Hypersthene: Euhedral, pale pink to pale green pleochroism.
Hornblende: Commonly twinned, pale brown to brown to green pleochroism; occasional reaction rims.
Opaque Minerals: As inclusions and disseminated in groundmass.

23. Locality: Eastern proximal June 12 pyroclastic flow deposit; eastern lobe.

Plagioclase: Phenocrysts and microlites; glass inclusions in cores of phenocrysts; normal, reverse and oscillatory zoning; carlsbad and polysynthetic twinning.
Hypersthene: Euhedral, pale pink to plae green pleochroism.
Hornblende: Commonly twinned, pale brown to brown to green pleochroism; occasional reaction rims.
Opaque Minerals: As inclusions and disseminated in groundmass.

24. Locality: Western distal July 22 pyroclastic flow deposit; eastern lobe.

Plagioclase: As microlites and euhedral phenocrysts; pink glass inclusions in phenocryst phase both throughout and parallel to zoning surfaces; normal, reverse and oscillatory zoning; carlsbad, polysynthetic and pericline twinning.
Hypersthene: Euhedral, pale pink to pale green pleochroism.
Hornblende: Phenocrysts with no or thin reaction rims are pleochroic light brown to dark brown, those with relatively thick rims of hypersthene microlites are light brown to olive green.
Opaque Minerals: As inclusions and disseminated in groundmass.
Clinopyroxene: As euhedral xenolith or clot containing twinned (parallel to 100) clinopyroxene (augite) of very light purple-brown color in ordinary light; other minerals in clot are euhedral hypersthene and anhedral opaques.

Sample

25. Locality: Distal June 12 pyroclastic flow deposit; western lobe "pumice pond".

Groundmass: Subtrachytic texture.
Plagioclase: Euhedral with a few subhedral and broken phenocrysts; the latter have clear cores with abundant pink glassy inclusions in the rims; microlites; normal, reverse, and oscillatory zoning; carlsbad, polysynthetic and pericline twinning.
Hypersthene: Euhedral, pale pink to pale green pleochroism.
Hornblende: Mostly anhedral slightly resorbed phenocrysts; twinning commmon; pleochroic brownish yellow to olive green.
Opaque Minerals: As inclusions and disseminated in groundmass.

26. Locality: Distal July 22 pyroclastic flow deposit; western lobe.

Plagioclase: Generally euhedral phenocrysts some with glassy inclusions; microlites; normal, reverse and oscillatory zoning; carlsbad, polysynthetic and pericline twinning.
Hypersthene: Euhedral, pale pink to pale green pleochroism.
Hornblende: Mostly anhedral slightly resorbed phenocrysts; twinning common; pleochroic brownish yellow to olive green.
Opaque Minerals: As inclusions and disseminated in groundmass.
Clinopyroxene: Subhedral phenocrysts with small hornblende inclusions.

27. Locality: Western distal July 22 pyroclastic flow deposit; western lobe.

Groundmass: Subtrachytic texture.
Plagioclase: Generally euhedral phenocrysts some with glassy inclusions; microlites; normal, reverse and oscillatory zonong; carlsbad, polysynthetic and pericline twinning.
Hypersthene: Euhedral, pale pink to pale green pleochroism.
Hornblende: Mostly anhedral slightly resorbed phenocrysts; twinning common; pleochroic brownish yellow to olive green.
Opaque Minerals: As inclusions and disseminated in groundmass.
Clinopyroxene: Single anhedral phenocryst.

Sample

28. Locality: Central distal July 22 pyroclastic flow deposit;
             western lobe.

        Plagioclase: Generally euhedral phenocrysts some with
        glassy inclusions; microlites; normal, reverse and oscilla-
        tory zoning; carlsbad, polysynthetic and pericline
        twinning.
        Hypersthene: Euhedral, pale pink to pale green
        pleochroism.
        Hornblende: Mostly anhedral slightly resorbed phenocrysts;
        twinning common; pleochroic brownish yellow to olive green.
        Opaque Minerals: As inclusions and disseminated in
        groundmass.

29. Locality: Western medial July 22 pyroclastic flow deposit;
             western lobe.

        Plagioclase: Generally euhedral phenocrysts some with
        glassy inclusions; microlites; normal, reverse and oscilla-
        tory zonong; carlsbad, polysynthetic and pericline
        twinning.
        Hypersthene: Euhedral, pale pink to pale green
        pleochroism.
        Hornblende: Mostly anhedral slightly resorbed phenocrysts;
        twinning common; pleochroic brownish yellow to olive green.
        Opaque Minerals: As inclusions and disseminated in
        groundmass.
        Clinopyroxene: As small clot of euhedral and subhedral
        crystals.

30. Locality: Central medial July 22 pyroclastic flow deposit;
             western lobe.

        Plagioclase: Generally euhedral phenocrysts some with
        glassy inclusions; microlites; normal, reverse and oscilla-
        tory zoning; carlsbad, polysynthetic and pericline
        twinning.
        Hypersthene: Euhedral, pale pink to pale green
        pleochroism.
        Hornblende: Mostly anhedral slightly resorbed phenocrysts;
        twinning common; pleochroic brownish yellow to olive green.
        Opaque Minerals: As inclusions and disseminated in
        groundmass.

Sample

31. Locality: Central medial July 22 pyroclastic flow deposit;
western lobe.

Plagioclase: Generally euhedral phenocrysts some with
glassy inclusions; microlites; normal, reverse and oscilla-
tory zoning; carlsbad, polysynthetic and pericline
twinning.
Hypersthene: Euhedral, pale pink to pale green
pleochroism.
Hornblende: Mostly anhedral slightly resorbed phenocrysts;
twinning common; pleochroic brownish yellow to olive green.
Clinopyroxene: As euhedral and subhedral phenocrysts
twinned parallel to 100.
Opaque Minerals: As inclusions and disseminated in
groundmass.
Xenolith or crystal cumulate: Euhedral and anhedral
hypersthene, plagioclase and opaques.

32. Locality: Central May 18 pyroclastic flow deposit; western
lobe.

Plagioclase: As generally euhedral phenocrysts with glassy
inclusions; microlites are smaller than in later pumice and
sparse, twinning and zoning are same in later pumice.
Hypersthene: Euhedral, pale pink to pale green
pleochroism.
Hornblende: Euhedral to subhedral phenocrysts with sharp
boundaries; no resorption or recrystallization apparent;
light brown to green to brown pleochroism.
Opaque Minerals: As inclusions and disseminated in
groundmass.

33. Locality: Central May 18 pyroclastic flow deposit; western
lobe.

Plagioclase: As generally euhedral phenocrysts with glassy
inclusions; microlites are smaller than in later pumice and
sparse, twinning and zoning are same as in later pumice.
Hypersthene: Euhedral, pale pink to pale green
pleochroism.
Hornblende: Euhedral to subhedral phenocrysts with sharp
boundaries; no resorption or recrystallization apparent;
light brown to green to brown pleochroism.
Opaque Minerals: As inclusions and disseminated in
groundmass.

Sample

35. Locality: Central Proximal October 19 pyroclastic flow
deposit; western lobe.

Plagioclase: As large euhedral phenocrysts with pink
glass inclusions; both phenocrysts and microlites are much
more abundant and coarser than in earlier flows; zoning and
twinning is essentially the same as earlier flows.
Hypersthene: Euhedral, pale pink to pale green
pleochroism.
Hornblende: Most of the smaller phenocrysts are completely
recrystallized to hypersthene microlites and opaques; large
phenocrysts have thick reaction rims.
Clinopyroxene: As both single euhedral to subhedral phe-
nocrysts and in xenolithic clots, twinning is common.

APPENDIX B

Sample Preparation

Pumice clasts were first cut into slices less than 1/4" thick to eliminate the possibility of including xenolith material in the analysis. The sawblade was cleaned thoroughly by using acetone to remove all paint and other impurities from its surface. The sliced pumice was washed thoroughly with deionized water and then dried in a dessication oven at 100°C for about 30 minutes. The dried slices were gently crushed into small pieces using agate mortar and pestle to prevent iron contamination. Some pulverization occurred during the crushing process. To prevent grain size bias, the entire sample, including both pieces and pulverized material was then dumped into the grinding vessel. The samples were ground in a spex shatterbox for approximately 10 to 15 minutes. The shatterbox vessels were cleaned thoroughly before each grinding by washing with deionized water, followed by an acetone drying bath.

Sample preparation for analysis on the ICPS of major and element oxides as accomplished in the following manner:

First, 0.1 gram of sample and 0.7 gram of $LiBO_2$ were weighed, mixed thoroughly and placed into a carbon crucible. The mixture was then fused at 1000°C for twenty minutes. The molten bead was poured into 50 milliliters (ml) of HNO_3 and dissolved with a teflon stirring bar. The solution was then transferred gravimetrically to a 100 ml volumetric flask where 3 ml of 5000 parts per million (ppm) La was added as an internal standard. The solution was then diluted to volume.

Trace element sample preparation included the following:

About 1.00 gram of sample was weighed into a teflon beaker to which 2 ml of concentrated HNO_3 were added. The mixture was covered and warmed on a hot plate for ½ hour. After cooling 10 ml of 48 percent HF, 3 ml of $HClO_4$ and 2 ml of HNO_3 were added. The mixture was then covered and allowed to sit overnight. The cover was then removed and the mixture was warmed until a clear solution was obtained. After transfer to a 100 ml volumetric flask the solution was brought back to 40 ml with 6.2 HCl (if it was necessary to do so), 5 ml of $HClO_4$ was added and the solution brought back to volume.